HHS Public Access

Author manuscript

Med Res Rev. Author manuscript; available in PMC 2019 September 01.

Published in final edited form as:

Med Res Rev. 2018 September ; 38(6): 1974–2023. doi:10.1002/med.21503.

Recent Advances in the Discovery and Development of Factor XI/XIa Inhibitors

Rami A. Al-Horani[1,*] and **Daniel K. Afosah**[2]

[1]Division of Basic Pharmaceutical Sciences, College of Pharmacy, Xavier University of Louisiana, New Orleans, Louisiana 70125

[2]Department of Medicinal Chemistry and Institute for Structural Biology, Drug Discovery and Development, Virginia Commonwealth University, Richmond, Virginia 23219

Abstract

Factor XIa (FXIa) is a serine protease homodimer that belongs to the intrinsic coagulation pathway. FXIa primarily catalyzes factor IX activation to factor IXa which subsequently activates factor X to factor Xa in the common coagulation pathway. Growing evidence suggests that FXIa plays an important role in thrombosis with a relatively limited contribution to hemostasis. Therefore, inhibitors targeting factor XI/XIa system have emerged as a paradigm-shifting strategy so as to develop a new generation of anticoagulants to effectively prevent and/or treat thromboembolic diseases without the life-threatening risk of internal bleeding. Several inhibitors of factor XI/XIa proteins have been discovered or designed over the last decade including polypeptides, active site peptidomimetic inhibitors, allosteric inhibitors, antibodies, and aptamers. Antisense oligonucleotides which ultimately reduce the hepatic biosynthesis of factor XI have also been introduced. A phase II study, which included patients undergoing elective primary unilateral total knee arthroplasty, revealed that a specific factor XI antisense oligonucleotide effectively protects patients against venous thrombosis with a relatively limited risk of bleeding. Initial findings have also demonstrated the potential of factor XI/XIa inhibitors in sepsis, listeriosis, and arterial hypertension. This review highlights various chemical, biochemical, and pharmacological aspects of factor XI/XIa inhibitors with the goal of advancing their development towards clinical use.

Keywords

Anticoagulants; factor XI/XIa; peptidomimetics; antibodies; oligonucleotides

INTRODUCTION

Hemostasis is a physiological clotting process that prevents excessive blood loss following a vascular injury. It sustains the blood fluidity and helps avoid insufficient perfusion of vital

[*]Address for correspondence: Dr. Rami A. Al-Horani, 1 Drexel Drive, Suite 327, New Orleans, LA 70125-1089. Phone: (504) 520-7603, Fax: (504) 520-7954, ralhoran@xula.edu.

CONFLICT OF INTEREST

Authors declare no competing financial conflict of interest.

organs. Dysregulation of this process may lead to excessive bleeding or thrombosis. Several factors may trigger such dysregulation including cancer, inflammation, and infections, yet acquired or inherited defects in components/mechanisms of physiological coagulation are the primary causes of dysregulated hemostasis [1, 2].

On the thrombosis front, thrombotic diseases are either venous or arterial diseases. Venous thrombosis (VT) comprises deep vein thrombosis (DVT) and pulmonary embolism (PE). Arterial thrombosis (ArT) mainly includes ischemic heart disease (IHD) and ischemic stroke (IS). Other examples of thrombotic diseases include atrial fibrillation, disseminated intravascular coagulation, and unstable angina. Wendelboe and Raskob (2016) reported that there have been about 1518.7 cases of IHD, 115–269 cases of VT, 139.3 cases of myocardial infarction, 114.3 cases of IS, and 137 cases of atrial fibrillation per hundred thousand people on the global stage. More seriously, global mortality rates of 105.5 for IHD, 42.3 for IS, 9.4–32.3 for VT, and 1.7 for atrial fibrillation per hundred thousand have been reported [3, 4]. Collectively, VT annually affects 7–14 million people worldwide. In the United States alone, VT is collectively responsible for more than 100,000 deaths annually. Furthermore, ArT causes more than 10 million deaths per year worldwide and this rate has increased by ~30% during the past two decades. Therefore, thrombotic diseases continue to be major causes of morbidity and mortality in developing and developed countries alike, and are indeed significant contributors to the global burden of diseases [3, 4].

Pathophysiologically, arterial and venous thrombi are fundamentally composed of three elements: red blood cells, platelets, and fibrin. Arterial thrombi (white thrombi) are platelet-rich whereas venous thrombi (red thrombi) are fibrin-rich, trapping more of red blood cells. Antithrombotic drugs are used to prevent and/or treat thrombosis and include anticoagulants, antiplatelet drugs, and fibrinolytic agents. Antiplatelet agents such as aspirin and clopidogrel are more widely used in ArT in which platelets play the major role through adhesion, activation, and aggregation. Fibrinolytic drugs such as streptokinase and alteplase (recombinant tPA) are therapeutically used to degrade thrombi. Fibrinolytics may be administered systemically in the treatment of acute myocardial infarction, acute IS, and cases of PE or can be applied directly into the thrombus via catheters to help degrade thrombi in the deep veins of the leg as well as peripheral arterial thrombi [1, 2, 5]. Anticoagulants represent the mainstay of the treatment and/or prevention strategies for venous thromboembolic diseases. Current anticoagulants directly or indirectly interfere with the physiological functions of the natural procoagulants of the coagulation process. Emerging anticoagulants are the subject of this review which will extensively describe recent efforts from the peer-reviewed literature domain that deal with the design and development of factor XIa (FXIa) inhibitors as a new line of effective anticoagulants with potentially no-to-limited risk of bleeding [6].

THE COAGULATION PROCESS AND CURRENT ANTICOAGULANTS

The platelets, blood vessel endothelium, coagulation process, and fibrinolytic apparatus work in harmony to control the blood flowing status. Particularly, the coagulation process, which represents a series of chemical bio-transformations, comprises the intrinsic pathway, the extrinsic pathway, and the common pathway (Figure 1). This process is primarily

initiated through the extrinsic pathway. Vascular injury allows tissue factor (TF) to get into systemic circulation which activates the zymogen factor VII (FVII) to factor VIIa (FVIIa) at the site of vessel damage. The binding of FVII/VIIa to TF subsequently activates factor X (FX) to factor Xa (FXa). The FVIIa–TF complex can also activate factor IX (FIX) to factor IXa (FIXa) which forms the tenase complex with factor VIIIa (FVIIIa) in the presence of phospholipids and Ca^{2+} ions. The tenase complex subsequently activates FX to FXa which starts the common coagulation pathway. Under similar conditions of phospholipids and Ca^{2+} ions, FXa forms the prothrombinase complex with FVIIIa. This complex facilitates the formation of thrombin (or factor IIa (FIIa)) by activating the corresponding zymogen i.e. prothrombin. Thrombin is a central serine protease in the whole process of coagulation. Among many physiological roles, thrombin converts soluble plasma fibrinogen to insoluble fibrin eventually leading to clot formation. Thrombin also activates the zymogen factor XIII (FXIII) to the transglutaminase factor XIIIa (FXIIIa) that covalently cross-links γ–chains and α-chains of fibrin molecules by forming new peptidic bonds between the ε-amino groups of lysine and the amide groups of glutamine residues. This crosslinking yields a more stable fibrin-rich clot which is resistant to proteolysis [1, 2, 5–7].

Likewise, FXa formation is also triggered by the intrinsic coagulation pathway, also known as the contact activation system. The intrinsic pathway involves factors VII, IX, XI, XII, prekallikrein, and high-molecular-weight kininogen (HK) as well as phospholipids and Ca^{2+} ions. The intrinsic pathway is generally initiated under “contact environment” in which factor XI (FXI), factor XII (FXII), prekallikrein, and HK are in contact with an anionic surface such as kaolin (in vitro activation) and extracellular DNA, RNA, and inorganic polyphosphates (in vivo activation). In this contact environment, FXII is activated to factor XIIa (FXIIa) upon proteolysis by kallikrein. FXIIa subsequently activates FXI to FXIa and also releases vasodilatory bradykinin from HK. In the presence of Ca^{2+} ions, FXIa activates FIX to FIXa which subsequently activates factor X to produce FXa by the intrinsic tenase complex [1, 2, 5–7]. To achieve the ultimate goal of hemostasis, the activity of procoagulant enzymes in the coagulation process is regulated and in many cases inhibited by internal proteins (endogenous anticoagulants) including tissue factor pathway inhibitor (TFPI) [8], activated protein C (APC) [9], and antithrombin (AT) [10]. Specifically, TFPI inhibits FXa whereas APC degrades FVa and FVIIIa. AT is the major regulator of factors IIa, Xa and IXa under physiological conditions [11] and can also inhibit FVIIa [12] and FXIa [13].

In recent history, our understanding of the contribution of the intrinsic coagulation pathway to thrombosis has significantly advanced [14–18]. Studies indicate that patients with a hereditary deficiency of FXII [19], prekallikrein [20], or HK [21, 22] do not exhibit bleeding problems. Likewise, hemophilia C patients who suffer from FXI deficiency generally have no bleeding problems [23]. Therefore, the intrinsic coagulation is largely seen as a pathway to primarily amplify FXa generation and ultimately thrombin formation through feedback mechanisms.

Anticoagulants are drugs that inhibit one or more of the coagulation proteins. Currently, factors IIa and Xa of the common coagulation pathway are the only coagulation proteases that have been successfully targeted by anticoagulant drugs. Clinically used anticoagulants exhibit pharmacological activity by either an indirect or a direct mechanism of inhibition.

The indirect inhibition mechanism involves the recruitment of an endogenous mechanism or protein, such as AT, to diminish the proteolytic activity of FIIa and/or FXa. In contrast, the direct inhibition mechanism targets FIIa or FXa directly by binding to their active sites or allosteric sites [1, 5]. Indirect anticoagulants include heparin (also known as unfractionated heparin (UFH)) and its variants of low molecular weight heparins (LMWHs) and the pentasaccharide fondaparinux as well as vitamin K antagonists i.e. coumarins such as warfarin [24–26]. Direct anticoagulants include FIIa inhibitors such as the bivalent peptidic inhibitors i.e. hirudins and bivalirudin and the active site peptidomimetic inhibitors i.e. dabigatran etexilate and argatroban. This class of anticoagulants also includes active site FXa inhibitors such as apixaban, edoxaban, and rivaroxaban. Heparins, hirudins, and argatroban are parenteral anticoagulants whereas warfarin, dabigatran etexilate, rivaroxaban, apixaban, and edoxaban are oral anticoagulants [24–26]. All current anticoagulants are reversible, and therefore, antidotes are available to reverse the action of many of them. Protamine sulfate, for example, is used as an antidote for UFH and LMWHs but not for fondaparinux whereas vitamin K is used to reverse the action of warfarin. Idarucizumab is approved for dabigatran reversal and andexanet alfa is under FDA review for reversal of rivaroxaban, apixaban, and edoxaban [27]. Ciraparantag (PER977) is also under development as a universal reversal agent for all direct-acting oral anticoagulants and heparin products [28].

Despite the clinical efficacy of the currently used anticoagulants, all are associated with several side effects and serious drawbacks [24–26]. UFH suffers from significant intra- and inter-patient response variation, which requires frequent laboratory monitoring. Heparin-induced thrombocytopenia, which occurs in 1–2% of patients who receive heparin, is a potentially lethal consequence of heparin therapy that may be associated with thrombosis. Additional limitations of UFH include the development of osteoporosis in patients receiving high dose therapy for relatively extended periods of time as well as the high risk of contamination with other glycosaminoglycans that may result in serious life-threatening hypersensitivity reactions. Many of these drawbacks are mitigated by the introduction of LMWHs and fondaparinux [24]. Warfarin suffers from a narrow therapeutic index and several drug–drug and drug–food interactions [25]. Hirudins also have narrow therapeutic windows and have variable levels of immunogenicity [24]. Although the safety profiles of newer oral active site inhibitors of thrombin and FXa are better than heparins, coumarins, and hirudins, the limited availability of standardized assays for measuring these drugs in biological fluids, their short half-lives, their relatively high cost, and potential contraindications in patients with severe renal dysfunction represent serious challenges for their therapeutic use [29, 30]. All three FXa inhibitors are CYP3A4 and P-glycoprotein substrates which carry potential drug-drug interaction issues [31]. Moreover, more studies are required to determine their use in specific patient populations including pregnant women [32, 33] and cancer patients [34, 35].

Importantly, all clinically used anticoagulants are associated with the life-threatening side effect of internal bleeding, particularly intracranial, gastrointestinal, and retroperitoneal bleeding [36–39]. For example, Agnelli *et al.* (2013) reported that the composite outcome of major or non-major clinically relevant bleeding episodes was encountered in 4.3% of the patients in the apixaban group, as compared with 9.7% of those in the enoxaparin/warfarin-

therapy group [36]. Buller *et al.* (2013) reported that the composite outcome of major or non-major clinically relevant bleeding episodes was encountered in 8.5% of the patients in the edoxaban group, as compared with 10.3% of those in the warfarin-therapy group [37]. van Es *et al.* (2014) reported that absolute risks of major bleeding, fatal bleeding, and intracranial bleeding were 1.1%, 0.1%, and 0.1%, respectively, in new oral anticoagulant therapy groups, as compared with 1.8%, 0.3%, and 0.2%, respectively, in warfarin therapy groups [38]. Furthermore, the annual rate of intracranial hemorrhage was found to be 0.3–0.6% for patients taking warfarin compared to 0.1–0.2% for patients on the new oral anticoagulants (4 drugs) [39]. Therefore, although many advances have been realized in recent years, there remains a serious need for developing new anticoagulants to prevent and/or treat thromboembolic diseases without being associated with a high risk of bleeding. As stated by Schmaier in a recent editorial of Thrombosis Research (2015) *"If one is an uninformed outsider looking into the pharmacological management of thrombosis, it seems bizarre that we prevent thrombosis by creating another potential bleeding state"* [40].

FACTOR XIa (FXIa): AN EMERGING PROTEIN TARGET FOR ANTICOAGULANTS

Structure and Function

Human FXIa is a 160-kDa serine protease disulfide homodimer belonging to the intrinsic coagulation pathway. It is a plasma protease that is primarily biosynthesized in hepatocytes and circulates systemically as a zymogen i.e. FXI, with an approximate concentration of 30 nM [41–43]. The two units of the zymogen dimer are connected by an interchain disulfide linkage between the Cys321 residues positioned in a structural loop in the A4 domain of each subunit. Furthermore, hydrophobic interactions between the Tyr329, Ile290, and Leu284 residues of the A4 domain interface, and the salt bridges between Lys331 from one monomer and Glu287 from the other monomer, also facilitate this dimerization. Each subunit of the FXIa homodimer is composed of 607 amino acid residues and contains an *N*-terminal heavy chain and a *C*-terminal light chain. The light chain is a trypsin-like catalytic domain whereas the heavy chain is made up of four repeats which are also known as the apple domains named A1 through A4 (Figure 2A/B). The catalytic domain sets on the apple domains, forming what has been described in literature as the cup and saucer configuration, and this appears to facilitate the proteolytic function of FXIa [41–43]. The apple domains present several binding sites for major macromolecules including thrombin in the A1 domain [44], HK in the A1/A2 domains [42, 45], platelet glycoprotein GPIb [46], the physiological substrate FIX [47], sulfated saccharides in the A3 domain [13, 48], and FXIIa in the A4 domain [49]. It is important to mention here that the amino acid sequence of FXI shows 58% identity with human plasma prekallikrein [50].

As with other serine proteases such as thrombin and FXa, the catalytic domain has the active site involving the trypsin-like catalytic triad of Ser557, Asp462, and His413. These residues correspond to Ser195, Asp102, and His57, respectively, in the chymotrypsin residue numbering system [50]. The Schechter and Berger nomenclature is conventionally used to label the subsites in the active site of proteolytic enzymes, including FXIa, and the amino acids in peptidic substrates. The numbering of subsites is S1′; S2′; S3′…*etc* from the

cleavage bond growing to the *C*-terminus of the enzyme and S1; S2; S3…*etc* growing in the direction of the *N*-terminus (Figure 2C). Likewise, the system is exploited to describe the binding of small molecules to the active site of FXIa, as S1 is the subsite that accommodates P1 part of the substrate/inhibitor molecule, S2 is the subsite for P2, S3 subsite for P3 part, and so forth [51]. The cleavage bond is between the amino acids P1 and P1′ of the peptidic substrate which bind to the corresponding subsites S1 and S1′, respectively. Considering this nomenclature, the active site of FXIa contains several subsites with characteristic features for substrate selectivity (S4–S3–S2–S1–S1′–S2′–S3′–S4′). The S1 specificity pocket has an aspartate residue (Asp189) at the base of the cleft, and therefore, it binds to an arginine residue in the high binding substrates/inhibitors including the physiological substrate FIX. The subsites S4, S3, S2, S1, S1′, S2′, S3′, and S4′ of FXIa predominantly bind to Lys/Asp, Leu/Phe, Thr/Pro, Arg, Val/Ala, Val/Glu, Gly/Thr, and Gly/Val, respectively [52].

Physiologically, FXI is activated through the cleavage of the Arg369-Ile370 bond by thrombin [53, 54] or FXIIa [55]. Auto-activation in the presence of polyanions, e.g. inorganic polyphosphate polymers is also possible [53]. Plasma serpins such as AT, α1-antitrypsin, C1-inhibitor, and protein Z–dependent protease inhibitor may physiologically inhibit FXIa [56, 57]. The physiological function of FXIa can also be inhibited by sulfated glycosaminoglycans such as heparin. Heparin can inhibit the proteolytic function of FXIa either directly by charge neutralization or allosteric modulation through binding to a select group of basic amino acids in FXIa's catalytic domain (Lys529, Arg530, Arg532, Lys535, and Lys539) [58, 59] or indirectly by enhancing the serpin-mediated template inhibition mechanism in which the A3 domain of FXIa (Lys252, Lys253, and Lys255) and the serpin bind to the same sequence of heparin forming an inhibitory ternary complex [56]. FXIa's primary physiological role is to activate FIX to FIXa which eventually results in thrombin generation. FXIa-mediated thrombin generation can also be brought about by activating factors V, VIII, and X [60, 61] as well as facilitating the proteolysis of TFPI [62].

Interestingly, hemophilia C i.e. genetic deficiency of FXI in humans, is generally associated with a relatively mild-to-moderate bleeding risk compared with the other two types of hemophilia i.e. FVIII deficiency (hemophilia A) or FIX deficiency (hemophilia B). Although excessive bleeding in severe FXI deficiency may occur in surgery or trauma, hemophilia C patients rarely suffer from spontaneous bleeding or significant bleeding complications [63–65]. These patients typically have a relatively long activated partial thromboplastin time (APTT) and normal prothrombin time (PT), suggesting a specific defect in the amplification phase of the coagulation process. In fact, studies strongly indicate that patients with severe FXI deficiency enjoy a relatively reduced risk of ischemic stroke [66] and deep vein thrombosis [67]. Likewise, epidemiological studies demonstrated that increased levels of FXI increase the risk for deep vein thrombosis [68], stroke [69–71], myocardial infarction [72], and cardiovascular diseases in women [73]. Furthermore, FXI-knockout mice were shown not to suffer from excessive bleeding while experiencing extended APTT and normal PT [23]. The FXI-knockout mice displayed significant antithrombotic activity in several arterial and venous thrombosis animal models [74–76]. Similar observations were recorded in rats [77] and higher animals including rabbits [78] and baboons [79, 80].

Overall, FXIa amplifies thrombin generation in thrombosis and appears to exhibit limited contribution to thrombin generation in hemostasis. FXIa may thus serve as a promising avenue to antithrombotics that are safer i.e. associated with significantly fewer bleeding complications than FXa and thrombin inhibitors. Recently, Weitz and Fredenburgh (2017) described specific potential indications for FXIa/FXI inhibitors for which existing therapies appear to be unsatisfactory [17]. These indications which focus on the prevention of arterial or venous thrombosis include: (1) prevention of cardiovascular events in patients with chronic kidney disease; (2) stroke prevention in atrial fibrillation patients at high bleeding risk; (3) prevention of thrombosis in patients with venous thromboembolism who are at an elevated risk of recurrent thrombosis upon discontinuation of anticoagulant therapy; (4) prevention of cardiovascular events in hemodialysis patients; (5) prevention of clotting in extracorporeal membrane oxygenation circuits; (6) prevention of thromboembolic events in patients with cardiac devices; and (7) prevention of stent thrombosis in acute coronary syndrome patients who need anticoagulant therapy in addition to antiplatelet therapy.

Inhibition Strategies Targeting Factor XI/XIa System

Inhibition strategies targeting FXI/FXIa proteins can generally be classified into seven categories: (1) polypeptides; (2) peptidomimetic active site inhibitors; (3) polymeric glycosaminoglycans (GAGs) and their saccharide mimetics; (4) nonpolymeric, nonsaccharide GAG mimetics; (5) antibodies; (6) antisense oligonucleotides (ASOs); and (7) aptamers. In subsequent sections, we extensively describe the chemical, biochemical, and pharmacological aspects of reported inhibitors of the FXI/FXIa system. Considering the historical aspects of the drug discovery process for FXI/FXIa-based potential therapeutics, we have chosen to start with the polypeptides category.

(1) Polypeptides—Several polypeptides have been reported to inhibit human FXIa. These include aprotinin (FXIa K_I=288 nM) [81, 82], corn Hageman factor inhibitor (FXIa K_I=5.4 μM) [83], Desmolaris (K_I=0.63 nM) [84], ecotin and mutants [85, 86], Fasxiator (FXIa K_D=20.2 nM) [87], human placental bikunin (FXIa K_I=6 nM) [88], *Ixodes ricinus* contact phase inhibitor (Ir-CPI) [89], nematode proteins of AcaNAP10 (FXIa K_I=25.8 nM) and AduNAP4 (FXIa K_I=42.5 nM) [90, 91], protease nexin-2 (PN-2) [92–96], simukunin (FXIa IC_{50}=56.7 nM) [97], and tissue factor pathway inhibitor-2 (also reported as KD1-WT) (FXIa K_I=15 nM) [98–101]. Considering the specificity of these polypeptides, Desmolaris, Fasxiator, and PN-2 are relatively the most interesting, and thus, are described in detail in the following sections.

Desmolaris: Desmolaris is a 21.5-kDa Kunitz 1-domainless variant of tissue factor pathway inhibitor-1 (TFPI-1) which was first extracted from the salivary gland of *Desmodus rotundus,* a vampire bat [84]. Desmolaris was found to be a tight, slow, and noncompetitive inhibitor of FXIa with a K_D value of 0.63 nM. Desmolaris also inhibited FXa with a K_D value of 16 nM. Moreover, Desmolaris inhibited kallikrein with a K_D value of 115 nM and reduced bradykinin generation in kaolin-activated plasma. Inhibition of FXIa and FXa by Desmolaris was enhanced in the presence of heparin. Interestingly, Desmolaris did not inhibit FXIIa, FVIIa/TF, thrombin, plasmin, tissue plasminogen activator, urokinase, matriptase, chymase, or proteinase-3 at the highest concentrations tested. However,

Desmolaris was found to substantially inhibit trypsin, α-chymotrypsin, neutrophil elastase, and neutrophil cathepsin G. At a concentration of 300 nM, Desmolaris dose-dependently extended the clotting times in APTT and PT assays by 9-fold and 2-fold, respectively.

Structure-activity relationship studies using mutated and truncated variants of Desmolaris indicated that the Arg32 residue in the Kunitz-1 domain is very important for protease inhibition. The studies also revealed that the Kunitz-2 and *C*-terminus domains facilitate interaction of Desmolaris with heparin and appear to be optimally required for FXa and FXIa inhibition. In $FeCl_3$-induced carotid artery thrombosis model, all mice treated with 100 μg/kg Desmolaris were resistant to arterial occlusion. At doses of 100 or 250 μg/kg, Desmolaris did not produce significant bleeding. In mouse models, Desmolaris also lessened epinephrine- and collagen-mediated thromboembolism and the polyphosphate-induced increase in vascular permeability [84].

Fasxiator: Fasxiator is a 7-kDa Kunitz-type protease inhibitor that was extracted from the venom of the snake *Bungarus fasciatus*. Fasxiator doubled clotting time in the APTT assay at a concentration of 3 μM without a significant effect on clotting time in the PT assay at a concentration as high as 100 μM. Pure recombinant Fasxiator was found to be a slow and potent inhibitor of FXIa with a K_D value of 20.2 nM (IC_{50}=1.5 μM). Fasxiator was also found to inhibit FXIa-mediated FIX activation with an IC_{50} value of 3 μM. Conversely, Fasxiator did not inhibit FXIIa, FXa, FIXa, FVIIa, thrombin, plasmin, urokinase, APC, and kallikrein at the highest concentration tested which was 120 μM suggesting a significant margin of selectivity of about 6000-fold. Nevertheless, Fasxiator inhibited chymotrypsin with an IC_{50} value of 1 μM [87].

To improve the potency and selectivity of Fasxiator, which has the scissile bond of Asn17–Ala18, a series of mutants were generated. Particularly, $Fasxiator_{N17\ R,L19E}$ was found to be a slow competitive inhibitor of FXIa with a K_i value of 0.86 nM (IC_{50}~1 nM) and a selectivity index of >100-fold over FVIIa, FXa, kallikrein, trypsin, chymotrypsin, APC, and plasmin. In human plasma, this mutant prolonged APTT in a dose-dependent manner with an effective concentration of 300 nM to double the clotting time. As expected, it had no significant effect on PT using a concentration as high as 40 μM. In $FeCl_3$-induced thrombosis murine model, $Fasxiator_{N17R,L19E}$ effectively delayed the occlusion of the carotid artery at a dose of 0.3 mg/animal. It is important to mention here that $Fasxiator_{N17R,L19E}$ is 10-fold more potent anticoagulant in human plasma than in murine plasma [87].

Protease nexin–2 (PN-2): PN-2 is a soluble form of amyloid beta-protein precursor (APP). It contains a Kunitz-type protease inhibitor (KPI) domain, and is released from activated platelets. PN-2 was found to be a potent, reversible, and competitive inhibitor of FXIa with a K_i value of 0.4 nM [92]. The mechanistic studies revealed that the inhibition proceeds by a slow equilibration process between the free enzyme and the inhibitor, and not via a loosely-associated complex. HK and Zn^{2+} ions were found to have opposite effects on the inhibition of FXIa by PN-2. Zn^{2+} augmented the PN-2-mediated inhibition of FXIa whereas HK dose-dependently protected FXIa from inhibition by PN-2 with an EC_{50} value of 61 nM [92]. Heparin was also found to enhance PN-2-mediated FXIa inhibition by 15-fold [93]. PN-2

KPI was also found to potently inhibit chymotrypsin and trypsin with K_i values of 6.0 and 0.02 nM, respectively, and to moderately inhibit plasmin as well as glandular and plasma kallikreins (K_i =42–82 nM) [94]. Mutagenesis in the reactive sequence of PN-2 (Gly^{12}–Pro–Cys–Arg–Ala–Met–Ile–Ser^{19}) has been reported to variably affect inhibition of FXIa, plasmin, and plasma kallikrein [95]. For example, P1 Arg→Lys and P2′Met→Lys/Arg enhanced the inhibitory activity against plasmin (K_i=8 nM) at the expense of the activity against FXIa and kallikrein [95]. KALI-DY, which differs from APP at 6 amino acid residues (Thr11Asp, Pro13His, Met17Ala, Ile18His, Ser19Pro, and Phe34Tyr), inhibited plasma kallikrein with a K_i value of 0.015 nM. KALI-DY also inhibited FXIa with a K_i value of 8.2 nM. KALI-DY did not inhibit FXIIa, FXa, FVIIa/TF, FIIa, plasmin, or APC. Consistent with the protease specificity, KALI-DY prolonged the clotting time only in the APTT assay by more than 3.5- fold at a concentration of 1 μM [95]. Likewise, the Kunitz domain of Alzheimer amyloid precursor protein homolog (KD APPH) was reported to inhibit FXIa with a K_i value of 14 nM. KD APPH also inhibited other serine proteases including trypsin (K_i =0.02 nM), glandular kallikrein (K_i =8.8 nM), plasma kallikrein (K_i =86 nM), plasmin (K_i =81 nM), and chymotrypsin (K_i =78 nM) [82, 94].

A co-crystal structure of recombinant KPI domain of PN-2 with a mutant form of the FXIa catalytic domain was reported (PDB ID: 1ZJD). In this complex, the disulfide-stabilized double loop structure of PN-2 KPI was found to fit into the FXIa active site with the P1 Arg15 residue occupying the S1 pocket. Single-point mutations in PN-2 KPI loop 1 ^{11}TGPCRAMISR^{20} and loop 2 ^{34}FYGGC^{38} indicated that the most important residues in PN-2 KPI for FXIa inhibition were Arg15> Phe34> Pro13>Arg20 [96].

(2) Peptidomimetics: Active Site Inhibitors—Despite the reports of co-crystal structures of recombinant human FXIa catalytic domain (rhFXIa(370–607)) and ecotin mutants, none of these structures was suitable for iterative structure-based drug design because ecotins interacted with rhFXIa(370–607) in a matrix-like fashion which was difficult to be displaced by small molecules [85]. In fact, it was not until 2005 that a co-crystal of a quadruple mutant of rhFXIa(370–607) (rhFXIa(370–607)-Ser434Ala, Thr475Ala, Cys482Ser, Lys437Ala) with a small molecule was obtained. Jin *et al.* (2005) reported that this FXIa mutant is readily co-crystallized with benzamidine which can easily be exchanged with other FXIa small-molecule inhibitors [102]. This method has subsequently facilitated the drug design of small-molecule active site inhibitors of human FXIa.

α-Ketothiazole arginine-containing peptidomimetics: Deng *et al.* (2006) reported the design and synthesis of tri-peptidomimetic FXIa inhibitors containing α-ketothiazole arginine moiety, represented by the generic structures I (8 derivatives), II (9 derivatives), and III (8 derivatives) (Figure 3) [103]. Usinga fluorogenic substrate hydrolysis assay under near physiological conditions, the molecules that exhibited the most potent inhibition toward FXIa were inhibitor **1** of generic structure I with an IC_{50} value of 2.25 μM, inhibitor **2** of generic structure II with an IC_{50} value of 0.48 μM, and inhibitor **3** of generic structure III with an IC_{50} value of 0.12 μM (Figure 3). The co-crystal structure of **3** (PDB ID: 2FDA) with the FXIa catalytic domain shows a salt bridge interaction between the P1 arginine

moiety of the inhibitor and Asp189 in the S1 pocket of the enzyme. Ketothiazole **3** (and others in this class) is a covalent inhibitor of FXIa because the keto group is covalently attached to Ser195 in the enzyme active site. The P2 Val side chain of the inhibitor appears to occupy the S2 pocket in FXIa's active site. The *N*-terminal carbonyl group forms an H-bond interaction with the backbone amino group of Gly216. The inhibitor also forms additional hydrophobic and H-bond interactions with residues in the S4 pocket and the backbone carbonyl group of Gly216, respectively (Figure 3) [103].

A set of 31 tetra-peptidomimetic FXIa inhibitors containing α-ketothiazole arginine moiety was synthesized and evaluated for FXIa inhibition by Lin *et al.* (2006) [104]. The tetra-peptidomimetic inhibitors were designed based on the chemical structures of two thrombin inhibitors, leupeptin (Leu-Leu-Arg-H) and PPACK (D-Phe-Pro-Arg-CH_2Cl). All resulting inhibitors exhibited FXIa IC_{50} values in the range of 6–26000 nM with variable selectivity over thrombin and FXa. Particularly, inhibitor **4** had an IC_{50} value of 6 nM (Figure 4) and demonstrated significant selectivity over thrombin (IC_{50}=2040 nM) and FXa (IC_{50}=1600 nM). Inhibitor **4** was also found to inhibit FVIIa, plasma kallikrein, APC, and trypsin with IC_{50} values of 38000, 10, 20700, and 12 nM, respectively [104]. The pharmacokinetic profile of inhibitor **4** was established via IV administration to rats and was shown to display a short $T_{0.5}$ (~45 min), a relatively high clearance rate (32 mL/kg/min), and a low Vdss (~236 mL/kg). It also doubled the clotting times in the APTT assay at a concentration of 2.4 μM and in the PT assay at a concentration of 25 μM. Continuous IV administration (0.25 mg/kg) of this molecule to rats inhibited the hypnotic saline/partial stenosis-induced thrombus formation in the inferior vena cava. The magnitude of the reduction was similar to that obtained using heparin at a dosing level of 50 units/kg (IV bolus) + 25 units/kg/hr (IV infusion). The effect of this inhibitor on rat mesenteric arteriole bleeding time was not evaluated. Instead, the authors examined the effect of another inhibitor **5** (which they reported to have similar *in vivo* efficacy). Inhibitor **5** had a FXIa IC_{50} value of 12 nM (Figure 4). It also inhibited thrombin and FXa with IC_{50} values of 1400 nM. It also doubled the clotting times in the APTT and the PT assays at concentrations of 2.4 μM and 31 μM, respectively. When administered at up to 1 mg/kg (4-fold more than the efficacious dose), this inhibitor led to 1.5-fold increase in the bleeding time relative to the control whereas 38 U/kg dose of heparin significantly resulted in more than 2.5-fold increase in the bleeding time relative to the control.

Furthermore, inhibitor **6** was used in X-ray crystallography experiments so as to develop better understanding of potential interactions between this class of tetrapeptidomimetic inhibitors and the FXIa active site. Inhibitor **6** had an IC_{50} value of 30 nM (Figure 4). The molecule also inhibited thrombin (IC_{50}=1100 nM) and FXa (IC_{50}=1900 nM). Inhibitor **6** doubled the clotting times in the APTT assay at a concentration of 1.35 μM and in the PT assay at a concentration of 48.6 μM. A detailed scheme of its key binding interactions with FXIa active site is described in figure 4B (PDB ID: 1ZOM). It appears that the lysine residue at position-192 is an important element in obtaining selective FXIa inhibition by this class of inhibitors [104]. No further development for this class of covalent and orthosteric FXIa inhibitors was reported.

Aryl boronic acid esters: Lazarova *et al.* (2006) reported the chemical synthesis and the biochemical evaluation of a group of aryl boronic acids as potential active site inhibitors of FXIa [105]. Generally, the molecules in this category had micromolar potency with very narrow selectivity over thrombin, FXa, and trypsin. Specifically, boronic acid esters **7** and **8** inhibited FXIa with IC_{50} values of 7.3 and 1.4 μM, respectively (Figure 5). Nevertheless, inhibitor **7** also inhibited thrombin, FXa, and trypsin with potencies of 30.8, 175.4, and 20.3 μM, respectively. Likewise, inhibitor **8** also inhibited thrombin and FXa with IC_{50} values of 12.3 and 43.6 μM, respectively. The crystal structure of inhibitor **8** with the catalytic domain of FXIa (PDB ID: 1ZLR) revealed that only the (*S*)-enantiomer binds into the active site. The inhibitor was co-crystallized as a glycerol boronate ester and its boron atom was found to form a covalent bond with the oxygen atom of Ser195 (Figure 5B). The inhibitor's guanidine group formed a salt bridge with the side-chain carboxylate of Asp189. The ester carbonyl in this inhibitor was also found to be within an H-bonding distance from the backbone nitrogen of Lys192. The pyridyl group was reported to have hydrophobic contacts with the Leu146 side chain [105]. Despite this initial discovery, no data was presented on aryl boronate esters' potential effect on human plasma clotting times. No further development for this class of covalent and orthosteric FXIa inhibitors was reported in the published literature.

Clavatadines: In the search for novel natural antithrombotics, an extract of the marine sponge *Suberea clavata* (Aplysinellidae) was screened against FXIa and showed significant inhibition, with an IC_{50} value of ~0.4 μg/μL. Bioassay-guided extract fractionation resulted in the isolation of two bromophenolic alkaloids, clavatadines A (**9**) and B (**10**) (Figure 6) [106]. Clavatadines A and B inhibited FXIa with IC_{50} values of 1.3 and 27 μM, respectively, and did not significantly inhibit FIXa at the highest concentration tested of 222 μM. A co-crystal structure of clavatadine A with FXIa was obtained (PDB ID: 3BG8) and revealed that the carbamate side chain is covalently attached to the active site residue Ser195 (Figure 6B) with the carbamate oxygen H-bonded to the backbone amide nitrogen of Gly193. The crystal structure also showed that the basic guanidine group binds to the carboxylate group of Asp189 by bidentate H-bonds and to the backbone amide oxygen of Gly218 by another H-bond. Furthermore, molecular docking studies suggested that the dibromophenol ring may occupy a pocket defined by Arg37D, Lys192, and Gly193 on one side and Leu39, Cys42–Cys58, and His57 on the other side. Clavatadine B is more than 20-fold less potent than clavatadine A, potentially due to the weak interactions between its amide (relative to carboxylate) and either Arg37D or Lys192.

Further purification of the active extracts of the marine sponge led to the isolation of six other marine alkaloids, named as clavatadines C-E, aerophobin 1, purealdin L, and aplysinamisine II [107]. Using 222 μM of each of these alkaloids in the S-2366 chromogenic substrate hydrolysis assay, FXIa was inhibited by clavatadine C **11** by ~17%, clavatadine D **12** by ~30%, clavatadine E **13** by ~37%, aerophobin 1 **14** by ~59%, purealdin L**15** by ~12%, and aplysinamisine II **16** by ~30% (Figure 6C). Interestingly, none of these alkaloids exhibited significant inhibition of FIXa at this concentration. No further studies have been reported in the published literature considering FXIa inhibition potential of these alkaloids.

β-Lactam derivatives: Schumacher *et al.* (2007) reported the hemostatic and antithrombotic effects of a small molecule FXIa inhibitor **17**, a 4-carboxy-2-azetidinone (β-lactam), (Figure 7A) in rats [77]. Inhibitor **17** is an irreversible inhibitor of human FXIa with an IC_{50} value of 2.8 nM. It is at least 170-fold more selective for FXIa considering other proteases in the coagulation process (thrombin, FXa, FIXa, FXIIa, and TF/FVIIa) and the fibrinolysis process (plasmin, urokinase, and tissue plasminogen activator) (Figure 7B). However, this molecule also inhibited human tryptase (IC_{50}=5 nM) as well as trypsin (IC_{50}=50 nM). β-Lactam **17** doubled the clotting time in the APTT assay in human and rat plasmas at concentrations of 0.14 and 2.2 μM, respectively. The inhibitor did not impact the PT at a concentration as high as 100 μM. Furthermore, a regimen of 12 mg/kg (IV bolus) +12 mg/kg/hr (IV infusion) of inhibitor **17** significantly resulted in maximum thrombus weight reductions of 97% and 73% in $FeCl_2$-induced thrombosis in rats in the carotid artery and the vena cava, respectively. In an *ex vivo* APTT assay, the dosing protocol of 12 mg/kg (IV bolus) +12 mg/kg/hr (IV infusion) of inhibitor **17** increased the clotting time about 3-fold. This dose level also inhibited the growth of arterial and venous thrombi upon administration after partial thrombus formation. The inhibitor was most potent against $FeCl_2$-induced venous thrombosis as it significantly decreased the thrombus weight by about 38% using a regimen of 0.2 mg/kg (IV bolus) + 0.2 mg/kg/hr (IV infusion). Nevertheless, regimens of up to 24 mg/kg (IV bolus) +24 mg/kg/hr (IV infusion) exhibited no effect on the *ex vivo* PT or the TF-induced venous thrombosis. Interestingly, inhibitor **17** administered at dose levels of 6+6, 12+12, and 24+24 (mg/kg + mg/kg/hr) did not extend cuticle, renal, or mesenteric bleeding times relative to vehicle treatment suggesting the lack of negative impact on hemostasis. In contrast, a heparin dose that produces similar antithrombotic effect to that of inhibitor **17** at a dose level of 24 mg/kg (IV bolus) +24 mg/kg/hr (IV infusion) was found to produce significant bleeding effects in all three bleeding models.

The antithrombotic and hemostatic effects of inhibitor **17** were also evaluated in rabbits [108]. In an *in vitro* setting, inhibitor **17** doubled the clotting time of rabbit plasma in the APTT assay at a concentration of 10.6 μM but had no effect on the PT, thrombin time (TT), or HeTest at 100 μM concentration. In an *in vivo* setting, inhibitor **17** dose-dependently promoted antithrombotic effects in rabbits with antithrombotic ED_{50} values of 0.4 mg/kg/hr IV in arteriovenous-shunt thrombosis model, 0.7 mg/kg/hr IV in venous thrombosis model, and 1.5 mg/kg/hr IV in electrolytic-mediated carotid arterial thrombosis model. Furthermore, platelet aggregation responses to collagen and adenosine diphosphate (ADP) were not substantially affected by inhibitor **17** at 10 mg/kg/hr IV infusion (vehicle: 74 ± 7% and 57 ± 4%, respectively, *vs.* inhibitor: 70 ± 5% and 63 ± 3%, respectively). Lastly, in the cuticle bleeding time model, inhibitor **17** did not significantly alter the bleeding time at 1 and 3 mg/kg/hr IV infusion, however, it significantly increased the bleeding time by 1.52 ± 0.07-fold at 10 mg/kg/hr IV infusion.

Another β-lactam-based FXIa inhibitor is molecule **17a** (EP-7041; Figure 7D). A phase I clinical trial for this inhibitor finished in 2017 [109]. The study revealed that EP-7041 was safe and well tolerated at all doses tested. Parenteral EP-7041 has rapid onset and offset as well as predictable dose-dependent increase in the APTT but not the PT [110].

Macrocyclic peptidomimetics: Cyclization of peptides and peptidomimetics is thought of as an effective chemical strategy to reduce the entropic penalty of a molecular recognition event, and therefore, to enhance dug candidate potency and to increase its metabolic stability and membrane permeability. Using this concept, the serine protease inhibitor **18** (Figure 8) was computationally exploited by Hanessian *et al.* (2010) to design a new class of macrocyclic peptidomimetic inhibitors of FXIa [111]. Inhibitor **18** was computationally modeled into the active site of human FXIa. The model revealed extensive H-bond interactions between the inhibitor's three amide bonds and the backbone of the protein (Gly218, Gly216, and Ser214), with the side chains of the Leu and cyclohexyl-Gly residues fitting into S2 pocket (proximal binding pocket) and S3 pocket (distal binding pocket), respectively. Based on the generated model, it was suggested that introducing a 4-carbon bridge between the methylene unit adjacent to the sulfonamide moiety and the benzamidine group would lead to a potent inhibitor. To further enhance the selectivity and the drug-like properties, the benzamidine moiety was replaced with a 5-chloroindole so to facilitate binding into the S1 subsite. A small library was also designed to investigate the significance of the sulfonamide and the aryl moieties extending towards a binding pocket formed by Thr143, Leu146, Arg147, and Lys192. Three linear and five macrocyclic molecules were eventually evaluated for their inhibitory activity on FXIa, thrombin, APC, and trypsin. The presence of a 5-chloroindole moiety as a P_1 motif was generally tolerated by FXIa, yet all tested molecules lacked significant selectivity as they all inhibited trypsin with submicromolar K_i values in the range of 0.02–1.22 μM and had moderate to strong inhibitory profiles against APC and thrombin. Molecule **19** (Figure 8) was the most potent macrocyclic FXIa inhibitor identified in this study with an IC_{50} value of 135.8 μM. This molecule did not inhibit thrombin at concentrations up to 300 μM but inhibited APC and trypsin with IC_{50} values of 144.5 μM and 0.26 μM, respectively. No crystallography data, studies in human plasma, studies in whole blood, or *in vivo* studies for the macrocyclic derivatives in this class have been reported thus far.

Along these lines, Gademann *et al.* (2010) reported the isolation and structural characterization of a natural cyclic peptide known as cyanopeptolin 1020 **20** (Figure 8) from a *Microcystis* strain as a potent inhibitor of FXIa with an IC_{50} value of 3.9 nM [112]. Cyanopeptolin 1020 belongs to the class of cyclic depsipeptides known as cyanopeptolins. These peptides are widely distributed secondary metabolites in cyanobacteria and contain the structural element of 3-amino-6-hydroxy-2-piperidone. Cyanopeptolin 1020 was also found to be a very potent inhibitor of trypsin with an IC_{50} value of 0.67 nM and human kallikrein with an IC_{50} value of 4.5 nM. Cyanopeptolin 1020 also inhibited plasmin (0.49 μM) and chymotrypsin (1.8 μM), but not the human enzymes of thrombin, plasminogen activator, or low molecular weight urokinase at concentrations below than 2.5 μM [112].

On a different front, two synthetic cyclic peptidomimetics **21** and **22** (Figure 8) were earlier developed as human plasmin inhibitors (Ki = 0.68 and 0.2 nM, respectively), yet they were also found to inhibit human FXIa with Ki values of 4.7 and 3.37 μM, respectively [113]. Furthermore, the peptidomimetic **21** inhibited the human enzymes of plasma kallikrein (0.32 μM), thrombin (13.87 μM), trypsin (0.062 μM), and urokinase (8.9 μM), whereas the peptidomimetic **22** inhibited human plasma kallikrein (1.0 μM), thrombin (26.42 μM), FXa

(25 μM), trypsin (0.038 μM), urokinase (6.5 μM), and urinary kallikrein (10 μM). Both inhibitors were selective over related human proteases including APC, FXIIa, FVIIa/TF, FIXa, tissue plasminogen activator, C1s, and C1r.

Advanced macrocyclic peptidomimetics will subsequently be discussed along with other FXIa inhibitors belonging to advanced subclasses of peptidomimetics.

Phenylalanines: Early derivatives with 1-(4-Chlorophenyl)-*1H*-tetrazole as the P1 group: In 2012, Fradera *et al.* reported the first crystal structures of FXIa catalytic domain in complex with two non-basic inhibitors **23** and **24** (Figure 9) possessing a chlorophenyl-tetrazole group as the P1 group [114]. The two crystal structures were also the first for FXIa catalytic domain in complex with peptidomimetic inhibitors binding to both the non-prime and prime sides of the active site. The two molecules **23** and **24** inhibited FXIa with EC_{50} values of 7.6 and 19.1 nM, respectively.. The two inhibitors were relatively selective against thrombin and FXa with less than 33% inhibition at 10 μM. As revealed by their co-crystal structures with the catalytic domain of FXIa (PDB IDs: 3SOS and 3SOR), the binding modes of the two inhibitors appear to be very similar, with the chlorophenyl-tetrazole moiety binding deep into the S1 pocket and the chlorine atom binding in a perpendicular fashion to the phenol ring of Tyr228. The tetrazole ring appears to be in close contact with the disulfide bond formed by Cys191 and Cys219. Both inhibitors have an ethylamide moiety at position-2 of the phenyl ring. The amide functionality forms H-bonding interactions with Ser195 and Gly193. The rest of each inhibitor binds in the prime side of the active site with the benzyl group interacting with His57, Tyr59A, and Leu39 in the S1′subsite. For inhibitor **23**, the benzyl ring has a face-to-face interaction with His57 whereas that of inhibitor **24** is arranged in an edge-to-face arrangement. Inhibitor **23** has an amide functionality in the S1′ subsite that is water-bridged to the backbone of Leu39. The S2′ site is occupied by the benzothiazinone ring which interacts with His38 and Tyr143. The Lys37D residue at the top of the phenyl and thiazinone rings further stabilizes the inhibitor binding through a cation–π interaction. Inhibitor **24** also has an amide functionality at the interface between S1′ and S2′ with the carbonyl group making an H-bond to a water molecule. The phenyl ring directly attached to the amide binds into the S2′ subsite and the acetate group makes polar interactions with the side chains of Lys37D and Tyr143. Looking closely at the co-crystal structures, selectivity over thrombin and FXa is mainly attributed to the benzyl moiety fitting into the relatively large S1′ subsite. Both thrombin and FXa have relatively small S1′ subsites and this feature prevents the benzyl moiety from binding. Furthermore, key differences in the S2′ subsite also exist. Tyr143 in FXIa is replaced by Arg (FXa) or Trp (thrombin) whereas Lys37D in FXIa is replaced by Glu residue in both FXa and thrombin. These residues directly bind to the benzothiazinone ring of inhibitor **23** and the acetate group of inhibitor **24**. Therefore, these inhibitors will not be able to form similar contacts in the active site of FXa or that of thrombin, and thus, they lose their inhibitory activity towards these two proteins. No further studies have been reported thus far for either inhibitor.

Likewise, Smith II *et al.* (2016) reported the development of phenylalanine diamides as a new chemotype of FXIa inhibitors, starting from the phenylalanine derivative **25** (Figure 10) [115]. Inhibitor **25** has a FXIa K_i value of 40.5 nM and a plasma kallikrein K_i value of 120

nM. Replacing the methylcarbamate moiety with a carboxylic acid group led to inhibitor **26** which has a FXIa K_i value of 2 nM, a plasma kallikrein K_i value of 140 nM, and APTT $EC_{1.5x}$ value of 4.2 μM. The X-ray crystal structure of inhibitor **26** bound in the active site of FXIa at 2.5 Å resolution was obtained (PDB ID:5E2O). The chlorophenyl tetrazole moiety was found to occupy the S1 pocket with the chlorine substituent in close contact with Tyr228 while the tetrazole N^2 atom was found to be close to the backbone amino group of Lys192 and the disulfide bridge (Cys191–Cys219). The tetrazole N^3 atom and the acidic tetrazole CH proton appear to interact with the amino group of Lys192 and the carbonyl of Gly216, respectively. The cinnamide carbonyl group forms several H-bonds with Gly193, Asp194, and Ser195 residues within the oxyanion hole. The benzyl side chain forms a hydrophobic edge-on interaction with the disulfide bridge (Cys42–Cys58) in the S1′ binding pocket. Lastly, the P2′ amide functionality makes direct and water-mediated H-bonds with His40, Leu41, and Tyr143 residues.

Several carboxylic acid bioisosteres were used including *N*-substituted tetrazole, C-substituted tetrazole (inhibitor **27**), imidazole, 1,2,4-triazole, 1,2,4-oxadiazol-5-one (inhibitor **28**), and 1,3,4-oxadiazol-2-one (Figure 10). Particularly, inhibitors **27** and **28** had FXIa K_i values of 1.4 and 2.0 nM, respectively, plasma kallikrein K_i values of 23 and 36 nM, respectively, and APTT $EC_{1.5X}$ values of 4.6 and 9.6 μM, respectively. Introduction of a fluorine substituent at postion-2 of the P1 phenyl of inhibitor **26** led to inhibitor **29** which had a significantly improved APTT potency (FXIa K_i =1.7 nM, plasma kallikrein K_i=46 nM, and APTT $EC_{1.5X}$=1.2 μM). Furthermore, the evaluation of the effect of substituents on the P1′ phenyl group revealed that groups such as propyl, phenyl, methylpiperazine-amide, and cyclopropyl-amide were all tolerated. Inhibitor **30** which has a methylpiperazine-amide substituent has a FXIa *Ki* value of 2.0 nM and APTT $EC_{1.5X}$=0.5 μM (plasma kallikrein K_i=59 nM). Likewise, inhibitor **31** which has a cyclopropyl-amide substituent has subnanomolar potency toward FXIa with a *Ki* value of 0.36 nM and APTT $EC_{1.5X}$=1.5 μM (plasma kallikrein K_i=7.5 nM). The reversed diamide **32** was also identified to have FXIa K_i =1.6 nM and APTT $EC_{1.5X}$=1.0 μM (plasma kallikrein K_i=110 nM) [115].

The pharmacokinetics of inhibitors **26**, **30**, and **32** were evaluated following IV administration in dogs. Generally, all inhibitors exhibited short half-lives (≤1 hr). Inhibitors **26** and **30** exhibited moderate clearance (~15 mL/min/kg) and low volume of distribution (0.6 L/kg) whereas inhibitor **32** had a relatively higher clearance (32 mL/min/kg) and a larger volume of distribution (1.3 L/kg). Lastly, all three inhibitors demonstrated excellent selectivity (>1000-fold) over serine proteases including FVIIa, FIXa, thrombin, APC, plasmin, trypsin, urokinase, and tissue plasminogen activator. Inhibitors **26** and **32** were also selective against FXa (K_i>9000 nM), yet inhibitor **26** inhibited FXa with K_i of 5200 nM. However, molecules **26**, **30**, and **32** inhibited chymotrypsin with K_i values of 7649, 280, and 1650 nM, respectively, and inhibited plasma kallikrein with K_i values of 122, 59, and 111 nM, respectively. In addition, it was found that regular diamides such as inhibitors **26** and **30** have good human liver stability ($T_{0.5}$= >120 min) whereas reversed diamides such as inhibitor **32** have poor human liver stability ($T_{0.5}$= 2–32 min). Inhibitor **30** relatively demonstrated better balance of selectivity, potency, and pharmacokinetic profile and was subsequently evaluated in the rabbit electrically-induced carotid arterial thrombosis (ECAT)

model. This inhibitor dose-dependently reduced thrombosis with an EC_{50} value of 2.8 μM. Using a dosing protocol of 0.75 mg/kg (IV bolus) + 3.6 mg/kg/hr (IV infusion), inhibitor **30** prolonged *ex vivo* APTT by 1.8-fold and had no effect on the PT which was consistent with the selective inhibition of the intrinsic coagulation pathway [115].

Advanced FXIa inhibitors with 1-(4-chlorophenyl)-1H-tetrazole moiety as the P1 group will subsequently be discussed along with other FXIa inhibitors belonging to advanced subclasses of peptidomimetics.

Tetrahydroquinoline (THQ), quinolin-2-one, and tetrahydroisoquinoline (THIQ) derivatives: Molecule **33**, a 1,2-phenylene THQ derivative (Figure 11), was identified as a potent inhibitor of human FXIa in a chromogenic substrate hydrolysis assay [116]. It was found to have a FXIa K_i value of 25 nM and approximately 40-fold and 4-fold selectivity over FXa and FVIIa, respectively. Replacement of the isobutyl amide moiety with a carboxylic group led to inhibitor **34** which had a FXIa K_i value of 8.5 nM and 100-fold and 30-fold selectivity over FXa and FVIIa, respectively. Subsequent efforts to convert 1,2-phenylene THQ to 1,3-phenylene-4-methyl-THQ led to inhibitors with improved affinity toward FXIa, enhanced chemical stability, and no atropisomerism issue as given by inhibitor **35** which exhibited a FXIa K_i value of 3.9 nM (FVIIa K_i =89 nM and FXa K_i =130 nM). A problem with the 1,3-phenylene molecules, however, was the high likelihood of the THQ ring aromatization which decreased FXIa inhibition potency by ~65-fold. Therefore, a methyl group was introduced at position-4 of the THQ ring (inhibitor **36**) to block the aromatization; yet, the newly introduced methyl group reduced FXIa binding affinity by about 15-fold (Figure 11) [116].

To enhance the potency and selectivity profile of this class of inhibitors, extensive structure-activity relationship study was conducted. Several structural modifications were tested at the *para*-position of the biaryl moiety of the C_4-methyl substituted THQ leading to a racemic inhibitor **37** with a FXIa K_i value of 1.5 nM and about 187-fold and 2000-fold selectivity over FVIIa and FXa, respectively. The *trans*-isomer of inhibitor **37** was found to be 17-fold less potent FXIa inhibitor than its racemic mixture. Following the chiral HPLC-facilitated separation of the two cis-enantiomers, the dextrorotary cis-enantiomer **38** was found to be at least 800-fold more potent than the levorotary cis-enantiomer with a FXIa K_i of 0.39 nM and about 6000-fold and 220-fold selectivity over FXa and FVIIa, respectively.

To further improve the selectivity profile of inhibitor **38** over FVIIa, a series of amides substituted at position-3 of the inner phenyl moiety were prepared and evaluated. The rationale behind such structural exploration was that FXIa has a relatively larger S2 subsite than FVIIa, and therefore, this structural difference can be probed in the pursuit of better selectivity. Selectivity relative to FVIIa generally increased as the size of the alkyl moiety increased whereas the selectivity over FXa diminished. Inhibitor **39** exhibited the most potent and selective profile in this series. Following separation using chiral HPLC, the dextrorotatory enantiomer **39** was found to have a FXIa K_i value of 0.20 nM, whereas the levorotary enantiomer was significantly less potent with a FXIa K_i value of 230 nM. Inhibitor **39** has >1700-fold selectivity for FXIa over many human serine proteases except for plasma kallikrein (23-fold) and APC (365-fold). An X-ray co-crystal structure of the

inhibitor **39** –FXIa catalytic domain complex was obtained (PDB ID: 4NA7) (Figure 11B). In the reported complex, the benzamidine group was found to tightly bind to the backbone carbonyl of Gly218 residue via an H-bond and Asp189 residue in the S1 pocket by an ionic bridge. Furthermore, the side chain hydroxyl group of Ser195 formed an H-bond with the N^1-H of the THQ ring. A potential stacking contact was noticed between the inner phenyl ring of inhibitor **39** and the His57 residue. The carboxylic group at the *ortho*-position of the outer phenyl ring forms H-bonds with His57 as well as the Gly193 and Ser195 residues of the oxyanion hole. The amide nitrogen at the *para*-position of the outer phenyl ring formed two H-bonds with the carbonyls of the His40 and Leu41 residues. The amide carbonyl was also found to interact with the Arg39 residue either directly or indirectly by a water molecule. The carbonyl of the isobutylamide in inhibitor **39** formed an H-bond with the hydroxyl group of Tyr58b in the S2 pocket, a unique characteristic to this inhibitor that is responsible for its enhanced selectivity profile [116].

Inhibitor **39** exhibited excellent *in vitro* anticoagulant activity in the APTT assay with the concentration required to double the clotting time reported to be 2.2 μM. Nevertheless, inhibitor **39** did not change the clotting time in the PT assay at the highest concentration tested of 20 μM. Inhibitor **39** was found to be a reversible competitive inhibitor of human FXIa using the small chromogenic tripeptide substrate and a mixed-type inhibitor using its physiological substrate FIX. Since similar selectivity and potency were observed for inhibitor **39** with rabbit and human enzymes, the inhibitor was studied in the rabbit AV shunt thrombosis model using the IV route of administration (loading dose [IV bolus] followed by maintenance dose [IV infusion]). A dose-dependent antithrombotic effect was observed for inhibitor **39** with an ID_{50} value of 0.95 mg/kg + 0.6 mg/kg/hr. Bleeding time was not increased compared to vehicle-treated animals and the clotting time in *ex vivo* settings was only prolonged under the APTT assay conditions but not under the PT assay conditions [116].

In a follow-up study, the *in vivo* activities of inhibitor **39** were evaluated in an ECAT model in rabbits and a cuticle bleeding assay [117]. In these models, inhibitor **39** or vehicle was intravenously administered before the induction of thrombosis or the cuticle transection. Preservation of 90 min-integrated carotid blood flow (iCBF) was utilized as an indication of antithrombotic efficacy. Inhibitor **39** produced 87 ± 10 % preservation of iCBF compared to 16 ± 3 % for the vehicle using the dose regimen of 0.37 mg/kg (IV bolus) + 0.27 mg/kg/hr (IV infusion). At the same dosing level, inhibitor **39** increased the cuticle bleeding time by about 1.2-fold. At a higher dose (1.1 mg/kg + 0.8 mg/kg/hr), the inhibitor increased the bleeding time by about 1.33-fold. The authors claimed that these results compared well with results previously obtained using equivalent anticoagulant doses of dabigatran and warfarin, two reference anticoagulants that are currently used in clinics. Lastly, results of *in vitro* platelet aggregation experiments suggest that inhibitor **39** has no direct antiplatelet activity with respect to collagen-, arachidonic acid-, or ADP-mediated platelet aggregation [117].

Fjellström *et al.* (2015) exploited a structure assisted, fragment-based exercise to obtain novel FXIa inhibitor leads [118]. In this exercise, fragments binding in the S1 pocket of the FXIa active site including the neutral 6-chloro-3,4-dihydro-1H-quinolin-2-one **40** (IC_{50} = 140 μM) and the weakly basic quinolin-2-amine **41** (IC_{50} = 240 μM) (Figure 12) were

identified by a dual-filter strategy of virtual screening followed by NMR screening. Aided by X-ray crystallography, these fragments were subsequently chemically extended to populate the binding pockets in the prime side of the FXIa active site resulting in several potent and moderately selective inhibitors of FXIa. Particularly, inhibitor **42** (Figure 12) inhibited FXIa with an IC_{50} value of 1.0 nM, yet it also inhibited plasma kallikrein with an IC_{50} value of 27 nM. This molecule did not significantly inhibit thrombin, FXa, FIXa, plasmin, tissue plasminogen activator, or trypsin at the highest concentration tested of 99 μM. Inhibitor **42** has a high polar surface area (153 $Å^2$), low permeability (<0.28 $\times 10^{-6}$ cm/s), high efflux (Efflux ratio >4.6), low/moderate *in vitro* intrinsic clearance (22 μL/min/1×10^6 cells) in rat hepatocytes, and high rat *in vivo* clearance (130 mL/min/kg). Further structural optimizations led to inhibitor **43** (Figure 12) with enhanced physicochemical properties. This molecule inhibited FXIa with an IC_{50} value of 0.82 μM and plasma kallikrein with an IC_{50} value of 8.4 μM. Nevertheless, the physicochemical properties of inhibitor **43** [moderate polar surface area (79 $Å^2$), high permeability (19×10^{-6} cm/s), low efflux (Efflux ratio 1.6), moderate rat *in vivo* clearance (18 mL/min/kg), and a measured rat oral bioavailability of 27%] have provided a promising avenue towards the goal of developing an oral FXIa inhibitor [118].

Very recently, Pinto *et al.* (2017) reported a new series of active site inhibitors of human FXIa in which the central phenylalanine domain of inhibitor **26** was replaced with either substituted pyrrolidine (inhibitor **44**), tetrahydroisoquinoline (THIQ)-3-carboxylate (inhibitor **45**), or THIQ-1-carboxylate (inhibitor **46**) (Figure 13) [119]. Inhibitor **44** showed a modest potency with a FXIa K_i value of 23 nM and APTT $EC_{1.5x}$ value of 36 μM. The two homochiral THIQ derivatives exhibited weaker potency (inhibitor **45**) or better potency (inhibitor **46**) with FXIa K_i values of 1.7 μM and 11 nM, respectively [119]. Attempts aimed at enhancing the potency of inhibitor **46** by replacing the THIQ-1-carboxylate moiety, which points to S1′ subsite in the active site of FXIa, with a host of bicyclic heteroaromatic systems failed. Likewise, attempts to enhance the potency of inhibitor **46** by replacing the *p*-aminobenzoic acid domain, which binds into the S2′ subsite, with a host of mono- and bi-cyclic hetroaromatic amines also failed. However, introducing a fluorine substituent to the *p*-chlorophenyl-tetrazole moiety, which binds into the S1 subsite, resulted in inhibitor **47** with a FXIa K_i value of 3.7 nM. Moreover, introducing a dimethylamino group at position-5 of the THIQ-1-carboxylate domain (inhibitor **48**) deemed rewarding for the inhibition potency (K_I=6 nM) but not for the effect on the clotting time in the APTT assay (APTT $EC_{1.5x}$ >40 μM). Considering the solubility at pH 6.5, the dimethylamino group in inhibitor **48** was replaced with several basic and nonbasic saturated cyclic polar systems which eventually resulted in the discovery of inhibitor **49** with an N^4-methyl-piperazine-2-one at position-5 of the THIQ-1-carboxylate moiety. This inhibitor exhibited a potent FXIa inhibition potency with a K_i value of 0.7 nM, a potent effect on the clotting time with an APTT $EC_{1.5x}$ value of 0.3 μM, and a good aqueous solubility of 0.88 mg/mL for parenteral administration [120]. A model of inhibitor **49** in the active site of FXIa showed that the N^4-methyl-piperazine-2-one P2 moiety establishes a significant contact with Tyr58B and Tyr94 residues in the S2 subsite whereas the *p*-aminobenzoic acid P2′ group and the chloro-fluoro-phenyl-tetrazole P1 group make significant interactions in the S2′ and S1 subsites, respectively, as previously described for similar inhibitors.

The pharmacokinetic studies of inhibitor **49** in rats indicated that it has a volume of distribution of 0.75 L/kg, a relatively rapid clearance rate of 16 ml/min/kg, and a short half-life of 0.88 hr. This half-life was almost consistent in other animal species including rabbit, dog, and cynomolgus monkeys. Given that the goal of this development program at Bristol-Myers Squibb Company was to discover an effective and safe anticoagulant for acute use in hospital settings, inhibitor **49** appeared to meet the initial selection critera, and therefore, it was subject to further studies. Inhibitor **49** demonstrated a significant selectivity profile over related human enzymes including FVIIa (>13 μM), FIXa (>27 μM), FXa (>9 μM), FXIIa (>3 μM), tissue kallikrein-1 (>10 μM), thrombin (>13 μM), trypsin (>6.2 μM), plasmin (>25 μM), APC (>21 μM), tissue plasminogen activator (>6.2 μM), and urokinase (>15 μM). This molecule inhibited human plasma kallikrein and chymotrypsin with K_i values of 0.31 and 11 μM, respectively. Furthermore, inhibitor **49** demonstrated no cytochrome inhibition activity (IC_{50} values > 40 μM), was stable in dog, rat, and human liver microsomes ($T_{0.5}$ =120, 59, and 108 min, respectively), and was Ames test negative, which suggested acceptable pharmaceutical properties considering the primary goal of the program [119].

To determine the antithrombotic efficacy of this molecule in animal models, the rabbit AV-shunt thrombosis model was used [120, 121]. Using a dose protocol of 0.23 mg/kg (IV bolus) + 1.55 mg/kg/hr (IV infusion), inhibitor **49** exhibited about 83 % inhibition of thrombus formation and increased the APTT up to 1.8-fold with no effect on the PT. Furthermore, a dose protocol of 0.46 mg/kg (IV bolus) + 3.1 mg/kg/hr (IV infusion) did not increase the bleeding time as compared to vehicle in the rabbit cuticle bleeding assay. Interestingly, the combination of inhibitor **49** (0.46 mg/kg + 3.1 mg/kg/hr) and aspirin (4 mg/kg/hr) resulted in bleeding times that were not higher than those noted for aspirin treatment alone [120, 121]. Overall, inhibitor **49** has been put forward as a potent, selective, reversible, direct, and active site inhibitor of FXIa and a clinical candidate for use as an acute antithrombotic agent in a hospital setting.

Imidazole-containing derivatives: Another chemotype that was recently introduced as FXIa orthosteric peptidomimetic inhibitors was the phenylimidazole class [122]. About 27 potential inhibitors were synthesized and tested for their inhibitory effect on a series of serine proteases including human FXIa. The first example in this series was inhibitor **50** (Figure 14) which was discovered by focused-deck screening. This unmodified phenylimidazole inhibited human FXIa and plasma kallikrein with K_i values of 120 and 330 nM, respectively. Furthermore, the inhibitor was selective against FVIIa (K_i > 10900 nM) and FXa (K_i > 8180 nM). This inhibitor also modestly increased clotting time in the APTT assay by 1.4-fold at a plasma concentration of 40 μM. Interestingly, inverting the stereochemistry of inhibitor **50** resulted in a 30-fold decrease in the inhibitory activity towards FXIa suggesting a stereospecific preferential recognition. Introducing various ester, amide, or sulfonamide substituents at the *meta*- or *para*-positions of the terminal phenyl moiety of inhibitor **50** always reduced its FXIa inhibition potency with one exception being inhibitor **51** (Figure 14) which has an unsubstituted amide functionality at the *para*-position. Inhibitor **51** was 4-fold more potent against FXIa with a K_i value of 30 nM and retained good selectivity against FVIIa (K_i>10900 nM) and FXa (K_i>9000 nM). However, it

inhibited human plasma kallikrein with a K_i value of 60 nM. The inhibitor also increased the APTT by 1.8-fold at a plasma concentration of 40 μM.

The X-ray crystal structure of inhibitor **51** bound to FXIa was obtained at 1.85 Å resolution and revealed several direct hydrophobic contacts as well as direct and indirect (water-mediated) H-bonds between the inhibitor and FXIa (PDB ID: 4TY6) (Figure 14B). The nitrogen of the unsubstituted amide at the *para*-position of the phenylimidazole moiety formed direct and water-mediated H-bonds to the backbone carbonyl and nitrogen of His40 of the S2′ pocket. The carbonyl of the unsubstituted amide also formed several water-mediated H-bonds with the backbone nitrogen of Ile151 and to the hydroxyl group of Tyr143. The phenyl ring formed a hydrophobic interaction with the side chain of Gly193 and Ile151 within the S2′ pocket. The N^1 atom of the imidazole ring formed several water-mediated H-bonds with the backbone nitrogens of the Gly218 and Gly216 residues. The N^3 atom of the imidazole ring also participated in a water-mediated H-bond with the backbone carbonyl of Leu41. The C-5 methine of the imidazole had a hydrophobic contact with the side chain of Lys192. The phenyl ring of the benzyl moiety had an edge-on hydrophobic interaction with Cys42 – Cys58 disulfide bridge in the S1′ pocket. The nitrogen of the amide linker (P1 group) formed water-mediated H-interactions with the Ser214 and Gly216 residues. The oxygen of the amide linker was over the oxyanion hole (Gly193, Asp194, and Ser195). The tranexamic acid group was found to fit into the S1 pocket forming a salt bridge between its primary amine group and the backbone carbonyl of Gly218 as well as the carboxylate of Asp189 residue [122].

Motivated by insights from the crystal structure, the terminal 3-aminoindazole moiety was introduced as in molecule **52** (Figure 14) which inhibited FXIa with a K_i value of 3 nM. It also inhibited plasma kallikrein with a K_i value of 50 nM and doubled the clotting time in the APTT assay at a plasma concentration of 2 μM. The inhibitor remained selective over FVIIa (K_i>10900 nM) and FXa (K_i>8180 nM). Introducing a chlorine atom at the C-5 methine position of the imidazole led to inhibitor **53** with further enhanced profile. Specifically, the inhibitor demonstrated sub-nanomolar potency against FXIa (K_i = 0.3 nM), potent *in vitro* APTT activity (EC_{2x} = 1 μM), 17-fold selectivity over plasma kallikrein, and >1000-fold selectivity over related serine proteases including thrombin, FXa, and FVIIa. The X-ray crystal data (2.09 Å resolution; PDB ID: 4TY7) demonstrated that the binding modes of inhibitors **51** and **53** are practically identical. The exocyclic nitrogen of the aminoindazole moiety was found to form several direct and indirect (water-mediated) H-bonds with the backbone carbonyl and nitrogen of the His40 residue. The N^1 and N^2 atoms of the indazole ring formed a direct H-bond with the hydroxyl group of Tyr143 and an indirect one with the backbone nitrogen of Ile151. The C-5 chlorine substituent formed a hydrophobic contact with the aliphatic side chain of Lys192. Other heterocycle replacements of the 4-phenylimidazole including 5-phenyl-oxazole, 3-phenyltriazole, 3-phenylpyrazole, 5-oxo-1-phenyltriazole, and 2-phenylimidazole were all tested and found to be less potent inhibitors of human FXIa [122].

Inhibitor **53** was found to be a reversible FXIa inhibitor with similar enzyme inhibition profiles for rabbit coagulation factors. The inhibitor is not orally bioavailable, and therefore, its pharmacokinetic parameters were measured in rabbits following the IV administration of

its bis-HCl salt at a dose level of 0.5 mg/kg. The inhibitor was found to have an 85% protein binding in rabbit serum, a small volume of distribution (0.7 L/kg), and a relatively rapid clearance rate (1.2 L/kg/hr). In the rabbit AV-shunt model, the inhibitor exhibited potent dose-dependent *in vivo* antithrombotic effect compared to vehicle controls with a calculated ID_{50} value of 0.6 mg/kg (loading IV bolus) + 1 mg/kg/hr (maintenance IV infusion) [122].

In subsequent studies, Pinto *et al.* (2015) reported on a series of structure-based efforts to enhance the antithrombotic profile of **53** [123]. All efforts were focused on improving the selectivity as well as oral bioavailability by using different less basic functionalities that bind to the S1 pocket. Accordingly, it was found that inhibitor **54** (Figure 14) had a K_i value of 1.2 nM toward human FXIa. This inhibitor doubled the clotting time in the APTT assay at a plasma concentration of 3 μM. In dogs, it had a volume of distribution of 0.8 L/kg, a clearance value of 16 mL/min/kg, and a $T_{0.5}$ of 2.2 hrs. However, it had no oral bioavailability in dogs. Replacing the aminoindazole moiety with a *para*-methylcarbamoyl-phenyl moiety led to inhibitor **56** (Figure 14) which had a FXIa K_i value of 2.7 nM, a volume of distribution of 1.6 L/kg, a clearance value of 9 mL/min/kg, a $T_{0.5}$ of 3.1 hrs, and an oral bioavailability of ~3% in dogs. This inhibitor increased the clotting time in the APTT assay by 1.5-fold at a plasma concentration of 5.3 μM. Interestingly, removing the chlorine atom from the imidazole moiety led to inhibitor **55** which had a FXIa K_i value of 6.7 nM, a volume of distribution of 3.4 L/kg, a clearance value of 20 mL/min/kg, a $T_{0.5}$ of 2.4 hrs, and an oral bioavailability of ~10.4% in dogs. This inhibitor increased the clotting time in the APTT assay by 1.5-fold at a plasma concentration of 8.6 μM. This inhibitor also demonstrated good selectivity over FVIIa (K_i>13000 nM), FIXa (K_i>60000 nM), FXa (K_i =1500 nM), thrombin (K_i >15000 nM), trypsin (K_i >6200 nM), plasma kallikrein (K_i =240 nM), tissue kallikrein (K_i >30000 nM), chymotrypsin (K_i =1300 nM), plasmin (K_i >41000 nM), and tissue plasminogen activator (K_i =17000 nM) [123].

Along those lines, Hu *et al.* (2015) reported the continued structural optimization efforts at the P1′ and P2′ regions of inhibitors **55** and **56** to further improve the potency, stability, and solubility of this chemotype [124]. These efforts eventually resulted in the discovery of a potent and efficacious parenteral FXIa inhibitor **57** (Figure 14) which inhibited FXIa with a K_i value of 0.04 nM, prolonged the clotting time with an APTT EC_{2x} of 1.0 μM, and had an aqueous solubility of 17 μg/mL in pH 6.5 buffer. In human liver microsome, this inhibitor had a half-life measured at >200 min. An X-ray crystal structure of inhibitor **57** bound in the active site of FXIa was obtained at 2.2 Å resolution. The X-ray structure (PDB ID: 4Y8Z) showed that the chlorophenyltetrazole moiety occupied the S1 pocket. The carbonyl group of the acrylamide moiety formed H-bond interactions with the oxyanion hole, and the N^3 atom of the imidazole ring formed water-mediated H-bonds with Ser195 hydroxyl group and Leu41 carbonyl group. The *N*-methyl piperazine bound near His57 and Tyr58B residues in the S2 pocket. In the S2′ region, the NH, carbonyl, and OH groups of quinolinone formed several H-bonds with His40 and Tyr143 residues.

Inhibitor **57** was highly selective for FXIa over other related serine proteases including FVIIa (>13.3 μM), FIXa (>60 μM), FXa (>9 μM), FXIIa (>20 μM), tissue kallikrein (>30 μM), urokinase (>1.6 μM), and APC (>5.4 μM) but not plasma kallikrein, trypsin, chymotrypsin, thrombin, and tissue plasminogen activator which were inhibited by this

molecule with K_i values of 0.007, 6.2, 0.4, 7.4, 29 μM, respectively. Inhibitor **57** demonstrated similar profiles in humans and rabbits (the species used for animal modeling) with respect to FXIa affinity (K_i values of 0.1 vs 0.58 nM, respectively) and effect on APTT ($EC_{1.5x}$ values of 0.28 vs 1 μM, respectively). In the pharmacokinetic studies, the inhibitor demonstrated high free fractions (2.6–18%) in the plasma protein binding studies across the different species used. The half-life was about 1–2 hrs across all tested species following IV administration. Inhibitor **57** was evaluated in the ECAT model in rabbits. The inhibitor produced a dose-dependent increase in integrated blood flow of the injured artery i.e. decrease in thrombus reduction at the injury site with an EC_{50} of 0.53 μM. In the rabbit cuticle bleeding time model, minimal bleeding time prolongation was observed for the inhibitor even at the highest dose studied (10 μM). At this largest dose, the inhibitor prolonged the APTT by 3.2-fold, but did not affect the PT or TT [124].

To improve the FXIa binding affinity and the APTT potency of inhibitor **56**, Corte *et al.* (2017) preorganized the inhibitor's conformation via the formation of a macrocyclic ring [125]. Macrocyclization has been recognized in drug discovery and development as an important chemical strategy to improve the chemical stability, binding affinity, selectivity, and pharmacokinetic properties of acyclic peptides or peptidomimetics [126–129]. The X-ray crystal structure of inhibitor **56** bound to FXIa showed the inhibitor occupying the S1 pocket (P1: *para*-chlorophenyl tetrazole moiety), S1′ pocket (P1′: benzyl moiety), and the S2′ pocket (P2′: methyl *N*-phenyl carbamate). Therefore, a macrocyclization strategy was devised to link the P1′ benzyl and the P2′ phenyl groups due to their close proximity. Molecular modeling was employed to help guide the initial choice of ring size i.e. linker length by running a conformational analysis of 11–14-membered macrocyclic rings. Interestingly, the 12- and 13-membered macrocyclic rings appeared to present conformations that were similar to the acyclic conformations, with no ring strain or redundant methylene units, and therefore, they were considered for synthesis.

Initially, eleven macrocyclic analogues of 12 and 13-membered rings were synthesized with saturated or *E*-unsaturated linkers. Some of those analogs had an ether bond. In the FXIa inhibition/binding assay, all analogs inhibited the enzyme with K_i values within the range of 42–3920 nM. Among them, only two inhibitors had potent impact on clotting time in the APTT assay, namely inhibitors **58** and **59** (Figure 15), which increased the APTT by 1.5-fold at plasma concentrations of 27 μM (FXIa K_i=42 nM) and 34 μM (FXIa K_i=68 nM), respectively [125].

Inspired by the crystal structure of inhibitor **59** with FXIa (PDB ID: 5TKS), it was predicted that an amide linker may afford additional H-bond interaction with the carbonyl of Leu41. Subsequently, ten more macrocyclic molecules having an amide linker and ring size of 12 or 13 were synthesized and evaluated for their FXIa inhibition potency, APTT effect, and human liver microsomal stability. The two most potent FXIa inhibitors were **60** and **61** (Figure 15). In one hand, inhibitor **60** had a K_i value of 0.16 nM, increased the APTT by 1.5-fold at a plasma concentration of 0.27 μM, and had human liver microsomal $T_{0.5}$ of 41 min. The inhibitor also had very good selectivity over a wide range of serine proteases including trypsin and chymotrypsin (K_i~1500 nM), plasmin (K_i>14200 nM), tissue plasminogen activator (K_i>6150 nM), urokinase (K_i=5050 nM), APC (K_i>21500 nM),

thrombin (K_i>11500 nM), FVIIa (K_i=1650 nM), FIXa (K_i>27100 nM), FXa (K_i>13300 nM), and FXIIa (K_i>3050 nM). In the other hand, inhibitor **61** had a K_i value of 1.0 nM, increased the APTT by 1.5-fold at a plasma concentration of 0.30 μM, and had human liver microsomal $T_{0.5}$ of 90 min. The inhibitor also had very good selectivity over a wide range of serine proteases including trypsin and chymotrypsin (K_i~3940–8390), plasmin (K_i>15200 nM), tissue plasminogen activator (K_i>6150 nM), urokinase (K_i>15100 nM), APC (K_i>21500 nM), thrombin (K_i>11500 nM), FVIIa (K_i=3190 nM), FIXa (K_i>27100 nM), FXa (K_i>13300 nM), and FXIIa (K_i>3050 nM). However, both inhibitors inhibited plasma kallikrein with K_i values of 16 and 70 nM, respectively. It is important to mention here that the crystal structure of inhibitor **60** with FXIa (PDB ID: 5TKU) confirmed the H-bond interaction between the installed amide linker and the carbonyl of Leu41 [125].

The pharmacokinetic profiles for inhibitors **60** and **61** were evaluated in dogs. The two inhibitors had high clearance values of 23 and 15 mL/hr/kg, respectively, short half-lives of ~1 hr, small volumes of distribution of 1.8 and 0.8 L/kg, respectively, low AUC values of 2.5 and 21 nM.hr, respectively, high dog liver microsomal stability ($T_{1/2}$>120 min), and high dog protein binding of ~90%. They both had very poor oral bioavailability of 1% and 6%, respectively, at tested doses [125]. Therefore, these two inhibitors were subject to further structural modifications which focused on the imidazole ring, the macrocyclic amide linker, and the P1 tetrazole-containing group [130]. Corte *et al* (2017) reported that 1) introducing a chlorine substituent to the imidazole ring enhanced the FXIa inhibition potency; 2) introducing small alkyl groups to the linker improved the inhibition potency considering the ring size, position of the introduced alkyl group, and its absolute stereochemistry; and 3) replacing the chlorophenyltetrazole cinnamide P1 group with *o,o*-difluoro-*p*-methylbenzoyl group decreased the polar surface area and increased the oral bioavailability of these inhibitors, yet at the expense of the inhibition potency. An example from this study is molecule **62** (Figure 15) which inhibited FXIa with an IC_{50} value of 0.07 nM and effectively prolonged the clotting time in APTT assay with an $EC_{1.5x}$ of 1.2 μM [130].

Recently, Wang *et al.* (2017) reported a macrocyclic molecule **63** (Figure 15) as a human FXIa inhibitor with a K_i value of 0.3 nM [131]. Molecule **63** also inhibited rabbit FXIa and rabbit plasma kallikrein with K_i values of 0.9 nM and 6 nM, respectively. The molecule showed >16000-fold selectivity over rabbit enzymes of FIIa, FIXa, FXa, and FXIIa. In rabbits, inhibitor **63** dose-dependently inhibited thrombus formation in the carotid artery and cerebral microembolic signals incidence in the middle cerebral artery induced by 30% $FeCl_3$. The integrated blood flow also increased from ~57% in the vehicle group to ~91% for the 3 mg/kg/hr inhibitor group, with an ED_{50} value of 0.003 mg/kg/hr. Clot weight also decreased from ~8.9 mg to ~0.0 with an ED_{50} value of 0.004 mg/kg/hr. Furthermore, inhibitor **63** significantly elevated the APTT, with an increase of 86.6% (at an IV infusion rate of 0.3 mg/kg/hr) and 220.3% (at an IV infusion rate of 3 mg/kg/hr) at 1 hour after treatment. The APTT increased by about 78.7% (at an IV infusion rate of 0.3 mg/kg/hr) and 290.4% (at an IV infusion rate of 3 mg/kg/hr) at 2 hours after treatment. Consistent with targeting FXIa in the intrinsic coagulation pathway, the inhibitor had no effect on the PT. Lastly, using 5 mg/kg/hr dosing level (>1250-fold of antithrombotic ED_{50}; IV infusion), inhibitor **63** led to statistically insignificant increase in bleeding time (~102% compared with

vehicle group) in a rabbit cuticle bleeding model. For comparison, at 3 mg/kg/hr dosing level (>75-fold of antithrombotic ED_{50}; IV infusion), apixaban (approved FXa inhibitor) led to a statistically significant increase in bleeding time (~291% compared with the vehicle group) in the same bleeding test in rabbits [131].

Pyridine, pyridinone, and pyrimidine-containing derivatives: In 2015, Corte *et al.* reported on the medicinal chemistry efforts to optimize the profile of inhibitor **53** (Figures 14 and 16) [130]. Initially, the imidazole ring was replaced by a series of six-membered heteroaromatic rings including pyridine, pyridine-*N*-oxide, pyrimidine, and benzene resulting in ten different FXIa inhibitors with K_i values in the range of 330–30207 nM. From this series of inhibitors, inhibitor **64** with the pyridine moiety was chosen for subsequent studies. Previously, it was shown that introducing a chlorine atom at position-5 of the imidazole ring increased the FXIa inhibition potency by 10-fold (as in inhibitors **52** and **53** (Figure 14)). Likewise, introducing a chlorine atom at position-6 in the pyridine ring improved the FXIa inhibition potency of inhibitor **64** from K_i value of 377 nM to 206 nM for inhibitor **65** (Figure 16). Hydroxyl group at the same position afforded much better results with a K_i value of 113 nM, amino group presented no effect (K_i = 227 nM), whereas methylamino, methoxy, and *N*-methyl pyridinone all decreased the FXIa inhibition potency of inhibitor **64** to 860, 949, and 479 nM, respectively.

Along those lines, the imidazole ring in inhibitor **52** (Figure 14) (K_i = 3.2 nM and APTT EC_{2X}=1–3 μM) was replaced by different stereoisomers and regioisomers of benzene and pyridine resulting in six different FXIa inhibitors with K_i values in the range of 8.4–6160 nM (APTT $EC_{1.5X}$ ≥4.5 μM). The most potent inhibitor in this series was **66** (Figure 16) which possessed a FXIa K_i value of 8.4 nM and APTT $EC_{1.5X}$=4.5 μM. In addition, the racemic mixture of inhibitor **67** (Figure 16), which has a pyridinone moiety, possessed a FXIa K_i value of 3.7 nM and APTT $EC_{1.5X}$=2.5 μM. Although inhibitor **66** was selective over FVIIa (K_i>10890 nM), FIXa (K_i>34860 nM), FXa (K_i>9000 nM), thrombin (K_i>12610 nM), APC (K_i>21400 nM), plasmin (K_i>22100 nM), tissue plasminogen activator (K_i>21900 nM), urokinase (K_i>14060 nM), and chymotrypsin (K_i>20780 nM), the molecule inhibited both trypsin (K_i=64 nM) and plasma kallikrein (K_i=24 nM) [132]. An X-ray crystal structure of the *(S)*-enantiomer of inhibitor **66** bound to the human FXIa active site (PDB ID: 4WXI, 2.6 Å resolution) was obtained. The overall binding mode is similar to what was described previously for the imidazole **53** (Figure 16).

The same research group reported further optimization of inhibitor **53** [133]. The aminoindazole group of S2′ pocket was replaced with an unsubstituted indazole, 3-hydroxyindazole, 3-aminobenzisoxazole, 4-amino-quinazoline, and 1-aminoisoquinoline. The racemic mixtures of these analogues as well as their enantiomerically pure (*S*)-stereoisomers were evaluated for their inhibitory effects on the activity of human FXIa as well as on the clotting time in the APTT assay. The most potent analog in this series was (*S*)-inhibitor **68** (Figure 16), 3-amino-benzoisoxazole analogue with a K_i value of 3.8 nM and APTT $EC_{1.5X}$ of 0.6 μM. This suggested that an H-bond acceptor is better for the interaction with Tyr143 residue in S2′ pocket. Other regioisomers of 3-aminoindazol-6-yl were also studied. For example, 3-aminoindazol-5-yl, indazol-5-yl, 3-hydroxyindazol-5-yl,

and 3-methoxyindazol-5-yl were synthesized and tested for their inhibitory effects toward human FXIa as well as their effects on the APTT. The most potent analogue in this series was (*S*)-inhibitor **69** (Figure 16) which has a K_i value of 3.7 nM and APTT $EC_{1.5X}$ of 0.4 μM. Furthermore, several monocyclic groups that bind to S2′ were also studied. These groups included 1-aminobenzoic acid-4-yl, benzoic acid-3-yl, aniline-4-yl, 2-aminopyridine-5-yl, and methylcarbamate-4-yl. The most potent analogue in this series was (*S*)-inhibitor **70** (Figure 16) which has a K_i value of 6.3 nM and APTT $EC_{1.5X}$ of 2.6 μM. Replacement of the pyridine group in this inhibitor with pyridinone led to inhibitor **71** (Figure 16) which has a K_i value of 2.4 nM and APTT $EC_{1.5X}$ of 0.4 μM [133].

Another set of molecules studied in the same report was that in which the basic cyclohexyl methyl amine P1 was replaced with a neutral *para*-chlorophenyltetrazole P1 in the regioisomeric pyridine, pyrimidine, and pyridinone analogs. The regioisomeric pyridine **73**, pyrimidine **74**, and pyridinone **75** (Figure 17) possessed improved FXIa binding activity and potency in the clotting assay compared to pyridine **72** (Figure 17). Nevertheless, these inhibitors were relatively less potent in the clotting assay than the corresponding derivatives with the basic cyclohexyl methyl amine as the P1 moiety. The loss of potency can be because of the increase in nonspecific binding to various plasma proteins. An X-ray structure of (S)-inhibitor **72** bound to FXIa (PDB ID: 5EXN; 1.49 Å resolution) was obtained and the overall binding mode was found to be similar to that described above, with the exception of the P1 domain. The chlorophenyl portion fits into the S1 pocket with the chlorine substituent forming a π–Cl interaction with Tyr228 residue. The tetrazole moiety interacts with the Cys191-Cys219 disulfide bridge. Moreover, the tetrazole N^4 nitrogen forms a water-mediated H-bond with the Gly218 residue [133].

Several compounds were evaluated in dogs in order to determine their pharmacokinetic profiles. Particularly, inhibitor **66** was found to have a volume of distribution of 3.4 L/kg, a clearance value of 50 mL/hr/kg, a half-life of 1.2 hrs, and no oral bioavailability. Inhibitor **70** demonstrated a volume of distribution of 10 L/kg, a clearance value of 54 mL/hr/kg, a half-life of 2.7 hrs, and 63% oral bioavailability. Inhibitor **71** was found to have a volume of distribution of 0.8 L/kg, a clearance value of 17 mL/hr/kg, a half-life of 1.1 hrs, and <1% oral bioavailability. Inhibitor **75** was found to have a volume of distribution of 1.6 L/kg, a clearance value of 30 mL/hr/kg, a half-life of 1.5 hrs, and no oral bioavailability. Interestingly, four other inhibitors demonstrated good oral bioavailability of 28–66%, even though they demonstrated relatively weaker FXIa K_i of 6.7 – 23 nM and APTT $EC_{1.5X}$ of 1.2 – >40 μM. Lastly, as with the previously published FXIa inhibitors, select inhibitors from this series were tested against other serine proteases including FVIIa, FIXa, FXa, thrombin, APC, plasmin, chymotrypsin, urokinase, and tissue plasminogen activator and were found to be significantly selective. Yet, they were found to moderately inhibit trypsin (selectivity index of 9 – 270-fold) and plasma kallikrein (selectivity index of 3 – 150-fold) [133].

Miscellaneous scaffolds: Few other peptidomimetic molecules were identified to inhibit human FXIa during the course of developing orthosteric inhibitors for other serine proteases in the coagulation process. Nar *et al.* (2001) reported three promiscuous benzimidazole

benzamidine derivatives **76** – **78** (Figure 18) that inhibited FXIa with K_i values of 9.0, 4.1, and 6.2 μM, respectively [134]. However, these molecules also inhibited thrombin (K_i = 20 – 780 nM), FXa (K_i = 15 – 57 nM), trypsin (K_i = 67 – 110 nM), two-chain urokinase (K_i = 6.5 – 44 μM), plasmin (K_i = 6.8 – 13 μM), FVIIa/TF (K_i >40 μM), and tissue type plasminogen activator (K_i = 6.8 – 13 μM).

Another chemotype that was originally developed to inhibit thrombin but was also found to inhibit FXIa is indolizidinones [135]. Particularly, indolizidinone **79** (Figure 18) was found to inhibit FXIa with a K_i value of 35 μM, yet it also inhibited thrombin, FVIIa, and plasmin with K_i values of 0.11, 0.52, and 71 μM, respectively. Furthermore, three enantiopure cyclicdiamines **80** – **82** (Figure 18) were found to inhibit FXIa with K_i values in the range of 6.7 – 10.2 μM [136]. These inhibitors were found to be slightly selective over FVIIa (>11 μM), chymotrypsin (>20 μM), plasma kallikrein (>6 μM), trypsin (>5 μM), APC (>21 μM), plasmin (>22 μM), tissue type plasminogen activator (>21 μM), and urokinase (>14 μM), yet they potently inhibited FXa (0.58, 0.5, and 0.64 nM, respectively) as well as thrombin (5.4, 4.0, and 4.0 μM, respectively). Some arylsulfonamidopiperidone derivatives with FXa inhibitory activity were also reported to inhibit FXIa [137]. For example, molecule **83** (Figure 18) inhibited FXIa with a K_i value of 13.3 μM. However, this inhibitor was found to be a potent promiscuous inhibitor for a wide range of serine proteases. In addition, a wide range of benzamidines **84** – **92** (Figure 19) was reported to have high nanomolar to micromolar inhibition potency toward FXIa. [138, 139]. Nevertheless, they were also potent inhibitors of FVIIa **84** – **89** and APC **90**– **92**. A series of biaryl acid derivatives **93** – **97** (Figure 20) was also reported to inhibit FXIa, in addition to other coagulation proteases, particularly FVIIa [140]. A substituted chromen-7-yl furan-2-carboxylate derivative was recently reported as an active site inhibitor of human FXIa [141]. This small molecule inhibited human FXIa with an IC_{50} of 0.77 μM and exhibited a substantial selectivity for FXIa inhibition over related serine proteases of digestive, coagulation, and fibrinolysis systems. The molecule also selectively doubled the APTT at a concentration of 72 μM in human plasma.

CU-2010 (renamed MDCO2010; **98**) (Figure 21) is a peptidomimetic inhibitor with a benzamidino moiety at the *C*-terminus mimicking the P1 domain [142]. CU-2010 inhibited several serine proteases including FXIa (K_I=18–26 nM), plasma kallikrein (K_I=0.019–0.04 nM), plasmin (K_I=2.2 nM), FXa (K_I=45–51 nM), FXIIa (K_I=892–5200 nM), and FIIa (K_I=1553–1700 nM). CU-2010 had a substantial effect on APTT (APTT EC_{2X}=1.4 μM) and a weaker effect on PT (PT EC_{2X}=9.1 μM). Clot lysis in human whole blood was inhibited by molecule **98** at 150 nM. CU-2010 half-life was 20 min in rats and dogs upon IV administration, which was increased to 45 min by pegylation (CU-2020). However, pegylation exerted variable effect on the inhibition potencies of FXIa (31-fold loss), plasma and plasma kallikrein (4-fold loss), FXIIa (4.5-fold gain), while retaining factors Xa and IIa inhibition potencies. CU-2020 had a significant effect on APTT (APTT EC_{2X}=32.8 μM) and as well as on PT (PT EC_{2X}=36.7 μM) [142–144]. In fact, CU-2010 and CU-2020 were evaluated for antifibrinolytic and anticancer activities, and not anticoagulant activity because of their prominent effect on the proteolytic activity of human plasmin [82].

Patented scaffolds: Motivated by the potential effective and safe anticoagulation properties of FXIa inhibitors, several inhibitor chemotypes have been introduced by various drug discovery programs in both academia and industry. In fact, a significant surge in the number of patents and patent applications for FXIa inhibitors has recently been witnessed, particularly over the past 3 years [6]. Importantly, about half of these applications have been filed and/or granted only since 2013 with about 80% of these applications being for small molecule active site or allosteric site inhibitors. The number of patents and patent applications for FXIa inhibitors was similar or exceeded those filed for thrombin or FXa inhibitors only starting 2010. Figure 22 shows different chemotypes of the recently patented active site FXIa inhibitors. Particularly, pyrrolidine-2-carboxamide **99**, piperidine-2-carboxamide **100**, dihydrobenzoxazine **101**, cyclopentapyridine-*N*-oxide **102**, and pyridine-*N*-oxide **103** inhibited human FXIa with nanomolar potency of 6, 0.4, 0.11, 0.38, and 1.34 nM, respectively. More details of patented FXIa inhibitors were reviewed recently [6].

(3) Polymeric GAGs and their Mimetics: Heparins, Dextran Sulfate, and Sulfated Lignins as Allosteric Inhibitors—GAGs are large linear polysaccharides constructed of repeating disaccharide units of an aminosugar, which could be galactosamine or glucosamine, and an uronic acid, which could be glucuronic acid and/or iduronic acid. With the exception of hyaluronic acid, all other GAGs including heparin/heparan, chondroitin, dermatan, and keratan are sulfated polysaccharides. Specifically, heparin is a highly sulfated, heterogeneous, and polydisperse mixture of linear polysaccharides with a wide range of biological, pathological, and pharmacological roles in thrombosis, infectious diseases, inflammation, and cancer among others [145–147]. Clinically, heparin and its variants, including LMWHs and fondaparinux, are used as anticoagulants to prevent and/or treat thromboembolic diseases. Mechanistically, heparin activates an endogenous anticoagulant serpin i.e. AT which subsequently and rapidly inhibits two coagulation proteases, thrombin and FXa, of the common coagulation pathway resulting in the anticoagulant activity [145–147].

In addition to its effect on thrombin and FXa, heparin plays a significant role in FXIa/FXI biology. The enzyme FXIa and its zymogen FXI have two anion-binding sites; one is in the catalytic domain (Lys529, Arg530, Arg532, Lys535, and Lys539) and the other is in the A3 apple domain (Lys252, Lys253, and Lys255) [13, 48, 56]. In one hand, the zymogen FXI is physiologically activated by thrombin and/or FXIIa and it may also undergo auto-activation in the presence of polyanions including heparin **104**, dextran sulfate **105** (Figure 23), and polyphosphates [53–53]. In the other hand, the active enzyme FXIa is physiologically inhibited by plasma serpins including AT, C1-inhibitor, α1-antitrypsin, protein Z-dependent protease inhibitor, and protease nexin-1 [56, 57]. Basic amino acids in the autolysis loop of FXIa's catalytic domain (Arg504, Lys505, Arg507, and Lys509) are the determinants of serpin specificity [148]. Heparin increases serpin-mediated FXIa inhibition by a template mechanism in which both the serpin and FXIa A3 domain bind to the same sequence of heparin. Nevertheless, heparin can also directly inhibit FXIa by allosteric modulation or charge neutralization through binding to anion-binding site in the catalytic domain [58, 59, 149, 150].

Al-Horani *et al.* (2014) reported on the binding affinities of UFH and heparin octasaccharide to two forms of human FXIa [58]. Using fluorescence spectroscopy at physiological conditions of pH 7.4, 37 °C, and 150 mM NaCl, UFH was found to bind to human FXIa with a K_D value of 1.1 ± 0.3 μM ($\Delta F_{max} = -75\%$) and human FXIa-DEGR (a variant of FXIa which contains the fluorophore dansyl at the end of the EGR tripeptide (P1–P3 residues) that is covalently attached to the catalytic Ser) with a K_D value of 1.6 ± 0.5 μM ($\Delta F_{max} = -29\%$). Likewise, heparin octasaccharide was found to bind to human FXIa and human FXIa-DEGR with K_D values of 0.9 ± 0.2 μM ($\Delta F_{max} = -68\%$) and 0.9 ± 0.2 μM ($\Delta F_{max} = -29\%$), respectively [58]. Furthermore, Sinha *et al.* (2004) reported on allosteric modification of FXIa functional activity upon binding to polyanions including two forms of dextran sulfate (Mr ~500000; DX500 and Mr ~10000; DX10) and two forms of heparin (64 disaccharide units, Mr ~14000; Hep64 and hypersulfated heparin, Mr ~12000; S-Hep) (Figure 23). Rates of hydrolysis of the chromogenic substrate S-2366 by FXIa in the absence and presence of different concentrations of DX500, DX10, Hep 64, and S-Hep were studied. All the polyanions inhibited the hydrolysis reaction in a concentration-dependent manner, with saturable inhibition observed at polyanion concentrations greater than 5 μg/mL (~0.1 nM DX500, ~0.5 μM Hep 64, S-Hep, and DX10) and variable maximal percent of inhibition (DX500 (83%), DX10 (56%), Hep 64 (58%), and S-Hep (48%)). Furthermore, all of the polyanions showed a concentration-dependent inhibition of FXIa-mediated activation of FIX with saturable maximal inhibition of 86%, 70%, 54%, and 51% by DX500, Hep 64, S-Hep, and DX 10, respectively [59]. Michaelis-Menten kinetics (wild type FXIa) and a series of fluorescence spectroscopy scanning and quenching experiments (fluorophore active site labeled FXIa; FXIa-DEGR) indicated that the inhibitory effect of the above polyanions was noncompetitive in nature [59]. Overall, the above results provided an evidence that FXIa binding to polyanions such as dextran sulfate and heparin, results in inhibition of the enzyme by an allosteric mechanism, and therefore, formed the foundation for the use of the GAG platform to design potent and selective sulfated nonsaccharide allosteric inhibitors of FXIa.

Along these lines, the Desai group developed sulfated low molecular weight lignins (LMWLs) as polymeric, nonsaccharide mimetics of heparin that exploit nonionic and ionic interactions in binding to heparin-binding proteins [151]. Three sulfated LMWLs **106** (CDSO3, FDSO3, and SDSO3) (Figure 23) were synthesized and found to be potent inhibitors of human FXIa in addition to other serine proteases [151]. Specifically, their FXIa IC_{50} values were 22, 105, and 176 nM, respectively, pointing to the significance of the aromatic scaffold, in addition to the sulfate groups, for FXIa inhibition by LMWLs. The LMWL polymers were chemo-enzymatically synthesized in two steps involving a horseradish peroxidase-catalyzed oxidative coupling of 4-hydroxycinnamic acid monomers followed by SO_3–$NEth_3$ -mediated sulfation. This chemo-enzymatic synthesis relies on a radical-mediated coupling reaction that results in polymers with multiple types of inter-residue bonds, heterogeneity, and polydispersity resembling LMWHs. The three sulfated LMWLs are reported to have an average molecular weight of 3500 Da, chain lengths of 5–15 units, and an average of 0.35 sulfate groups per unit [152].

(4) Nonpolymeric GAG Mimetics: Nonpolymeric Allosteric Site Inhibitors— Several small, sulfated, nonsaccharide, GAG mimetics were designed and/or discovered to

inhibit human FXIa, and therefore, to promote anticoagulant activity [58, 149, 150, 153–156]. Al-Horani *et al.* (2013) reported the discovery of sulfated pentagalloyl glucopyranoside (SPGG) as a potent, selective, and allosteric inhibitor of human FXIa [149]. Using a chromogenic substrate hydrolysis assay, a specific variant of SPGG, named as SPGG2 **107** (Figure 24), inhibited human FXIa with an IC_{50} value of 551 nM (1.2 μg/mL; K_I=0.4 μM) under physiological conditions of pH7.4, 37 °C, and NaCl concentration of 150 mM. SPGG2 was found to be at least 200-fold selective for FXIa over a host of human serine proteases including FXa (IC_{50}~266 μg/mL), FIXa (IC_{50}~1141 μg/mL), FXIIa (IC_{50}~256 μg/mL), thrombin (IC_{50}~1219 μg/mL), FVIIa (IC_{50}>3700 μg/mL), trypsin (IC_{50}>1800 μg/mL), and chymotrypsin (IC_{50}>1800 μg/mL). SPGG2 (3 μM) also inhibited FXIa-mediated activation of FIX, the physiological substrate of FXIa. Michaelis–Menten kinetics as well as competitive studies with UFH, short and long polyphosphate polymers, and GPIbα using the wild type full length FXIa or a species of FXIa only containing the catalytic domain were exploited to study the mechanism of inhibition of SPGG2. Results indicated that SPGG2 binds to or in the vicinity of the heparin-binding site in the catalytic domain suggesting an allosteric inhibition phenomenon. In fact, subsequent mutagenesis studies using single-point and multiple-point mutants precisely determined that the most active species of SPGG2 may interact with the Arg532, Arg530 and Lys529 residues of the catalytic domain of FXIa [58, 149, 150]. The allosteric phenomenon was thought to be responsible for the significant selectivity of SPGG2 over other serine proteases as allosteric sites on these proteases are typically less conserved in relative to their orthosteric sites. In another study, SPGG2 was also found to be at least 200–300-fold selective over APC, plasma kallikrein, and FXIIIa using UV-based as well as fluorescence-based *in vitro* assays [150]. In contrast to many covalent active site inhibitors of FXIa, SPGG2 inhibited FXIa reversibly with protamine and polybrene dose-dependently restoring 30–42% and 76–92%, respectively, of FXIa activity after incubation with 5 and 250 μg/mL SPGG2. Interestingly, SPGG2-mediated FXIa inhibition was also dose-dependently compromised by bovine albumin and the zymogen FXI, suggesting other reversal avenues [150].

In normal human plasma PT and APTT assays, SPGG2 was found to double the clotting time in the APTT assay at a concentration of 45±3 μM whereas the concentration required to double clotting time in the PT assay was found to be 373±26 μM. In FXI-deficient human plasma, the APTT EC_{2x} was 114±8 μM and in AT/heparin cofactor II deficient human plasma, the APTT EC_{2x} was 40±6 μM. These results suggested that SPGG2 anticoagulant activity primarily stems from inhibiting the intrinsic coagulation pathway [150]. Furthermore, SPGG2 demonstrated very good anticoagulant activity in human whole blood as established by thrombo-elastography [149], with results in this exercise being consistent with the previous findings.

Structurally, SPGG2 was characterized by UPLCMS and was found to be a mixture of variably sulfated pentagalloyl glucopyranoside with the decasulfated species being the most predominant species. Considering the steric factor, the 3,5-disulfated benzoyl moiety appears to represent the predominant sulfation pattern [149, 157]. Various thermodynamic studies conducted to understand the structural basis for SPGG2 interaction with human FXIa revealed that the negatively charged sulfate groups are crucial for potent inhibition of FXIa.

However, about 89% of the binding energy of SPGG2 came from non-ionic forces [58]. A library of GAG analogs including UFH, chondroitin sulfates A-C, enoxaparin, fondaparinux, and sucrose octasulfate was also tested against human FXIa under physiologically relevant conditions (pH 7.4, 150 mM NaCl, and 37 °C). In addition, SPGG2-OH **108** (Figure 24), an SPGG2 analog in which the *p*-phenolic group was substituted with a hydrogen atom, was also studied. Interestingly, none of the GAGs inhibited FXIa at concentrations as high as 50 μM. In contrary, SPGG2 and SPGG2-OH inhibited FXIa with IC_{50} values of 0.50 ± 0.02 and 1.4 ± 0.1 μM, respectively. This suggested that the aromatic units in SPGG2 and SPGG2-OH are essential for FXIa inhibition, in addition to the sulfate moieties [149, 150].

SPGG2 was initially prepared by a 2-hr microwave-mediated sulfation protocol. Different variants of SPGG2 were also prepared using the same protocol but at different reaction times of 0.5 hrs, 1 hr, 4 hrs, 6 hrs, and 8 hrs so as to evaluate the effect of degree of sulfation on FXIa inhibition potency and selectivity [58]. Furthermore, three variants of SPGG8 (prepared by 8-hr microwave-assisted sulfation) were prepared with different stereochemical orientations for the substituent at the anomeric carbon including α-stereochemistry, β-stereochemistry, and α,β-stereochemistry. Overall, eight variants were studied and results indicated that a high level of sulfation, as with SPGG8, appears to increase inhibition toward thrombin and FXa in addition to FXIa (IC_{50}=76 nM) suggesting a 2–3-fold loss of selectivity whereas a low level of sulfation, as with SPGG0.5, significantly reduces the potency of FXIa inhibition (IC_{50}=920 nM). A moderate level of sulfation that corresponds to a decasulfated SPGG scaffold, as with SPGG1 (IC_{50}=521 nM) or SPGG2 (IC_{50}=408 nM), appears to exhibit an optimal combination of potency and specificity. Furthermore, the three stereochemical SPGG8 variants exhibited similar FXIa inhibition potencies suggesting the insignificance of stereochemistry of the anomeric carbon. Yet, α-SPGG8 and α,β-SPGG8 inhibited thrombin as well as FXa moderately suggesting that the β-stereochemistry of the anomeric carbon is important to achieve a significant level of selectivity. Given the above results, an approximate optimal SPGG structure that can be expected to show the desired inhibition function without a loss of specificity is that with a β-anomeric carbon and 10 equally distributed sulfate groups at the *meta*-positions i.e. positions-3 and -5 of the five aromatic rings at carbons-1, -2, -3, -4, and -6 of the glucopyranose moiety [58]. To further advance this line of FXIa inhibitors as effective and safe anticoagulants, sulfated, hexasubstituted inositol-based GAG mimetics were recently introduced. One particular mimetic demonstrated similar potency, selectivity, and allosteric mechanism of FXIa inhibition to those of SPGG2, yet it is structurally dodecasulfated chemical species that is homogeneous [158]. This line of sulfated, nonpolymeric, and nonsaccharide GAG mimetics is currently under investigation in multiple animal models of thrombosis and bleeding.

Another strategy that was used to develop allosteric inhibitors of FXIa is the dual-element recognition strategy. In this strategy, a Coulombic attraction of an anionic scaffold to the cationic heparin-binding site of FXIa is thought to initially take place, followed by a hydrophobic interaction with a neighboring hydrophobic patch [153]. Using this strategy, sulfated quinazolinone homodimers were identified with micromolar inhibition potencies toward human FXIa. The most potent inhibitors identified in this study were molecules **109** and **110** (Figure 24) with IC_{50} values of 59 μM (K_I=37 μM) and 52 μM (K_I=38 μM),

respectively. Despite significant selectivity over thrombin, FXa, trypsin, and chymotrypsin, these two molecules showed poor effect on clotting times in the APTT and PT assays with concentrations to double clotting times of >950 μM [153].

Other allosteric inhibitors of human FXIa that were identified while developing allosteric inhibitors for thrombin and/or FXa are the benzofuran trimer **111** [154] and the sulfated coumarin dimer **112** [155] (Figure 24) among others [156]. Specifically, screening a chemically diverse library of 65 sulfated molecules with different scaffolds and sulfation levels resulted in the identification of monosulfated benzofuran trimer **111** as a potent FXIa inhibitor with an IC_{50} value of 0.82 μM [154]. Michaelis-Menten kinetics studies indicated a noncompetitive mechanism of inhibition for benzofuran **111**. In addition to competitive studies with UFH and fluorescence quenching studies, molecular modeling studies proposed a site near Lys255 on the A3 domain of FXIa as a putative binding site for this inhibitor. This result was further supported by the significantly compromised inhibition potency of this benzofuran toward a variant of FXIa lacking the A3 domain. However, this trimer also inhibited thrombin with an IC_{50} value of 5.8 μM [159]. The sulfated coumarin **112** inhibited human FXIa with an IC_{50} value of 31 μM, yet it also inhibited thrombin (IC_{50}= 0.2 μM) and FXa (IC_{50}=163 μM) [155].

(5) Antibodies

Polyclonal antihuman FXI antibody (aFXI): In 2003, Gruber and Hanson investigated the role of FXI-dependent thrombus propagation under arterial flow conditions in baboons [79]. In this study, porcine heparin (50 U/kg IV bolus and IV infusion of 50 U/kg/hr for 70 minutes) or affinity-purified monospecific antihuman FXI polyclonal goat antibody (aFXI; GAFXI-AP) (16 to 50 mg/kg IV bolus) were used. Coagulation tests indicated that aFXI pretreatment prolonged the clotting time in the APTT assay 3-foldfor at least 25 hrs post treatment, suggesting an impairment of the intrinsic coagulation pathway. There was no significant effect on the PT or template bleeding time. Furthermore, the *in vivo* anticoagulation profile of aFXI was evaluated in a thrombosis model in baboons in which thrombosis was triggered by knitted dacron or TF-presenting Teflon grafts positioned into AV shunts. Interestingly, the antithrombotic effects of heparin and aFXI were comparable as bothreduced fibrin deposition to 31–38% and 29–38%, respectively. As with heparin, aFXI significantly reduced the net platelet accumulation rate in thrombi. In fact, heparin reduced the platelet count in thrombi to 9–27% whereas aFXI reduced the thrombi platelet count to 7–35%. Overall, this study suggested that anticoagulation mediated by aFXI through FXIa inhibition did not stop the initiation of thrombogenesis, but substantially reduced thrombus propagation over time independent of the initiating factor. Thus, it was concluded that this antibody may not decrease the frequency at which initial thrombotic events take place, yet it may diminish thrombus mass, thrombus growth rate, and thrombo-occlusion [79].

Monoclonal antihuman FXI/FXIa antibody (XI-5108): Yamashita *el al.* (2006) reported a mouse monoclonal antibody named XI-5108 that acts against FXI and FXIa [160]. The XI-5108 antibody interacts with the catalytic domains of rabbit and human FXI/FXIa with K_D values of 0.11 and 0.46 nM, respectively. XI-5108 inhibited FXIa-initiated generation of FXa and FXIa, however, XI-5108 did not inhibit thrombin- and FXIIa-mediated generation

of FXIa. Further studies indicated that XI-5108 does not inhibit the amidolytic activity of FXIa as determined by S-2366, a chromogenic substrate. Instead, it appeared that XI-5108 structurally inhibits the binding of the large molecular weight substrates to FXIa. In rabbits, IV administration of 3.0 mg/kg of XI-5108 significantly prolonged the APTT for 4 hrs from 16.2 seconds to 38 seconds, whereas the PT and collagen-induced platelet aggregation were not substantially affected. Furthermore, the bleeding time did not significantly change. In fact, the bleeding times before and after the IV administration of XI-5108 were 128±26 seconds vs 101±26 seconds, respectively. These results further confirmed that XI-5108 effectively blocked the intrinsic coagulation pathway at an IV dose of 3.0 mg/kg. Similar effects were observed at an IV dose of 10 mg/kg. In a model of balloon-induced injured neointima of the rabbit iliac artery, an IV dose of 3.0 mg/kg of XI-5108 significantly reduced thrombus growth [160]. Subsequent studies by Takahashi *et al.* (2010) demonstrated that XI-5108 significantly diminished *ex vivo* ellagic acid but not TF-mediated plasma thrombin generation, as well as *in vivo* thrombus formation in rabbit jugular vein promoted by vessel ligation or endothelial denudation. XI-5108 significantly reduced thrombus surface areas covered by platelets and fibrin. The antibody was also found to limit thrombin generation at low shear rate in flow chambers [161].

Monoclonal antihuman FXI antibody (aXIMab or O1A6): Tucker *et al.* (2009) investigated the effect of an antihuman FXI monoclonal antibody (aXIMab; also known as O1A6; 2 mg/kg) on thrombus formation in a primate thrombosis model [80]. aXIMab has been reported to bind to an epitope on the apple domains of human FXI, particularly the A3 domain. aXIMab inhibited FXIa activity with an *in vitro* IC_{50} value of 2.5 nM. Reduced platelet activation and thrombin generation were also observed in aXIMab-treated baboons. Relative to controls, platelet activation at the thrombus surface was 86% lower at 30 mins in samples distal to thrombi in aXIMab-treated animals. Furthermore, local level of thrombin-AT complex, systemic level of thrombin-AT complex, and systemic level of β-thromboglobulin were all lower in aXIMab-treated animals than in controls by up to 98% at 40 mins, 81% at 60 mins, and 42% at 60 mins, respectively. No increase in D-dimer release from thrombi was observed. Indeed, pretreatment of baboons with aXIMab diminished plasma level of FXI by more than 99% for 10 days post treatment and inhibited thrombin-AT complex and β-thromboglobulin formation when their levels were measured downstream from thrombi occurring within collagen-coated vascular grafts [80].

Moreover, FXI inhibition with aXIMab was found to significantly diminish the 60-min platelet deposition and the end-point fibrin deposition in 4-mm diameter grafts by 63% and 81%, respectively. In addition, treatment with aXIMab prevented graft occlusion over 60 minutes in all grafts, whereas vehicle treatment in controls did not stop graft occlusion, which occurred in 8 of 9 grafts within about 27 minutes. Lastly, FXI inhibition by aXIMab did not prolong the standard template bleeding in baboons, which was similar in aXIMab- (3.5 mins) and vehicle-treated animals (3.4 mins). In contrast, pretreatment with aspirin at dose level of 32 mg/kg did not prevent graft occlusion and did prolong bleeding times [80].

Monoclonal antimouse FXI antibody (14E11): The immunoglobulin G 14E11 is a monoclonal antibody that was raised against mouse FXI in mice deficient of FXI and was

identified for its ability to prolong the APTT of mouse plasma by targeting FXI [162]. 14E11 was found to bind to the apple domain A2 of mouse and human FXI/FXIa with apparent K_D values of 0.002–0.003 nM. The antibody was also found to prolong the APTT of human and mouse plasma with maximum inhibition being achieved at 25–50 nM. As expected, 14E11 did not prolong the PT of human plasma. Subsequently, various studies indicated that 14E11 affects FXI activation by FXIIa or in HK-dependent system, but not FXIa activity or thrombin-mediated FXI activation. Similar to adding the antibody directly to mouse plasma, IV infusion or intraperitoneal injection of 14E11 into wild-type mice at a dose level of 1.0 mg/kg effectively prolonged the APTT. In the 7.5% $FeCl_3$-induced thrombosis model in mice, 1.0 mg/kg dose of 14E11 protected the mice from carotid artery occlusion with the antithrombotic effect lasting about 48 hours. Infusion of 1.0 mg/kg 14E11 before TF infusion also significantly prolonged mice survival in TF-mediated lethal pulmonary embolism mouse model compared with the untreated wild-type mice. In the baboon thrombosis model of collagen-coated Gore-Tex grafts, 1 mg/kg 14E11 was found to increase the APTT 2.3-fold with the effect lasting 4 days. The antibody 14E11 did not affect the platelet deposition on the graft surface. The antibody also prevented or significantly diminished the downstream thrombus growth and fibrin deposition within the grafts which were inserted into arteriovenous shunts [162].

14E11 was also tested in a murine model of acute ischemic stroke which was initiated by middle cerebral artery occlusion (MCAO). In this model, the APTT of mouse plasma was prolonged by more than 2.5-fold at 24 hrs following 14E11 administration compared with the APTT in the vehicle-treated animals and it remained prolonged for at least 2 days. The antibody did not affect the PT test. The tail bleeding times in 14E11-treated mice were similar to those in vehicle-treated animals indicating the absence of significant impairment for the primary hemostasis by 14E11. Furthermore, it was determined that 14E11 pretreatment improves cortical reperfusion after MCAO and that the neurological performance of 14E11-treated mice was substantially better than that of vehicle-treated controls with sustained benefits for at least 7 days following the acute stroke. Although the administration of 14E11 did not reduce mortality following acute ischemic stroke, yet 2 mg/kg 14E11 substantially deceased the fibrin deposition and the infarct size without intracranial bleeding. Overall, this study indicated that inhibition of FXIIa-mediated activation of FXI by 14E11 protects the mice from an experimentally-induced acute ischemic stroke [163].

In another mouse model of bowel perforation-induced peritoneal sepsis, about 30% improvement in overall survival was demonstrated in the 14E11-treated group over vehicle-treated animals. Early 14E11-mediated anticoagulation significantly decreased the systemic level of thrombin-AT complex as well as the levels of IL-6 and TNF-α. It also significantly diminished the platelet consumption in the circulation and the subsequent deposition in the blood vessels. These results indicated that inhibiting FXIIa-mediated FXI activation by 14E11 substantially reduces coagulopathy and inflammation, and improves the survival of mice in polymicrobial sepsis [164]. Therefore, this strategy appears to be effective in limiting the development of disseminated intravascular coagulation without increasing the risk of bleeding. Lastly, inhibition of FXIIa-mediated FXI activation by 14E11 significantly

reduced inflammation, coagulopathy, and bacterial growth in a mouse model of listeriosis by a lethal dose of *Listeria monocytogenes* [165].

Monoclonal antihuman FXI/FXIa antibodies (αFXI-203 and αFXI-175): These two antibodies dose-dependently prevented the normal plasma clotting with a maximum inhibition of ~85% [166]. The antibodies reacted with both FXIa and FXI with K_D values of 3–5 nM. In one hand, αFXI-203 primarily recognizes the A2 apple domain, and therefore, it prevents the binding of FXI(a) to HK. In the other hand, αFXI-175 predominantly recognizes the A4 apple domain, and thus, it appears that αFXI-175 interferes with FXIa-mediated activation of FIX. In the $FeCl_3$-induced thrombosis mouse model, the inferior vena cava was patent (stayed open) for 12.5 min in αFXI-203- treated animals and for 25 min in mice treated with αFXI-175. These times were significantly longer compared to placebo in which the inferior vena cava remained patent for only 5 mins. Furthermore, the two antibodies inhibited the intrinsic pathway-initiated thrombin generation with none-to-very limited effect on tissue factor-initiated thrombin generation. Lastly, tail bleeding times in antibody-treated animals appeared to be similar to those in placebo-treated animals indicating lack of severe bleeding risk [166].

Monoclonal antihuman FXI/FXIa antibodies (076D-M007-H04 and 076D-M028-H17): Two human monoclonal antibodies, namely 076D-M007-H04 and 076D-M028-H17, were also recently reported [167]. 076D-M007-H04 is a competitive inhibitor of human and rabbit FXIa whereas 076D-M028-H17 is an inhibitor of thrombin- and/or FXIIa-mediated activation of human and rabbit FXI. Both antibodies dose-dependently decreased the weight of thrombus in $FeCl_3$-induced arterial thrombosis model in rabbits without affecting the ear bleeding times. Similar results were also obtained in baboons using collagen-initiated arteriovenous shunt thrombosis model and template skin bleeding test [167]. These antibodies appear to be similar to those reported by David *et al* (2016) [168].

Fusion protein of an anti-CD14 antibody and a modified domain of bikunin (MR1007): Very recently, Nakamura *et al.* (2017) reported that simultaneous targeting of CD14 and FXIa by a fusion protein (MR1007) consisting of an anti-CD14 antibody and the modified second domain of bikunin enhances the survival of rabbits in sepsis models [169]. MR1007 binds to CD14 with a K_D value of 1 nM and inhibits human FXIa in a chromogenic substrate hydrolysis assay with an IC_{50} value of 48.2 nM. MR1007 dose-dependently inhibited lipopolysaccharide (LPS)-induced TNF-α production in human and rabbit peripheral blood mononuclear cells with IC_{50} values of 0.752 and 1.96 μg/ml, respectively. Likewise, MR1007 dose-dependently inhibited LPS-induced IL-6 production in human endothelial cells and suppressed the elevation of E-selectin expression in the same cells with an IC_{50} value of 0.640 μg/mL. MR1007 prolonged APTT in a concentration-dependent manner in human and rabbit platelet-poor plasma with $EC_{1.5x}$ values of 45.8 μg/mL and 131 μg/mL, respectively. Furthermore, MR1007 inhibited thromboplastin-induced thrombin generation in a concentration-dependent fashion in human and rabbit platelet-rich plasma with 50% inhibition achieved at 30 μg/mL and 300 μg/mL, respectively. Consistent with FXIa inhibition, MR1007 did not increase the ear bleeding time in rabbits at a dose as high

as 30 mg/kg indicating that the anticoagulant effects of MR1007 may be suitable to prevent excessive coagulation without impairing hemostasis.

In *ex vivo* settings of healthy rabbits, IV administration of 3 and 10 mg/kg MR1007 prolonged the APTT in a dose-dependent manner. MR1007 suppressed LPS-induced TNF-α production with the effect maintained 24 hrs (at 3 mg/kg) and 48 hrs (10 mg/kg) after MR1007 administration. In a rabbit sublethal endotoxemia model, IV administration of MR1007 at 0.3–3 mg/kg doses significantly decreased the reduction of white blood cell counts in a dose-dependent fashion. Likewise, MR1007 at 1–3 mg/kg doses also prevented the increase in plasma levels of TNF-α, IL-6, D-Dimer, and AT activity in a dose-dependent manner. The reduction of platelet counts was dose-independent and only slightly prevented at ≥1 mg/kg. These results suggested that MR1007 effectively suppressed LPS-induced pro-inflammatory and pro-coagulation responses in rabbits. In the same model, IV administration of 3 mg/kg MR1007 significantly increased survival in treated animals relative to the control group even at 8 and 24 hrs. The survival rates at 48 hrs were 67% and 0% in MR1007-treated animals and control animals, respectively. Furthermore, IV administration of 10 mg/kg MR1007 also significantly improved survival 2 hrs post cecal ligation and puncture. The survival rates at 72 hrs were 44%, and 0% in the MR1007-treated group and control group, respectively. Lastly, 30 mg/kg MR1007 did not increase bacterial counts in blood, lung, liver, or spleen relative to the control group. This indicates that the fusion protein does not compromise the host's ability to clear bacterial infection in the sepsis model [169]. Overall, targeting FXIa, as demonstrated partially by MR1007, appears to be a clinically relevant approach for the treatment of severe sepsis and septic shock.

(6) Antisense Oligonucleotides (ASOs)—ASOs are relatively short, chemically modified single-stranded nucleic acid sequences that selectively pair to specific regions of mRNA, and therefore, regulate its translation into functional proteins [170–174]. By binding to a complementary RNA following Watson-Crick base pairing, ASOs can suppress gene expression by different mechanisms including RNase H activation, RNA splicing modulation, and endogenous microRNAs sequestration. Several advantages have been reported for ASOs including their high target specificity, predictable clinical pharmacokinetics, long half-life, and lack of common drug–drug interactions [170–174]. However, the physiological phosphodiester backbone of RNA and DNA is susceptible to degradation by nuclease which limits their therapeutic uses. Thus, chemical modifications of the backbone may improve the metabolic stability of oligonucleotides, and therefore, may enhance their therapeutic uses. One of the most commonly used modifications in oligonucleotide therapeutics is the phosphorothioate modification in which a non-bridging oxygen atom in the phosphodiester linkage is substituted with a sulfur atom (Figure 25). The resulting chemically modified nucleotide sequences not only have enhanced chemical stability but also improved protein binding and cellular uptake properties [170–174].

FXI ASO: ISIS404071: Considering FXI, several oligonucleotides composed of 20 nucleotides in length and chemically modified with phosphorothioate in the backbone and 2′-O-methoxyethyl on the wings with a central deoxy gap ("5-10-5" design) were synthesized and reported by Zhang *et al.* (2010) [175]. In mice, treatment with one particular

FXI ASO (ISIS404071) resulted in a dose-dependent reduction of FXI mRNA levels in liver with an approximate maximal reduction of ~98%. This reduction in FXI mRNA levels correlated well with the reduction in circulating FXI plasma protein level and FXIa activity. Furthermore, FXI ASO was highly specific for FXI and did not affect other coagulation factor mRNAs. FXI antisense therapy resulted in a dose-dependent prolongation of APTT and no effect on PT. Subcutaneous injection of 50 mg/kg FXI ASO resulted in a time-dependent reduction in FXI mRNA levels with an onset of action of ~1 day. This activity was maintained at maximal inhibition from 2 to 7 days, followed by a gradual return to basal levels between days 14 and 28. Likewise, FXI ASO-mediated APTT prolongation increased and then returned to baseline over the same time course. The data also indicated that ~60% reduction in FXI mRNA levels is required to promote anticoagulant activity in mice.

In 10% $FeCl_3$-induced inferior vena cava thrombosis model, FXI ASO produced a dose-dependent reduction in thrombus formation with maximal effects observed at doses between 5 and 10 mg/kg. In contrast to warfarin, enoxaparin, and FII ASO, FXI ASO treatment had no effect on bleeding at the highest doses tested in the tail vein bleeding test or the partial hepatectomy surgical bleeding model compared with the control treatment. In 10% $FeCl_3$-induced mesenteric vein thrombosis mouse model, FXI ASO treatment (50 mg/kg) completely prevented occlusion of the mesenteric vein up to 40 minutes after 10% $FeCl_3$ exposure. Although small thrombi initially formed, their formation was significantly delayed in time, their density, stability, and size were significantly decreased, and they were ultimately cleared. FXI ASO treatment also dose-dependently reduced thrombus formation in the stenosis-induced inferior vena cava thrombosis model. Importantly, treatment with FXI protein concentrate rapidly normalized the FXI ASO-mediated APTT prolongation suggesting an avenue to a reversal strategy. Lastly, FXI ASO improved the antithrombotic effect of enoxaparin and clopidogrel in the inferior vena cava mouse model of venous thrombosis and the $FeCl_3$-induced descending aorta model of arterial thrombosis, respectively, and significantly decreased their associated risk of bleeding in tail bleeding assays. In another study, similar FXI ASO (50 mg/kg) reduced thrombus formation and fibrin deposition on atherosclerotic plaque rupture in the carotid arteries of $ApoE^{(-/-)}$ mice without inducing a bleeding tendency [176]. Clots were not only smaller but also more unstable in FXI ASO–treated animals. Moreover, collagen deposition as well as macrophage infiltration was relatively limited in the carotid arteries of FXI ASO-treated animals with no neutrophil infiltration in thrombi. This study in mice indicated that FXI ASO can safely prevent thrombus formation on acutely ruptured atherosclerotic plaques with much less severe inflammatory response and with no bleeding complications.

FXI ASO: ISIS416858 (ISIS-FXIRx): ISIS 416858 is a single-stranded antisense oligodeoxynucleotide of 20 nucleotides (ACGGCATTGGTGCACAGTTT) [177]. It contains a phosphorothioate linkage in the place of a phosphodiester linkage in the DNA backbone and 2′-O-methoxyethyl modifications on the sugar moieties of the 5 outermost nucleotides at the 3′ and 5′ ends (Figure 25). ISIS 416858 was administered (4, 8, 12, or 40 mg/kg; SC) to healthy cynomolgus monkeys via a 2-week loading dose regimen followed by once weekly dosing for up to 13 weeks. Dose- and duration-dependent reductions in liver FXI mRNA and FXI plasma activity were detected along with a parallel increase in APTT. For

example, using a dose of 12 mg/kg, liver FXI mRNA expression was significantly reduced by ~50% and ~75% after 6 and 13 weeks of treatment, respectively. This level almost returned to normal after 26 weeks. Elevations in APTT were also produced at the 12 mg/kg dose level at 2 weeks, and after 13 weeks of treatment APTT was elevated by ~20%. ISIS 416858-mediated elevations in APTT progressively decreased following cessation of treatment and returned to the baseline level by the end of the 13-week treatment-free period. No change in PT was detected. Likewise, 20 mg/kg SC administration of ISIS 416858 produced reduced plasma FXI activity by 50% or 70% after 2 or 6 weeks of treatment, respectively, with a corresponding 30% elevation in APTT. At this dose, ISIS 416858 did not affect the bleeding time or blood volume loss following partial tail amputation or gum or skin laceration. However, monkeys that received a single dose of enoxaparin (2 mg/kg) experienced 2- and 3-fold increases in bleeding time and blood volume loss, respectively, after a partial tail amputation. Bleeding time following gum laceration was also increased by 60% following enoxaparin treatment. Generally, ISIS 416858 was clinically well tolerated up to the highest dose tested which was 40 mg/kg with dose-dependent formation of basophilic granules in multiple tissues [177].

This oligonucleotide was also administered to four baboons at a dose level of 25 mg/kg, given three times per week. Both FXI level and FXIa plasma activity were significantly diminished in all animals, with similar kinetic profiles. A 50% inhibition of FXIa plasma activity was achieved by day 25 in all animals with the maximum inhibition of ~70% being reached by the end of the infusion time. FXI protein levels were similarly reduced during the infusions. After treatment discontinuation, the levels of both FXI protein and activity slowly increased over multiple months. The APTT readings increased over the treatment time, and aligned well with the decrease in FXI protein level and FXIa activity levels after discontinuation. FXI ASO-treated baboons were also protected from collagen-initiated thrombus propagation. Furthermore, the antithrombotic effect of FXI ASO in baboons was found to be facilitated by inhibiting/reducing platelet activation, thrombin generation, and fibrin mesh formation. In the standard template skin bleeding test, FXI ASO treatment did not impair hemostasis in baboons [178].

A double blind, single-dose study in healthy subjects indicated that 200 mg or 300 mg SC administration of ISIS-FXIRx significantly reduced FXI antigen level and activity 1 week after dosing. Likewise, in a multiple ascending-dose study, treatment with ISIS- FXIRx (50–300 mg; SC) exhibited a significant, sustained, and dose-dependent decrease in the FXI antigen and activity with the maximum reduction observed within 1–2 weeks post-dosing. In both cases, there was significant APTT prolongation and no bleeding events were noted. ISIS-FXIRx also did not cause clinically significant changes in vital signs, electrocardiogram, renal function, hepatic function, or hematology. Preliminary pharmacokinetic analysis indicated that hepatic $T_{0.5}$ of ISIS-FXIRx was ~20 days [179].

This FXI ASO was also tried in an open-label, parallel-group Phase II study in patients undergoing elective primary unilateral total knee arthroplasty [180]. Patients received 200 mg FXI ASO, 300 mg FXI ASO, or 40 mg enoxaparin once daily. In one hand, venous thromboembolism occurred only in 27% of patients receiving 200 mg FXI ASO, 4% of those receiving 300 mg FXI ASO, and 30% of those receiving 40 mg enoxaparin. Thus, 300

mg FXI ASO regimen was superior to enoxaparin whereas 200 mg FXI ASO regimen was noninferior to enoxaparin. In the other hand, nonmajor bleeding occurred in 3% of the patients on FXI-ASO treatment and in 8% of the patients receiving enoxaparin. Overall, this study indicated that this specific FXI ASO effectively protects patients undergoing total knee arthroplasty against venous thrombosis with a relatively limited risk of bleeding.

FXI ASO: ISIS564673: Yau *et al.* (2014) reported that the administration of 15 mg/kg, twice weekly for 5 weeks, of FXI ASO (ISIS564673; GTAACATGTGCCCTTTCCTT) to rabbits decreased FXI activity by 99%, prolonged APTT by 4.7-fold, and delayed catheter thrombosis by 2.3-fold with no effect on the PT [181]. An interesting prospect for FXI ASO was recently put forward by Kossmann *et al.* (2017) who demonstrated a potential use of FXI/FXIa-based anticoagulants in treating hypertension [182]. A similar FXI ASO inhibited thrombin propagation on platelets, angiotensin II-induced endothelial dysfunction, and vascular leukocyte infiltration in mice and rats. In rats with arterial hypertension, FXI ASO also reduced high blood pressure as well as vascular and kidney dysfunctions.

(7) Aptamers—Very recently, Donkor *et al.* (2017) reported the selection and characterization of a DNA aptamer that inhibits FXIa [183]. Aptamers are small sequences of nucleic acids that are capable of binding to a target protein with high affinity. Such aptamers are useful as research, diagnostic, or therapeutic tools. Using 'Systematic Evolution of Ligands by Exponential Enrichment' (SELEX), the first nucleic acid-based FXIa inhibitory aptamer was obtained and named as Factor ELeven Inhibitory Aptamer (FELIAP). FELIAP is an 80 base, single-stranded DNA that has a hypervariable central sequence 5′-AACCTATCGGACTATTGTTAGTGATTTTTATAGTGT-3′. FELIAP competitively bind to FXIa with a K_D value of 1.8 nM as determined by surface plasmon resonance. Furthermore, FELIAP inhibited FXIa-catalyzed S2366 cleavage, FIX activation, and complex formation with AT, with no effect on FXI activation. FELIAP also significantly inhibited thrombin generation and plasma clotting relative to control aptamers.

CONCLUSION AND FUTURE DIRECTIONS

The global burden of thromboembolic diseases is enormous, and therefore, the pursuit of "ideal" effective and safe strategies to treat and/or prevent these diseases continues. Clinically used anticoagulant drugs are very effective and directly or indirectly target proteins in the common coagulation pathway i.e. factors IIa and Xa. Indeed, studies have demonstrated that these two proteases contribute to the physiology and pathology of blood flowing status i.e. hemostasis and thrombosis, respectively. Therefore, anticoagulants that target these two proteins are likely to cause bleeding complications which in many cases can become life-threatening. In addition to the animal models, the pathophysiology and epidemiology of thromboembolic diseases indicate that inhibiting enzymes in the intrinsic coagulation phase, also known as the contact phase system, may satisfy the goal of effective anticoagulation without bleeding consequences. Among the different proteins in the intrinsic coagulation pathway, FXIa appears to be a very attractive drug target and the development of molecules that interfere with its physiological functions, or even inhibit its hepatic biosynthesis, appears to have gained momentum in both industry and academia.

Strategies to inhibit FXI/FXIa system involve polypeptides, active site peptidomimetic inhibitors, allosteric inhibitors, monoclonal antibodies, ASOs, and aptamers. The different strategies available to target FXI/FXIa system present multiple therapeutic opportunities so as to address the different medical needs of thrombotic patients. For example, active site and allosteric FXIa inhibitors have the potential to be used orally and/or parenterally whereas ASOs, antibodies, and aptamers are suitable for parenteral administration. Moreover, ASOs are expected to have a relatively delayed onset of action with long duration of action which makes them appropriate for chronic indications. However, all the other options are relatively associated with immediate action and could be suitable for acute or chronic indications depending on their half-lives. While consideration of hepatic metabolism and renal clearance is variable depending on the chemical structure of active site or allosteric site inhibitors, the two pharmacokinetic aspects become less important in anticoagulant therapies that use ASOs, antibodies, or aptamers. As indicated earlier, potential indications for FXI/FXIa-based therapeutics include the prevention of cardiovascular events in patients associated with chronic kidney disease, hemodialysis, elevated risk of recurrent thrombosis, or cardiac devices. Therapeutics that target FXI/FXIa system may also benefit atrial fibrillation patients at high bleeding risk as well as acute coronary syndrome patients who need anticoagulant therapy in addition to antiplatelet therapy [17].

Early results of FXI ASO [ISIS416858 (ISIS-FXIRx)] (parenteral) in healthy volunteers are very encouraging in terms of the absence of the bleeding events and the absence of clinically significant changes in vital signs, cardiac function, renal function, hepatic function, or hematology. Phase II studies of this FXI ASO (NCT01713361) have also established its efficacy in patients undergoing elective primary unilateral total knee arthroplasty. Likewise, the results of the safety, pharmacokinetics, and pharmacodynamics of ISIS416858 in patients with end-stage renal disease receiving chronic hemodialysis (NCT02553889) were positive [184] with more trials are planned. Furthermore, two active site peptidomimetic inhibitors of FXIa BMS986177 (oral; chemical structure appears to be not disclosed; multiple clinical trials) [185] and EP-7014 **17a** (parenteral; Figure 7D) (NCT02914353) [109, 110] have just completed Phase I trials. Moreover, active site peptidomimetic FXIa inhibitor **49** (parenteral) (Figure 13) has been put forward as a clinical candidate for use as an acute antithrombotic agent in a hospital setting.

Interestingly, FXI/FXIa-targeting therapeutics have shown significant potential in animal models of severe sepsis (monoclonal antibody 14E11 and anti-CD14 antibody MR1007) [169] as well as those of arterial hypertension (FXI ASO: ISIS564673) [182]. Although more studies are required, these findings open new avenues to mechanistically novel and therapeutically effective treatment strategies. In addition, nonpolymeric GAG mimetics which target allosteric sites on FXIa present a new concept in modulating coagulation that is rapidly developing. Although, the efficacy of these mimetics has yet to be established in animal models, nevertheless the molecules offer many advantages that may be suitable for use in acute thrombotic episodes in hospital settings, particularly during surgery. Nonpolymeric GAG mimetics possess high water solubility, low cellular and central nervous system toxicity, and the advantage of synthetic feasibility [149, 150].

Despite the promising results at many fronts in developing FXI/FXIa-targeting therapeutics, substantial efforts are still required to advance these therapeutics to enter the clinic. Finding appropriate routes of administration and delivery systems as well as developing molecules with optimal pharmacokinetic profiles appear to be the focus of most of the programs targeting FXI/FXIa. Importantly, the non-selectivity of the active site peptidomimetic inhibitors, particularly toward plasma kallikrein [186], trypsin, and/or chymotrypsin appears to be an issue, although diverse drug design strategies have been considered (Figure 26). Furthermore, an effective antidote to treat cases of excessive anticoagulation may be needed and perhaps should be considered. Overall, given the significant attention that this protein target has been receiving over the last decade, a clinical approval of FXI/FXIa inhibitors will represent a major paradigm-shift in the way we treat thromboembolic diseases.

Acknowledgments

This publication was made possible by funding to RAAH from the Research Centers in Minority Institutions (RCMI) Program from the National Institute on Minority Health and Health Disparities of the National Institutes of Health under grant number 5G12MD007595. This publication was also supported by an Institutional Development Award (IDeA) from the National Institute of General Medical Sciences of the National Institutes of Health under grant numbers 5 P20 GM103424-15 and 3 P20 GM103424-15S1 to RAAH. The contents are solely the responsibility of the authors and do not necessarily represent the official views of the NIH.

ABBREVIATIONS

APC	Activated protein C
APP	Amyloid beta-protein precursor
APTT	Activated partial thromboplastin time
ArT	Arterial thrombosis
ASO	Antisense oligonucleotide
AT	Antithrombin
DVT	Deep vein thrombosis
ECAT	Electrically-induced carotid arterial thrombosis
FIIa	Factor IIa
FVIIa	Factor VIIa
FVIIIa	Factor VIIIa
FXa	Factor Xa
FXIa	Factor XIa
FXIIa	Factor XIIa
FXIIIa	Factor XIIIa
FELIAP	Factor eleven inhibitory aptamer

GAGs	Glycosaminoglycans
HK	High molecular weight kininogen
iCBF	Integrated carotid blood flow
IHD	Ischemic heart disease
Ir-CPI	*Ixodes ricinus* contact phase inhibitor
IS	Ischemic stroke
IV	Intravenous
KD APPH	Kunitz domain of Alzheimer amyloid precursor protein homolog
KPI	Kunitz-type protease inhibitor
LMWHs	Low molecular weight heparins
LMWLs	Low molecular weight lignins
LPS	Lipopolysaccharide
MCAO	Middle cerebral artery occlusion
PE	Pulmonary embolism
PL	Phospholipid
PN-2	Protease nexin-2
PT	Prothrombin time
SC	Subcutaneous
SELEX	Systematic evolution of ligands by exponential enrichment
SPGG	Sulfated pentagalloylglucopyranoside
THQ	Tetrahydroquinoline
TF	Tissue factor
TFPI	Tissue factor pathway inhibitor
TFPI-1	Tissue factor pathway inhibitor-1
UFH	Unfractionated heparin
VT	Venous thrombosis

References

1. Henry BL, Desai UR. Anticoagulants: Drug discovery and development. In: Rotella D, Abraham DJ, editorsBurger's medicinal chemistry. 7. New York: John Wiley and Sons; 2010. 365–408.

2. Freedman JE, Loscalzo J. Arterial and venous thrombosis. In: Kasper D, Fauci A, Hauser S, Longo D, Jameson JL, Loscalzo J, editorsHarrison's principles of internal medicine. 19. Vol. Chapter 142. New York: McGraw-Hill Education; 2015.

3. Wendelboe AM, Raskob GE. Global burden of thrombosis: Epidemiologic aspects. Circ Res. 2016; 118(9):1340–7. [PubMed: 27126645]

4. Raskob GE, Angchaisuksiri P, Blanco AN, Buller H, Gallus A, Hunt BJ, Hylek EM, Kakkar A, Konstantinides SV, McCumber M, Ozaki Y, Wendelboe A, Weitz JI. Thrombosis: a major contributor to the global disease burden. J Thromb Haemost. 2014; 12(10):1580–90. [PubMed: 25302663]

5. LUMC. Antithrombotics, thrombolytics, antiplatelets, and coagulants. In: Lemke TL, Williams DA, Roche VF, Zito SW, editorsFoye's principles of medicinal chemistry. 7. Vol. Chapter 25. Philadelphia: Lippincott Williams & Wilkins; 2013. 841–876.

6. Al-Horani RA, Desai UR. Factor XIa inhibitors: A review of the patent literature. Expert Opin Ther Pat. 2016; 26(3):323–45. [PubMed: 26881476]

7. Gross PL, Murray RK, Weil PA, Rand ML. Hemostasis and thrombosis. In: Rodwell VW, Bender DA, Botham KM, Kennelly PJ, Weil PA, editorsHarper's illustrated biochemistry. 30. Vol. Chapter 55. New York: McGraw-Hill Education; 2015.

8. Wood JP, Ellery PE, Maroney SA, Mast AE. Biology of tissue factor pathway inhibitor. Blood. 2014; 123(19):2934–43. [PubMed: 24620349]

9. Griffin JH, Fernández JA, Gale AJ, Mosnier LO. Activated protein C. J Thromb Haemost. 2007; 5(Suppl 1):73–80. [PubMed: 17635713]

10. Björk I, Olson ST. Antithrombin. A bloody important serpin. Adv Exp Med Biol. 1997; 425:17–33. [PubMed: 9433486]

11. Olson ST, Swanson R, Raub-Segall E, Bedsted T, Sadri M, Petitou M, Hérault JP, Herbert JM, Björk I. Accelerating ability of synthetic oligosaccharides on antithrombin inhibition of proteinases of the clotting and fibrinolytic systems. Comparison with heparin and low-molecular-weight heparin. Thromb Haemost. 2004; 92(5):929–39. [PubMed: 15543318]

12. Larsen KS, Østergaard H, Bjelke JR, Olsen OH, Rasmussen HB, Christensen L, Kragelund BB, Stennicke HR. Engineering the substrate and inhibitor specificities of human coagulation Factor VIIa. Biochem J. 2007; 405(3):429–38. [PubMed: 17456045]

13. Zhao M, Abdel-Razek T, Sun MF, Gailani D. Characterization of a heparin binding site on the heavy chain of factor XI. J Biol Chem. 1998; 273(47):31153–9. [PubMed: 9813019]

14. Wheeler AP, Gailani D. The Intrinsic pathway of coagulation as a target for antithrombotic therapy. Hematol Oncol Clin North Am. 2016; 30(5):1099–114. [PubMed: 27637310]

15. Gailani D, Gruber A. Factor XI as a therapeutic target. Arterioscler Thromb Vasc Biol. 2016; 36(7):1316–22. [PubMed: 27174099]

16. Gailani D. Future prospects for contact factors as therapeutic targets. Hematology Am Soc Hematol Educ Program. 2014; 2014(1):52–9. [PubMed: 25696834]

17. Weitz JI, Fredenburgh JC. Factors XI and XII as targets for new anticoagulants. Front Med (Lausanne). 2017; 4:19. [PubMed: 28286749]

18. Fredenburgh JC, Gross PL, Weitz JI. Emerging anticoagulant strategies. Blood. 2017; 129(2):147–154. [PubMed: 27780803]

19. Pauer HU, Renné T, Hemmerlein B, Legler T, Fritzlar S, Adham I, Müller-Esterl W, Emons G, Sancken U, Engel W, Burfeind P. Targeted deletion of murine coagulation factor XII gene-a model for contact phase activation in vivo. Thromb Haemost. 2004; 92:503–508. [PubMed: 15351846]

20. Revenko AS, Gao D, Crosby JR, Bhattacharjee G, Zhao C, May C, Gailani D, Monia BP, MacLeod AR. Selective depletion of plasma prekallikrein or coagulation factor XII inhibits thrombosis in mice without increased risk of bleeding. Blood. 2011; 118:5302–5311. [PubMed: 21821705]

21. Merkulov S, Zhang WM, Komar AA, Schmaier AH, Barnes E, Zhou Y, Lu X, Iwaki T, Castellino FJ, Luo G, McCrae KR. Deletion of murine kininogen gene 1 (mKng1) causes loss of plasma kininogen and delays thrombosis. Blood. 2008; 111:1274–1281. [PubMed: 18000168]

22. Langhauser F1, Göb E, Kraft P, Geis C, Schmitt J, Brede M, Göbel K, Helluy X, Pham M, Bendszus M, Jakob P, Stoll G, Meuth SG, Nieswandt B, McCrae KR, Kleinschnitz C. Kininogen

deficiency protects from ischemic neurodegeneration in mice by reducing thrombosis, blood-brain-barrier damage and inflammation. Blood. 2012; 120(19):4082–92. [PubMed: 22936662]

23. Gailani D, Lasky NM, Broze GJ Jr. A murine model of factor XI deficiency. Blood Coagul Fibrinolysis. 1997; 8:134–144. [PubMed: 9518045]
24. Garcia DA, Baglin TP, Weitz JI, Samama MM. American College of Chest Physicians. Parenteral anticoagulants: Antithrombotic therapy and prevention of thrombosis, 9th ed: American college of chest physicians evidence-based clinical practice guidelines. Chest. 2012; 141(2 Suppl):e24S–43S. [PubMed: 22315264]
25. Ageno W, Gallus AS, Wittkowsky A, Crowther M, Hylek EM, Palareti G. American College of Chest Physicians. Oral anticoagulant therapy: Antithrombotic therapy and prevention of thrombosis, 9th ed: American college of chest physicians evidence-based clinical practice guidelines. Chest. 2012; 141(2 Suppl):e44S–88S. [PubMed: 22315269]
26. Weitz JI, Eikelboom JW, Samama MM. American College of Chest Physicians. New antithrombotic drugs: Antithrombotic therapy and prevention of thrombosis, 9th ed: American college of chest physicians evidence-based clinical practice guidelines. Chest. 2012; 141(2 Suppl):e120S–51S. [PubMed: 22315258]
27. Weitz JI. Reversal of direct oral anticoagulants: Current status and future directions. Semin Respir Crit Care Med. 2017; 38(1):40–50. [PubMed: 28208197]
28. Leitch J, van Vlymen J. Managing the perioperative patient on direct oral anticoagulants. Can J Anaesth. 2017; 64(6):656–672. [PubMed: 28429198]
29. Kim JH, Lim KM, Gwak HS. New anticoagulants for the prevention and treatment of venous thromboembolism. Biomol Ther (Seoul). 2017; doi: 10.4062/biomolther.2016.271
30. Mekaj YH, Mekaj AY, Duci SB, Miftari EI. New oral anticoagulants: their advantages and disadvantages compared with vitamin K antagonists in the prevention and treatment of patients with thromboembolic events. Ther Clin Risk Manag. 2015; 11:967–77. [PubMed: 26150723]
31. Cabral KP, Jack E, Ansell JE. The role of factor Xa inhibitors in venous thromboembolism treatment. Vasc Health Risk Manag. 2015; 11:117–123. [PubMed: 25673997]
32. Ginsberg JS, Crowther MA. Direct oral anticoagulants (DOACs) and pregnancy: A plea for better information. Thromb Haemost. 2016; 116(4):590–1. [PubMed: 27608925]
33. Beyer-Westendorf J, Michalski F, Tittl L, Middeldorp S, Cohen H, Abdul Kadir R, Arachchillage DJ, Arya R, Ay C, Marten S. Pregnancy outcome in patients exposed to direct oral anticoagulants - and the challenge of event reporting. Thromb Haemost. 2016; 116(4):651–8. [PubMed: 27384740]
34. Ravikumar R, Lim CS, Davies AH. The role of new oral anticoagulants (NOACs) in cancer patients. Adv Exp Med Biol. 2017; 906:137–148. [PubMed: 27620312]
35. Verso M, Agnelli G, Prandoni P. Pros and cons of new oral anticoagulants in the treatment of venous thromboembolism in patients with cancer. Intern Emerg Med. 2015; 10(6):651–6. [PubMed: 25840679]
36. Agnelli G, Buller HR, Cohen A, Curto M, Gallus AS, Johnson M, Masiukiewicz U, Pak R, Thompson J, Raskob GE, Weitz JI. AMPLIFY Investigators. Oral apixaban for the treatment of acute venous thromboembolism. N Engl J Med. 2013; 369(9):799–808. [PubMed: 23808982]
37. Büller HR, Décousus H, Grosso MA, Mercuri M, Middeldorp S, Prins MH, Raskob GE, Schellong SM, Schwocho L, Segers A, Shi M, Verhamme P, Wells P. Hokusai-VTE Investigators. Edoxaban versus warfarin for the treatment of symptomatic venous thromboembolism. N Engl J Med. 2013; 369(15):1406–15. [PubMed: 23991658]
38. van Es N, Coppens M, Schulman S, Middeldorp S, Büller HR. Direct oral anticoagulants compared with vitamin K antagonists for acute venous thromboembolism: evidence from phase 3 trials. Blood. 2014; 124(12):1968–75. [PubMed: 24963045]
39. Steiner T, Weitz JI, Veltkamp R. Anticoagulant-associated intracranial hemorrhage in the era of reversal agents. Stroke. 2017; 48(5):1432–1437. [PubMed: 28400486]
40. Schmaier AH. Medically-induced hemophilia C to treat thrombosis. Thromb Res. 2015; 136(2): 185–6. [PubMed: 26024825]
41. He R, Chen D, He S. Factor XI: hemostasis, thrombosis, and antithrombosis. Thromb Res. 2012; 129(5):541–50. [PubMed: 22197449]

42. Emsley J, McEwan PA, Gailani D. Structure and function of factor XI. Blood. 2010; 115(13): 2569–77. [PubMed: 20110423]
43. Gailani D, Smith SB. Structural and functional features of factor XI. J Thromb Haemost. 2009; 7(Suppl 1):75–8. [PubMed: 19630773]
44. Baglia FA, Walsh PN. A binding site for thrombin in the apple 1 domain of factor XI. J Biol Chem. 1996; 271:3652–8. [PubMed: 8631976]
45. Renne T, Gailani D, Meijers JC, Muller-Esterl W. Characterization of the H-kininogen-binding site on factor XI: a comparison of factor XI and plasma prekallikrein. J Biol Chem. 2002; 277:4892–9. [PubMed: 11733491]
46. Baglia FA, Gailani D, Lopez JA, Walsh PN. Identification of a binding site for glycoprotein Ibalpha in the Apple 3 domain of factor XI. J Biol Chem. 2004; 279:45470–6. [PubMed: 15317813]
47. Sun MF, Zhao M, Gailani D. Identification of amino acids in the factor XI apple 3 domain required for activation of factor IX. J Biol Chem. 1999; 274:36373–8. [PubMed: 10593931]
48. Ho DH, Badellino K, Baglia FA, Walsh PN. A binding site for heparin in the apple 3 domain of factor XI. J Biol Chem. 1998; 273:16382–90. [PubMed: 9632702]
49. Baglia FA, Jameson BA, Walsh PN. Identification and characterization of a binding site for factor XIIa in the Apple 4 domain of coagulation factor XI. J Biol Chem. 1993; 268:3838–44. [PubMed: 8440679]
50. Fujikawa K, Chung DW, Hendrickson LE, Davie EW. Amino acid sequence of human factor XI, a blood coagulation factor with four tandem repeats that are highly homologous with plasma prekallikrein. Biochemistry. 1986; 25:2417–24. [PubMed: 3636155]
51. Drag M, Salvesen GS. Emerging principles in protease-based drug discovery. Nat Rev Drug Discov. 2010; 9(9):690–701. [PubMed: 20811381]
52. Rawlings ND, Waller M, Barrett AJ, Bateman A. MEROPS: the database of proteolytic enzymes, their substrates and inhibitors. Nucleic Acids Res. 2014; 42:D503–D509. [PubMed: 24157837]
53. Naito K, Fujikawa K. Activation of human blood coagulation factor XI independent of factor XII. Factor XI is activated by thrombin and factor XIa in the presence of negatively charged surfaces. J Biol Chem. 1991; 266:7353–8. [PubMed: 2019570]
54. Kravtsov DV, Matafonov A, Tucker EI, Sun MF, Walsh PN, Gruber A, Gailani D. Factor XI contributes to thrombin generation in the absence of factor XII. Blood. 2009; 114:452–8. [PubMed: 19351955]
55. Bouma BN, Griffin JH. Human blood coagulation factor XI. Purification, properties, and mechanism of activation by activated factor XII. J Biol Chem. 1977; 252:6432–7. [PubMed: 893417]
56. Yang L, Sun MF, Gailani D, Rezaie AR. Characterization of a heparin-binding site on the catalytic domain of factor XIa: mechanism of heparin acceleration of factor XIa inhibition by the serpins antithrombin and C1-inhibitor. Biochemistry. 2009; 48:1517–24. [PubMed: 19178150]
57. Zhang J, Tu Y, Lu L, Lasky N, Broze GJ Jr. Protein Z-dependent protease inhibitor deficiency produces a more severe murine phenotype than protein Z deficiency. Blood. 2008; 111:4973–8. [PubMed: 18344422]
58. Al-Horani RA, Desai UR. Designing allosteric inhibitors of factor XIa. Lessons from the interactions of sulfated pentagalloylglucopyranosides. J Med Chem. 2014; 57(11):4805–4818. [PubMed: 24844380]
59. Sinha D, Badellino KO, Marcinkiewicz M, Walsh PN. Allosteric modification of factor XIa functional activity upon binding to polyanions. Biochemistry. 2004; 43:7593–7600. [PubMed: 15182201]
60. Whelihan MF, Orfeo T, Gissel MT, Mann KG. Coagulation procofactor activation by factor XIa. J Thromb Haemost. 2010; 8:1532–1539. [PubMed: 20456758]
61. Matafonov A, Cheng Q, Geng Y, Verhamme IM, Umunakwe O, Tucker EI, Sun MF, Serebrov V, Gruber A, Gailani D. Evidence of factor IX-independent roles for factor XIa in blood coagulation. J Thromb Haemost. 2013; 11:2118–2127. [PubMed: 24152424]

62. Puy C, Tucker EI, Matafonov A, Cheng Q, Zientek KD, Gailani D, Gruber A, McCarty OJ. Activated factor XI increases the procoagulant activity of the extrinsic pathway by inactivating tissue factor pathway inhibitor. Blood. 2015; 125(9):1488–96. [PubMed: 25587039]

63. James P, Salomon O, Mikovic D, Peyvandi F. Rare bleeding disorders – bleeding assessment tools, laboratory aspects and phenotype and therapy of FXI deficiency. Haemophilia. 2014; 20(Suppl 4): 71–75. [PubMed: 24762279]

64. Seligsohn U. Factor XI deficiency in humans. J Thromb Haemost. 2009; 7(Suppl 1):84–87. [PubMed: 19630775]

65. Salomon O, Steinberg DM, Seligshon U. Variable bleeding manifestations characterize different types of surgery in patients with severe factor XI deficiency enabling parsimonious use of replacement therapy. Haemophilia. 2006; 12:490–493. [PubMed: 16919078]

66. Salomon O, Steinberg DM, Koren-Morag N, Tanne D, Seligsohn U. Reduced incidence of ischemic stroke in patients with severe factor XI deficiency. Blood. 2008; 111:4113–4117. [PubMed: 18268095]

67. Salomon O, Steinberg DM, Zucker M, Varon D, Zivelin A, Seligsohn U. Patients with severe factor XI deficiency have a reduced incidence of deep-vein thrombosis. Thromb Haemost. 2011; 105(2): 269–73. [PubMed: 21057700]

68. Meijers JC, Tekelenburg WL, Bouma BN, Bertina RM, Rosendaal FR. High levels of coagulation factor XI as a risk factor for venous thrombosis. N Engl J Med. 2000; 342(10):696–701. [PubMed: 10706899]

69. Yang DT, Flanders MM, Kim H, Rodgers GM. Elevated factor XI activity levels are associated with an increased odds ratio for cerebrovascular events. Am J Clin Pathol. 2006; 126:411–415. [PubMed: 16880142]

70. Suri MF, Yamagishi K, Aleksic N, Hannan PJ, Folsom AR. Novel hemostatic factor levels and risk of ischemic stroke: the Atherosclerosis Risk in Communities (ARIC) Study. Cerebrovasc Dis. 2010; 29:497–502. [PubMed: 20299790]

71. Siegerink B, Govers-Riemslag JW, Rosendaal FR, Ten Cate H, Algra A. Intrinsic coagulation activation and the risk of arterial thrombosis in young women: results from the Risk of Arterial Thrombosis in relation to Oral contraceptives (RATIO) case-control study. Circulation. 2010; 122:1854–1861. [PubMed: 20956210]

72. Doggen CJ, Rosendaal FR, Meijers JC. Levels of intrinsic coagulation factors and the risk of myocardial infarction among men: Opposite and synergistic effects of factors XI and XII. Blood. 2006; 108:4045–4051. [PubMed: 16931632]

73. Berliner JI, Rybicki AC, Kaplan RC, Monrad ES, Freeman R, Billett HH. Elevated levels of Factor XI are associated with cardiovascular disease in women. Thromb Res. 2002; 107:55–60. [PubMed: 12413590]

74. Wang X1, Cheng Q, Xu L, Feuerstein GZ, Hsu MY, Smith PL, Seiffert DA, Schumacher WA, Ogletree ML, Gailani D. Effects of factor IX or factor XI deficiency on ferric chloride induced carotid artery occlusion in mice. J Thromb Haemost. 2005; 3:695–702. [PubMed: 15733058]

75. Wang X, Smith PL, Hsu MY, Gailani D, Schumacher WA, Ogletree ML, Seiffert DA. Effects of factor XI deficiency on ferric chloride-induced vena cava thrombosis in mice. J Thromb Haemost. 2006; 4:1982–8. [PubMed: 16961605]

76. Rosen ED, Gailani D, Castellino FJ. FXI is essential for thrombus formation following $FeCl_3$-induced injury of the carotid artery in the mouse. Thromb Haemost. 2002; 87:774–776. [PubMed: 12008966]

77. Schumacher WA, Seiler SE, Steinbacher TE, Stewart AB, Bostwick JS, Hartl KS, Liu EC, Ogletree ML. Antithrombotic and hemostatic effects of a small molecule factor XIa inhibitor in rats. Eur J Pharmacol. 2007; 570(1–3):167–74. [PubMed: 17597608]

78. Yamashita A, Nishihira K, Kitazawa T, Yoshihashi K, Soeda T, Esaki K, Imamura T, Hattori K, Asada Y. Factor XI contributes to thrombus propagation on injured neointima of the rabbit iliac artery. J Thromb Haemost. 2006; 4:1496–1501. [PubMed: 16839345]

79. Gruber A, Hanson SR. Factor XI-dependence of surface- and tissue factor-initiated thrombus propagation in primates. Blood. 2003; 102:953–955. [PubMed: 12689935]

80. Tucker EI, Marzec UM, White TC, Hurst S, Rugonyi S, Mccarty OJ, Gailani D, Gruber A, Hanson SR. Prevention of vascular graft occlusion and thrombus-associated thrombin generation by inhibition of factor XI. Blood. 2009; 113:936–944. [PubMed: 18945968]

81. Pedicord DL, Seiffert D, Blat Y. Substrate-dependent modulation of the mechanism of factor XIa inhibition. Biochemistry. 2004; 43(37):11883–8. [PubMed: 15362874]

82. Al-Horani RA, Desai UR. Recent advances on plasmin inhibitors for the treatment of fibrinolysis-related disorders. Med Res Rev. 2014; 34(6):1168–216. [PubMed: 24659483]

83. Korneeva VA, Trubetskov MM, Korshunova AV, Lushchekina SV, Kolyadko VN, Sergienko OV, Lunin VG, Panteleev MA, Ataullakhanov FI. Interactions outside the proteinase-binding loop contribute significantly to the inhibition of activated coagulation factor XII by its canonical inhibitor from corn. J Biol Chem. 2014; 289(20):14109–20. [PubMed: 24706752]

84. Ma D, Mizurini DM, Assumpção TC, Li Y, Qi Y, Kotsyfakis M, Ribeiro JM, Monteiro RQ, Francischetti IM. Desmolaris, a novel factor XIa anticoagulant from the salivary gland of the vampire bat (Desmodus rotundus) inhibits inflammation and thrombosis in vivo. Blood. 2013; 122:4094–4106. [PubMed: 24159172]

85. Jin L, Pandey P, Babine RE, Gorga JC, Seidl KJ, Gelfand E, Weaver DT, Abdel-Meguid SS, Strickler JE. Crystal structures of the FXIa catalytic domain in complex with ecotin mutants reveal substrate-like interactions. J Biol Chem. 2005; 280(6):4704–12. [PubMed: 15545266]

86. Seymour JL, Lindquist RN, Dennis MS, Moffat B, Yansura D, Reilly D, Wessinger ME, Lazarus RA. Ecotin is a potent anticoagulant and reversible tight-binding inhibitor of factor Xa. Biochemistry. 1994; 33(13):3949–58. [PubMed: 8142399]

87. Chen W, Carvalho LP, Chan MY, Kini RM, Kang TS. Fasxiator, a novel factor XIa inhibitor from snake venom, and its site-specific mutagenesis to improve potency and selectivity. J Thromb Haemost. 2015; 13(2):248–61. [PubMed: 25418421]

88. Delaria KA, Muller DK, Marlor CW, Brown JE, Das RC, Roczniak SO, Tamburini PP. Characterization of placental bikunin, a novel human serine protease inhibitor. J Biol Chem. 1997; 272(18):12209–14. [PubMed: 9115295]

89. Decrem Y, Rath G, Blasioli V, Cauchie P, Robert S, Beaufays J, Frère JM, Feron O, Dogné JM, Dessy C, Vanhamme L, Godfroid E. Ir-CPI, a coagulation contact phase inhibitor from the tick Ixodes ricinus, inhibits thrombusformation without impairing hemostasis. J Exp Med. 2009; 206(11):2381–95. [PubMed: 19808248]

90. Li D, He Q, Kang T, Yin H, Jin X, Li H, Gan W, Yang C, Hu J, Wu Y, Peng L. Identification of an anticoagulant peptide that inhibits both fXIa and fVIIa/tissue factor from the blood-feeding nematode Ancylostoma caninum. Biochem Biophys Res Commun. 2010; 392:155–159. [PubMed: 20059979]

91. Gan W, Deng L, Yang C, He Q, Hu J, Yin H, Jin X, Lu C, Wu Y, Peng L. An anticoagulant peptide from the human hookworm, Ancylostoma duodenale that inhibits coagulation factors Xa and XIa. FEBS Lett. 2009; 583(12):1976–80. [PubMed: 19446556]

92. Scandura JM, Zhang Y, Van Nostrand WE, Walsh PN. Progress curve analysis of the kinetics with which blood coagulation factor XIa is inhibited by protease nexin-2. Biochemistry. 1997; 36(2): 412–420. [PubMed: 9003194]

93. Smith RP, Higuchi DA, Broze GJ. Platelet coagulation factor XIa-inhibitor, a form of Alzheimer amyloid precursor protein. Science. 1990; 248(4959):1126–1128. [PubMed: 2111585]

94. Petersen LC, Bjørn SE, Norris F, Norris K, Sprecher C, Foster DC. Expression, purification and characterization of a Kunitz-type protease inhibitor domain from human amyloid precursor protein homolog. FEBS Lett. 1994; 338(1):53–7. [PubMed: 8307156]

95. Navaneetham D, Jin L, Pandey P, Strickler JE, Babine RE, Abdel-Meguid SS, Walsh PN. Structural and mutational analyses of the molecular interactions between the catalytic domain of factor XIa and the Kunitz protease inhibitor domain of protease nexin 2. J Biol Chem. 2005; 280(43):36165–36175. [PubMed: 16085935]

96. Dennis MS, Herzka A, Lazarus RA. Potent and selective Kunitz domain inhibitors of plasma kallikrein designed by phage display. J Biol Chem. 1995; 270(43):25411–7. [PubMed: 7592708]

97. Tsujimoto H, Kotsyfakis M, Francischetti IM, Eum JH, Strand MR, Champagne DE. Simukunin from the salivary glands of the black fly Simulium vittatum inhibits enzymes that regulate clotting and inflammatory responses. PLoS One. 2012; 7:e29964. [PubMed: 22383955]

98. Bajaj MS, Ogueli GI, Kumar Y, Vadivel K, Lawson G, Shanker S, Schmidt AE, Bajaj SP. Engineering kunitz domain 1 (KD1) of human tissue factor pathway inhibitor-2 to selectively inhibit fibrinolysis: properties of KD1-L17R variant. J Biol Chem. 2011; 286(6):4329–40. [PubMed: 21115497]

99. Kong D, Ma D, Bai H, Guo H, Cai X, Mo W, Tang Q, Song H. Expression and characterization of the first kunitz domain of human tissue factor pathway inhibitor-2. Biochem Biophys Res Commun. 2004; 324:1179–1185. [PubMed: 15504338]

100. Petersen LC, Sprecher CA, Foster DC, Blumberg H, Hamamoto T, Kisiel W. Inhibitory properties of a novel human Kunitz-type protease inhibitor homologous to tissue factor pathway inhibitor. Biochemistry. 1996; 35(1):266–72. [PubMed: 8555184]

101. Chand HS, Schmidt AE, Bajaj SP, Kisiel W. Structure-function analysis of the reactive site in the first Kunitz-type domain of human tissue factor pathway inhibitor-2. J Biol Chem. 2004; 279(17):17500–7. [PubMed: 14970225]

102. Jin L, Pandey P, Babine RE, Weaver DT, Abdel-Meguid SS, Strickler JE. Mutation of surface residues to promote crystallization of activated factor XI as a complex with benzamidine: an essential step for the iterative structure-based design of factor XI inhibitors. Acta Crystallogr D Biol Crystallogr. 2005; 61(Pt 10):1418–25. [PubMed: 16204896]

103. Deng H, Bannister TD, Jin L, Babine RE, Quinn J, Nagafuji P, Celatka CA, Lin J, Lazarova TI, Rynkiewicz MJ, Bibbins F, Pandey P, Gorga J, Meyers HV, Abdel-Meguid SS, Strickler JE. Synthesis, SAR exploration, and X-ray crystal structures of factor XIa inhibitors containing an α-ketothiazole arginine. Bioorg Med Chem Lett. 2006; 16(11):3049–3054. [PubMed: 16524727]

104. Lin J, Deng H, Jin L, Pandey P, Quinn J, Cantin S, Rynkiewicz MJ, Gorga JC, Bibbins F, Celatka CA, Nagafuji P, Bannister TD, Meyers HV, Babine RE, Hayward NJ, Weaver D, Benjamin H, Stassen F, Abdel-Meguid SS, Strickler JE. Design, synthesis, and biological evaluation of peptidomimetic inhibitors of factor XIa as novel anticoagulants. J Med Chem. 2006; 49(26): 7781–7791. [PubMed: 17181160]

105. Lazarova TI, Jin L, Rynkiewicz M, Gorga JC, Bibbins F, Meyers HV, Babine R, Strickler J. Synthesis and in vitro biological evaluation of aryl boronic acids as potential inhibitors of factor XIa. Bioorg Med Chem Lett. 2006; 16(19):5022–5027. [PubMed: 16876411]

106. Buchanan MS, Carroll AR, Wessling D, Jobling M, Avery VM, Davis RA, Feng Y, Xue Y, Oster L, Fex T, Deinum J, Hooper JN, Quinn RJ. Clavatadine A, a natural product with selective recognition and irreversible inhibition of factor XIa. J Med Chem. 2008; 51(12):3583–3587. [PubMed: 18510371]

107. Buchanan MS, Carroll AR, Wessling D, Jobling M, Avery VM, Davis RA, Feng Y, Hooper JN, Quinn RJ. Clavatadines C-E, guanidine alkaloids from the Australian sponge *Suberea clavata*. J Nat Prod. 2009; 72(5):973–975. [PubMed: 19379003]

108. Wong PC, Crain EJ, Watson CA, Schumacher WA. A small-molecule factor XIa inhibitor produces antithrombotic efficacy with minimal bleeding time prolongation in rabbits. J Thromb Thrombolysis. 2011; 32(2):129–37. [PubMed: 21614454]

109. [Accessed 14 January 2018] Study to evaluate safety, PK and PD of single and multiple ascending doses of EP-7041 in healthy subjects (Identifier: NCT02914353). https://clinicaltrials.gov

110. Hayward NJ, Goldberg DI, Morrel EM, Friden PM, Bokesch PM. Phase 1a/1b study of EP-7041: A novel, potent, selective, small molecule FXIa inhibitor. Circulation. 2017; 136:A13747.

111. Hanessian S, Larsson A, Fex T, Knecht W, Blomberg N. Design and synthesis of macrocyclic indoles targeting blood coagulation cascade factor XIa. Bioorg Med Chem Lett. 2010; 20:6925–28. [PubMed: 21035339]

112. Gademann K, Portmann C, Blom JF, Zeder M, Jüttner F. Multiple toxin production in the cyanobacterium microcystis: isolation of the toxic protease inhibitor cyanopeptolin 1020. J Nat Prod. 2010; 73:980–984. [PubMed: 20405925]

113. Saupe SM, Leubner S, Betz M, Klebe G, Steinmetzer T. Development of new cyclic plasmin inhibitors with excellent potency and selectivity. J Med Chem. 2013; 56:820–831. [PubMed: 23294255]

114. Fradera X, Kazemier B, Carswell E, Cooke A, Oubrie A, Hamilton W, Dempster M, Krapp S, Nagel S, Jestel A. High-resolution crystal structures of factor XIa coagulation factor in complex with nonbasic high-affinity synthetic inhibitors. Acta Crystallogr Sect F Struct Biol Cryst Commun. 2012; 68(Pt 4):404–8.

115. Smith LM 2nd, Orwat MJ, Hu Z, Han W, Wang C, Rossi KA, Gilligan PJ, Pabbisetty KB, Osuna H, Corte JR, Rendina AR, Luettgen JM, Wong PC, Narayanan R, Harper TW, Bozarth JM, Crain EJ, Wei A, Ramamurthy V, Morin PE, Xin B, Zheng J, Seiffert DA, Quan ML, Lam PY, Wexler RR, Pinto DJ. Novel phenylalanine derived diamides as factor XIa inhibitors. Bioorg Med Chem Lett. 2016; 26(2):472–478. [PubMed: 26704266]

116. Quan ML, Wong PC, Wang C, Woerner F, Smallheer JM, Barbera FA, Bozarth JM, Brown RL, Harpel MR, Luettgen JM, Morin PE, Peterson T, Ramamurthy V, Rendina AR, Rossi KA, Watson CA, Wei A, Zhang G, Seiffert D, Wexler RR. Tetrahydroquinoline derivatives as potent and selective factor XIa inhibitors. J Med Chem. 2014; 57(3):955–969. [PubMed: 24405333]

117. Wong PC, Quan ML, Watson CA, Crain EJ, Harpel MR, Rendina AR, Luettgen JM, Wexler RR, Schumacher WA, Seiffert DA. In vitro, antithrombotic and bleeding time studies of BMS-654457, a small-molecule, reversible and direct inhibitor of factor XIa. J Thromb Thrombolysis. 2015; 40(4):416–23. [PubMed: 26249722]

118. Fjellström O, Akkaya S, Beisel HG, Eriksson PO, Erixon K, Gustafsson D, Jurva U, Kang D, Karis D, Knecht W, Nerme V, Nilsson I, Olsson T, Redzic A, Roth R, Sandmark J, Tigerström A, Öster L. Creating novel activated factor XI inhibitors through fragment based lead generation and structure aided drug design. PLoS One. 2015; 10(1):e0113705. [PubMed: 25629509]

119. Pinto DJP, Orwat MJ, Smith LM Ii, Quan ML, Lam PYS, Rossi KA, Apedo A, Bozarth JM, Wu Y, Zheng JJ, Xin B, Toussaint N, Stetsko P, Gudmundsson O, Maxwell BD, Crain EJ, Wong PC, Lou Z, Harper TW, Chacko SA, Myers JE, Sheriff S, Zhang H, Hou X, Mathur A, Seiffert DA, Wexler RR, Luettgen JM, Ewing WR. Discovery of a parenteral small molecule coagulation Factor XIa inhibitor clinical candidate (BMS-962212). J Med Chem. 2017; doi: 10.1021/acs.jmedchem.7b01171

120. Luettgen JM, Wong PC, Perera V, Wang Z, Russo C, Chen W, Dorizio SM, Frost CE, Dierks E, Pinto DJP, Ewing WR, Wexler RR, DeSouza MM, LaCreta FP, Gordon DA, Seiffert DA, Frost RJ. Preclinical and early clinical characterization of a parenterally administered direct factor XIa inhibitor. Stroke. 2017; 48:TMP117.

121. Perera V, Frost CE, Yones CL, Wang Z, Dorizio S, Russo C, Chen W, Ueno T, Akimoto M, Cirincione B, Xu X, Seiffert DA, Desouza MM, Mugnier P, LaCreta F, Frost RJ. Pharmacokinetics, pharmacodynamics, safety and tolerability of a novel factor XIa inhibitor administered as IV infusion in non-Japanese and japanese healthy subjects. American Society for Clinical Pharmacology and Therapeutics Clin Pharmacol Ther. 2017; 101:S5–S99.

122. Hangeland JJ, Friends TJ, Rossi KA, Smallheer JM, Wang C, Sun Z, Corte JR, Fang T, Wong PC, Rendina AR, Barbera FA, Bozarth JM, Luettgen JM, Watson CA, Zhang G, Wei A, Ramamurthy V, Morin PE, Bisacchi GS, Subramaniam S, Arunachalam P, Mathur A, Seiffert DA, Wexler RR, Quan ML. Phenylimidazoles as potent and selective inhibitors of coagulation factor XIa with in vivo antithrombotic activity. J Med Chem. 2014; 57(23):9915–32. [PubMed: 25405503]

123. Pinto DJ, Smallheer JM, Corte JR, Austin EJ, Wang C, Fang T, Smith LM 2nd, Rossi KA, Rendina AR, Bozarth JM, Zhang G, Wei A, Ramamurthy V, Sheriff S, Myers JE Jr, Morin PE, Luettgen JM, Seiffert DA, Quan ML, Wexler RR. Structure-based design of inhibitors of coagulation factor XIa with novel P1 moieties. Bioorg Med Chem Lett. 2015; 25(7):1635–1642. [PubMed: 25728130]

124. Hu Z, Wong PC, Gilligan PJ, Han W, Pabbisetty KB, Bozarth JM, Crain EJ, Harper T, Luettgen JM, Myers JE Jr, Ramamurthy V, Rossi KA, Sheriff S, Watson CA, Wei A, Zheng JJ, Seiffert DA, Wexler RR, Quan ML. Discovery of a Potent Parenterally Administered Factor XIa Inhibitor with Hydroxyquinolin-2(1H)-one as the P2′ Moiety. ACS Med Chem Lett. 2015; 6(5):590–595. [PubMed: 26005539]

125. Corte JR, Fang T, Osuna H, Pinto DJ, Rossi KA, Myers JE, Sheriff S, Lou Z, Zheng JJ, Harper TW, Bozarth JM, Wu Y, Luettgen JM, Seiffert DA, Decicco CP, Wexler RR, Quan ML. Structure-based design of macrocyclic factor XIa inhibitors: Discovery of the macrocyclic amide linker. J Med Chem. 2017; 60(3):1060–1075. [PubMed: 28085275]

126. Marsault E, Peterson ML. Macrocycles are great cycles: applications, opportunities, and challenges of synthetic macrocycles in drug discovery. J Med Chem. 2011; 54:1961–2004. [PubMed: 21381769]

127. Mallinson J, Collins I. Macrocycles in new drug discovery. Future Med Chem. 2012; 4:1409–38. [PubMed: 22857532]

128. Nantermet PG, Barrow JC, Newton CL, Pellicore JM, Young M, Lewis SD, Lucas BJ, Krueger JA, McMasters DR, Yan Y, Kuo LC, Vacca JP, Selnick HG. Design and synthesis of potent and selective macrocyclic thrombin inhibitors. Bioorg Med Chem Lett. 2003; 13:2781–2784. [PubMed: 12873514]

129. Priestley ES, Cheney DL, DeLucca I, Wei A, Luettgen JM, Rendina AR, Wong PC, Wexler RR. Structure-based design of macrocyclic coagulation factor VIIa inhibitors. J Med Chem. 2015; 58:6225–6236. [PubMed: 26151189]

130. Corte JR, Yang W, Fang T, Wang Y, Osuna H, Lai A, Ewing WR, Rossi KA, Myers JE Jr, Sheriff S, Lou Z, Zheng JJ, Harper TW, Bozarth JM, Wu Y, Luettgen JM, Seiffert DA, Quan ML, Wexler RR, Lam PYS. Macrocyclic inhibitors of factor XIa: Discovery of alkyl-substituted macrocyclic amide linkers with improved potency. Bioorg Med Chem Lett. 2017; 27(16):3833–3839. [PubMed: 28687203]

131. Wang X, Kurowski S, Wu W, Castriota GA, Zhou X, Chu L, Ellsworth KP, Chu D, Edmondson S, Ali A, Andre P, Seiffert D, Erion M, Gutstein DE, Chen Z. Inhibition of factor XIa reduces the frequency of cerebral microembolic signals derived from carotid arterial thrombosis in rabbits. J Pharmacol Exp Ther. 2017; 360(3):476–483. [PubMed: 28035007]

132. Corte JR, Fang T, Hangeland JJ, Friends TJ, Rendina AR, Luettgen JM, Bozarth JM, Barbera FA, Rossi KA, Wei A, Ramamurthy V, Morin PE, Seiffert DA, Wexler RR, Quan ML. Pyridine and pyridinone-based factor XIa inhibitors. Bioorg Med Chem Lett. 2015; 25(4):925–930. [PubMed: 25592713]

133. Corte JR, Fang T, Pinto DJ, Orwat MJ, Rendina AR, Luettgen JM, Rossi KA, Wei A, Ramamurthy V, Myers JE Jr, Sheriff S, Narayanan R, Harper TW, Zheng JJ, Li YX, Seiffert DA, Wexler RR, Quan ML. Orally bioavailable pyridine and pyrimidine-based factor XIa inhibitors: Discovery of the methyl N-phenyl carbamate P2 prime group. Bioorg Med Chem. 2016; 24(10): 2257–2272. [PubMed: 27073051]

134. Nar H, Bauer M, Schmid A, Stassen JM, Wienen W, Priepke HW, Kauffmann IK, Ries UJ, Hauel NH. Structural basis for inhibition promiscuity of dual specific thrombin and factor Xa blood coagulation inhibitors. Structure. 2001; 9(1):29–37. [PubMed: 11342132]

135. Hanessian S, Therrien E, Granberg K, Nilsson I. Targeting thrombin and factor VIIa: design, synthesis, and inhibitory activity of functionally relevant indolizidinones. Bioorg Med Chem Lett. 2002; 12(20):2907–11. [PubMed: 12270173]

136. Qiao JX, Wang TC, Wang GZ, Cheney DL, He K, Rendina AR, Xin B, Luettgen JM, Knabb RM, Wexler RR, Lam PY. Enantiopure five-membered cyclicdiamine derivatives as potent and selective inhibitors of factor Xa. Improving in vitro metabolic stability via core modifications. Bioorg Med Chem Lett. 2007; 17(18):5041–8. [PubMed: 17643988]

137. Shi Y, O'Connor SP, Sitkoff D, Zhang J, Shi M, Bisaha SN, Wang Y, Li C, Ruan Z, Lawrence RM, Klei HE, Kish K, Liu EC, Seiler SM, Schweizer L, Steinbacher TE, Schumacher WA, Robl JA, Macor JE, Atwal KS, Stein PD. Arylsulfonamidopiperidone derivatives as a novel class of factor Xa inhibitors. Bioorg Med Chem Lett. 2011; 21(24):7516–21. [PubMed: 22041058]

138. Shiraishi T, Kadono S, Haramura M, Kodama H, Ono Y, Iikura H, Esaki T, Koga T, Hattori K, Watanabe Y, Sakamoto A, Yoshihashi K, Kitazawa T, Esaki K, Ohta M, Sato H, Kozono T. Factor VIIa inhibitors: target hopping in the serine protease family using X-ray structure determination. Bioorg Med Chem Lett. 2008; 18(16):4533–7. [PubMed: 18674905]

139. Bach P, Knerr L, Fjellström O, Hansson K, Mattsson C, Gustafsson D. Design, synthesis, and SAR of a series of activated protein C (APC) inhibitors with selectivity against thrombin for the treatment of haemophilia. Bioorg Med Chem Lett. 2014; 24(3):821–7. [PubMed: 24418773]

140. Bolton SA, Sutton JC, Anumula R, Bisacchi GS, Jacobson B, Slusarchyk WA, Treuner UD, Wu SC, Zhao G, Pi Z, Sheriff S, Smirk RA, Bisaha S, Cheney DL, Wei A, Schumacher WA, Hartl KS, Liu E, Zahler R, Seiler SM. Discovery of nonbenzamidine factor VIIa inhibitors using a biaryl acid scaffold. Bioorg Med Chem Lett. 2013; 23(18):5239–43. [PubMed: 23927973]
141. Obaidullah AJ, Al-Horani RA. Discovery of chromen-7-yl furan-2-carboxylate as a potent and selective factor XIa inhibitor. Cardiovasc Hematol Agents Med Chem. 2017; 15(1):40–8. [PubMed: 28552062]
142. Dietrich W, Nicklisch S, Koster A, Spannagl M, Giersiefen H, van de Locht A. CU-2010-a novel small molecule protease inhibitor with antifibrinolytic and anticoagulant properties. Anesthesiology. 2009; 110:123–130. [PubMed: 19104179]
143. Steinmetzer T, Schweinitz A, Stuerzebecher J, Steinmetzer P, Soffing A, Van deLocht A, Nicklisch S, Reichelt C, Ludwig F-A, Schulze A, Daghisch M, Heinicke J. Trypsin-like serine protease inhibitors, and their preparation and use. US Patent Application. 20100022781. 2010.
144. Szabo G, Veres G, Radovits T, Haider H, Krieger N, Bahrle S, Miesel-Groschel C, Niklisch S, Karck M, van de Locht A. Effects of novel synthetic serine protease inhibitors on postoperative blood loss, coagulation parameters, and vascular relaxation after cardiac surgery. J Thorac Cardiovasc Surg. 2010; 139:181–188. [PubMed: 20106364]
145. Mulloy B, Hogwood J, Gray E, Lever R, Page CP. Pharmacology of heparin and related drugs. Pharmacol Rev. 2016; 68(1):76–141. [PubMed: 26672027]
146. Gandhi NS, Mancera RL. The structure of glycosaminoglycans and their interactions with proteins. Chem Biol Drug Des. 2008; 72:455–482. [PubMed: 19090915]
147. Vaidyanathan D, Williams A, Dordick JS, Koffas MAG, Linhardt RJ. Engineered heparins as new anticoagulant drugs. Bioeng Transl Med. 2017; 2(1):17–30. [PubMed: 28516163]
148. Rezaie AR, Sun MF, Gailani D. Contributions of basic amino acids in the autolysis loop of factor XIa to serpin specificity. Biochemistry. 2006; 45(31):9427–33. [PubMed: 16878977]
149. Al-Horani RA, Ponnusamy P, Mehta AY, Gailani D, Desai UR. Sulfated pentagalloylglucoside is a potent, allosteric, and selective inhibitor of factor XIa. J Med Chem. 2013; 56(3):867–878. [PubMed: 23316863]
150. Al-Horani RA, Gailani D, Desai UR. Allosteric inhibition of factor XIa. Sulfated non-saccharide glycosaminoglycan mimetics as promising anticoagulants. Thromb Res. 2015; 136(2):379–87. [PubMed: 25935648]
151. Henry BL, Thakkar JN, Liang A, Desai UR. Sulfated, low molecular weight lignins inhibit a select group of heparin-binding serine proteases. Biochem Biophys Res Commun. 2012; 417(1): 382–6. [PubMed: 22155248]
152. Monien BH, Henry BL, Raghuraman A, Hindle M, Desai UR. Novel chemo-enzymatic oligomers of cinnamic acids as direct and indirect inhibitors of coagulation proteinases. Bioorg Med Chem. 2006; 14(23):7988–98. [PubMed: 16914317]
153. Karuturi R, Al-Horani RA, Mehta SC, Gailani D, Desai UR. Discovery of allosteric modulators of factor XIa by targeting hydrophobic domains adjacent to its heparin-binding site. J Med Chem. 2013; 56(6):2415–2428. [PubMed: 23451707]
154. Argade MD, Mehta AY, Sarkar A, Desai UR. Allosteric inhibition of human factor XIa: Discovery of monosulfated benzofurans as a class of promising inhibitors. J Med Chem. 2014; 57(8):3559–3569. [PubMed: 24666186]
155. Verespy S 3rd, Mehta AY, Afosah D, Al-Horani RA, Desai UR. Allosteric partial inhibition of monomeric proteases. Sulfated coumarins induce regulation, not just inhibition, of thrombin. Sci Rep. 2016; 6:24043. [PubMed: 27053426]
156. Sidhu PS, Zhou Q, Desai UR. A simple, general approach of allosteric coagulation enzyme inhibition through monosulfated hydrophobic scaffolds. Bioorg Med Chem Lett. 2014; 24(24): 5716–5720. [PubMed: 25453807]
157. Al-Horani RA, Karuturi R, Verespy S 3rd, Desai UR. Synthesis of glycosaminoglycan mimetics through sulfation of polyphenols. Methods Mol Biol. 2015; 1229:49–67. [PubMed: 25325944]
158. Al-Horani RA, Desai UR. Sulfated inositol-based glycosaminoglycan mimetics are homogeneous, potent, selective, and allosteric inhibitors of factor XIa. Circulation. 2017; 136(Suppl 1):A13636.

159. Sidhu PS, Abdel Aziz MH, Sarkar A, Mehta AY, Zhou Q, Desai UR. Designing allosteric regulators of thrombin. Exosite 2 features multiple subsites that can be targeted by sulfated small molecules for inducing inhibition. J Med Chem. 2013; 56(12):5059–70. [PubMed: 23718540]

160. Yamashita A, Nishihira K, Kitazawa T, Yoshihashi K, Soeda T, Esaki K, Imamura T, Hattori K, Asada Y. Factor XI contributes to thrombus propagation on injured neointima of the rabbit iliac artery. J Thromb Haemost. 2006; 4(7):1496–501. [PubMed: 16839345]

161. Takahashi M, Yamashita A, Moriguchi-Goto S, Sugita C, Matsumoto T, Matsuda S, Sato Y, Kitazawa T, Hattori K, Shima M, Asada Y. Inhibition of factor XI reduces thrombus formation in rabbit jugular vein under endothelial denudation and/or blood stasis. Thromb Res. 2010; 125:464–470. [PubMed: 20089298]

162. Cheng Q, Tucker EI, Pine MS, Sisler I, Matafonov A, Sun MF, White-Adams TC, Smith SA, Hanson SR, McCarty OJ, Renné T, Gruber A, Gailani D. A role for factor XIIa-mediated factor XI activation in thrombus formation in vivo. Blood. 2010; 116:3981–3989. [PubMed: 20634381]

163. Leung PY, Hurst S, Berny-Lang MA, Verbout NG, Gailani D, Tucker EI, Wang RK, McCarty OJ, Gruber A. Inhibition of factor XII-mediated activation of factor XI provides protection against experimental acute ischemic stroke in mice. Transl Stroke Res. 2012; 3:381–9. [PubMed: 23634198]

164. Tucker EI, Verbout NG, Leung PY, Hurst S, McCarty OJ, Gailani D, Gruber A. Inhibition of factor XI activation attenuates inflammation and coagulopathy while improving the survival of mouse polymicrobial sepsis. Blood. 2012; 119:4762–4768. [PubMed: 22442348]

165. Luo D, Szaba FM, Kummer LW, Johnson LL, Tucker EI, Gruber A, Gailani D, Smiley ST. Factor XI-deficient mice display reduced inflammation, coagulopathy, and bacterial growth during listeriosis. Infect Immun. 2012; 80:91–99. [PubMed: 22006565]

166. van Montfoort ML, Knaup VL, Marquart JA, Bakhtiari K, Castellino FJ, Hack CE, Meijers JC. Two novel inhibitory anti-human factor XI antibodies prevent cessation of blood flow in a murine venous thrombosis model. Thromb Haemost. 2013; 110:1065–1073. [PubMed: 23925504]

167. Bayer Pharma, Germany. Preparation of human antibodies capable of binding to the coagulation factor XI and/or its activated form factor XIa for treatment of thrombosis. WO2013167669A1. 2013.

168. David T, Kim YC, Ely LK, Rondon I, Gao H, O'Brien P, Bolt MW, Coyle AJ, Garcia JL, Flounders EA, Mikita T, Coughlin SR. Factor XIa-specific IgG and a reversal agent to probe factor XI function in thrombosis and hemostasis. Sci Transl Med. 2016; 8(353):353ra112.

169. Nakamura M, Takeuchi T, Kawahara T, Hirose J, Nakayama K, Hosaka Y, Furusako S. Simultaneous targeting of CD14 and factor XIa by a fusion protein consisting of an anti-CD14 antibody and the modified second domain of bikunin improves survival in rabbit sepsis models. Eur J Pharmacol. 2017; 802:60–68. [PubMed: 28249709]

170. Kole R, Krainer AR, Altman S. RNA therapeutics: Beyond RNA interference and antisense oligonucleotides. Nat Rev Drug Discov. 2012; 11(2):125–140. [PubMed: 22262036]

171. DeVos SL, Miller TM. Antisense oligonucleotides: treating neurodegeneration at the level of RNA. Neurotherapeutics. 2013; 10:486–497. [PubMed: 23686823]

172. Lippi G, Harenberg J, Mattiuzzi C, Favaloro EJ. Next generation antithrombotic therapy: focus on antisense therapy against coagulation factor XI. Semin Thromb Hemost. 2015; 41:255–262. [PubMed: 25703390]

173. Cosmi B. An update on the pharmaceutical management of thrombosis. Expert Opin Pharmacother. 2016; 12:1–16.

174. Heestermans M, van Vlijmen BJM. Oligonucleotides targeting coagulation factor mRNAs: use in thrombosis and hemophilia research and therapy. Thromb J. 2017; 15:7. [PubMed: 28286423]

175. Zhang H, Löwenberg EC, Crosby JR, MacLeod AR, Zhao C, Gao D, Black C, Revenko AS, Meijers JC, Stroes ES, Levi M, Monia BP. Inhibition of the intrinsic coagulation pathway factor XI by antisense oligonucleotides: a novel antithrombotic strategy with lowered bleeding risk. Blood. 2010; 116:4684–4692. [PubMed: 20807891]

176. van Montfoort ML, Kuijpers MJ, Knaup VL, Bhanot S, Monia BP, Roelofs JJ, Heemskerk JW, Meijers JC. Factor XI regulates pathological thrombus formation on acutely ruptured

atherosclerotic plaques. Arterioscler Thromb Vasc Biol. 2014; 34:1668–1673. [PubMed: 24947525]

177. Younis HS, Crosby J, Huh JI, Lee HS, Rime S, Monia B, Henry SP. Antisense inhibition of coagulation factor XI prolongs APTT without increased bleeding risk in cynomolgus monkeys. Blood. 2012; 119:2401–2408. [PubMed: 22246038]
178. Crosby JR, Marzec U, Revenko AS, Zhao C, Gao D, Matafonov A, Gailani D, MacLeod AR, Tucker EI, Gruber A, Hanson SR, Monia BP. Antithrombotic effect of antisense factor XI oligonucleotide treatment in primates. Arterioscler Thromb Vasc Biol. 2013; 33:1670–1678. [PubMed: 23559626]
179. Que Liu ED, Claudette B, Dessouki E, Grundy J, Monia BP, Bhanot S. Isis-fxirx, a novel and specific antisense inhibitor of factor xi, significantly reduces fxi antigen and activity and increases APTT without causing bleeding in healthy volunteers. Blood. 2011; 118:209.
180. Büller HR, Bethune C, Bhanot S, Gailani D, Monia BP, Raskob GE, Segers A, Verhamme P, Weitz JI. FXI-ASO TKA Investigators. Factor XI antisense oligonucleotide for prevention of venous thrombosis. N Engl J Med. 2015; 372:232–40. [PubMed: 25482425]
181. Yau JW, Liao P, Fredenburgh JC, Stafford AR, Revenko AS, Monia BP, Weitz JI. Selective depletion of factor XI or factor XII with antisense oligonucleotides attenuates catheter thrombosis in rabbits. Blood. 2014; 123:2102–2107. [PubMed: 24501216]
182. Kossmann S, Lagrange J, Jäckel S, Jurk K, Ehlken M, Schönfelder T, Weihert Y, Knorr M, Brandt M, Xia N, Li H, Daiber A, Oelze M, Reinhardt C, Lackner K, Gruber A, Monia B, Karbach SH, Walter U, Ruggeri ZM, Renné T, Ruf W, Münzel T, Wenzel P. Platelet-localized FXI promotes a vascular coagulation-inflammatory circuit in arterial hypertension. Sci Transl Med. 2017; 9(375):eaah4923. [PubMed: 28148841]
183. Donkor DA, Bhakta V, Eltringham-Smith LJ, Stafford AR, Weitz JI, Sheffield WP. Selection and characterization of a DNA aptamer inhibiting coagulation factor XIa. Sci Rep. 2017; 7(1):2102. [PubMed: 28522812]
184. Bethune C, Walsh M, Jung B, Yu R, Geary RS, Bhanot S. Pharmacokinetics and pharmacodynamics of Ionis-FXIRx, an antisense inhibitor of factor XI, in patients with end-stage renal disease on hemodialysis. Blood. 2017; 130:1116.
185. [Accessed 14 January 2018] A study to evaluate the safety and pharmacokinetics of BMS-986177 in participants with end-stage renal dysfunction on chronic stable hemodialysis treatment (Identifier: NCT02902679). https://clinicaltrials.gov
186. Fischer PM. Design of small-molecule active-site inhibitors of the S1A family proteases as procoagulant and anticoagulant drugs. J Med Chem. 2017; doi: 10.1021/acs.jmedchem.7b00772

Biographies

Rami A. Al-Horani is is assistant professor of medicinal chemistry at the Division of Basic Pharmaceutical Sciences of College of Pharmacy in Xavier University of Louisiana. Dr. Al-Horani received his PhD in pharmaceutical sciences from School of Pharmacy of Virginia Commonwealth University. Dr. Al-Horani's research area of interest is the chemical, biochemical, and pharmacological design and development of saccharide and nonsaccharide glycosaminoglycan mimetics which can serve as novel therapeutics to treat cardiovascular diseases, cancer, or viral infections and/or chemical probes to investigate unknown mechanism of physiological and pathologic conditions of significance to human health.

Daniel K. Afosah was born in Accra, Ghana and earned his B.Sc. in Pharmacy in 2007 from the Kwame Nkrumah University of Science and Technology, Kumasi, Ghana. He obtained his M.Sc. in Pharmaceutical Analysis and Quality Control in 2010 at the same university under the supervision of Professor John S. K. Ayim. He worked as a quality control pharmacist at Ernest Chemists Limited, Ghana, and a regulatory officer at the Food and

Drugs Authority, Ghana, before enrolling in PhD Pharmaceutical Sciences program (Medicinal Chemistry) at the Virginia Commonwealth University (VCU) in 2012. He graduated from the program in 2017 under the supervision of Professor Umesh R. Desai and is currently a postdoctoral research fellow at the Department of Medicinal Chemistry and Institute of Structural Biology Drug Discovery and Development, VCU. His research focuses on the study of glycosaminoglycans (GAGs) and their mimetics, and their interaction with GAG-binding proteins.

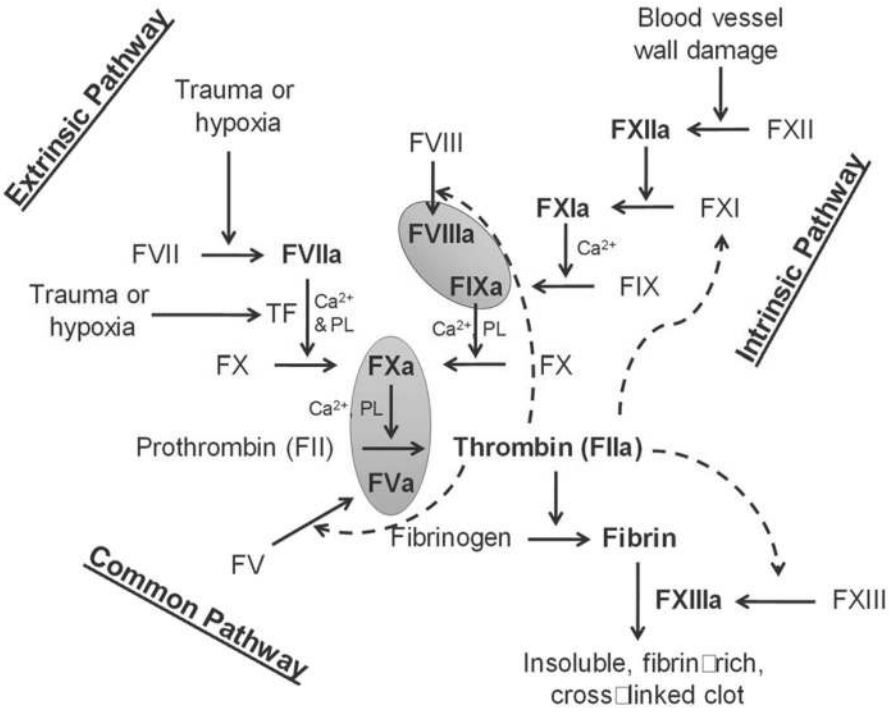

Figure 1. An overview of the coagulation process

The coagulation process is a major player in maintaining hemostasis. The coagulation cascade is a series of chemical bio-transformations that comprises the intrinsic (FXII/XIIa, FXI/XIa, FIX/IXa, and FX/Xa), extrinsic (TF, FVII/FVIIa, and FX/Xa), and common pathways (FX/Xa, FII/IIa, and FXIII/XIIIa). The coagulation process is primarily initiated through the extrinsic pathway. FXa formation is also triggered by the intrinsic coagulation pathway, also known as the contact activation system. Both pathways lead into the common pathway that results in thrombin generation and the formation of insoluble, fibrin-rich, cross-linked clot. Natural anticoagulant proteins (not shown) are also available to regulate the activity of those procoagulant proteins. FXIa is a serine protease in the intrinsic pathway which gets activated by FXIIa and thrombin (in addition to auto-activation) and in turn activates FIX to FIXa. The intrinsic pathway is largely seen to amplify FXa and ultimately thrombin formation through feedback mechanisms, and therefore, to significantly contribute to thrombus formation.

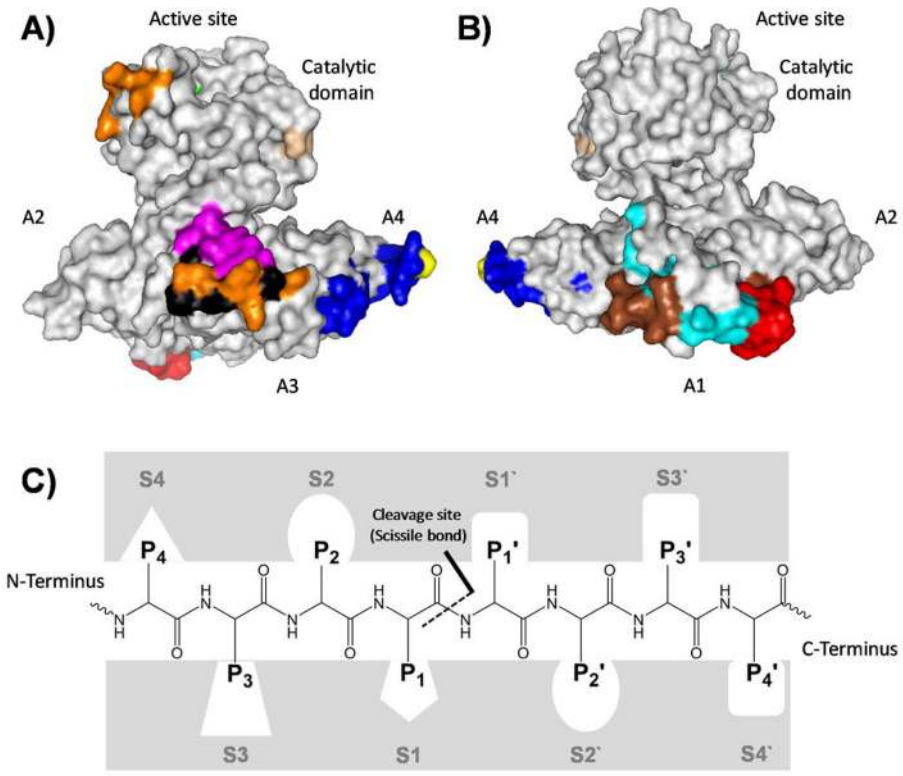

Figure 2. Cartoon depiction of a monomeric human FXI structure (PDB ID: 2F83) showing the "cup and saucer" arrangement

A) A side view showing the catalytic domain involving the active site (green), activation loop cleavage site (tint), and heparin binding site (orange) as well as the apple domains A2 involving some residues important for HK binding, A3 involving FIX binding site (pink), platelet GPIb binding site (black), and heparin binding site (orange), and A4 involving FXIIa binding site (blue) and Cys321 (yellow) for dimerization. B) Another side view showing the catalytic domain, apple domains A2 and A4 as well as apple domain A1 involving thrombin binding site (red and brown) and HK binding site (cyan and brown). C) A representation of the active site subsites of proteases, in this case FXIa. The Schechter and Berger nomenclature is used to number the subsites in the active site of FXIa and the amino acids on the substrate peptide. The system has also been exploited to describe the binding of small molecules to the active site of FXIa. See text for details.

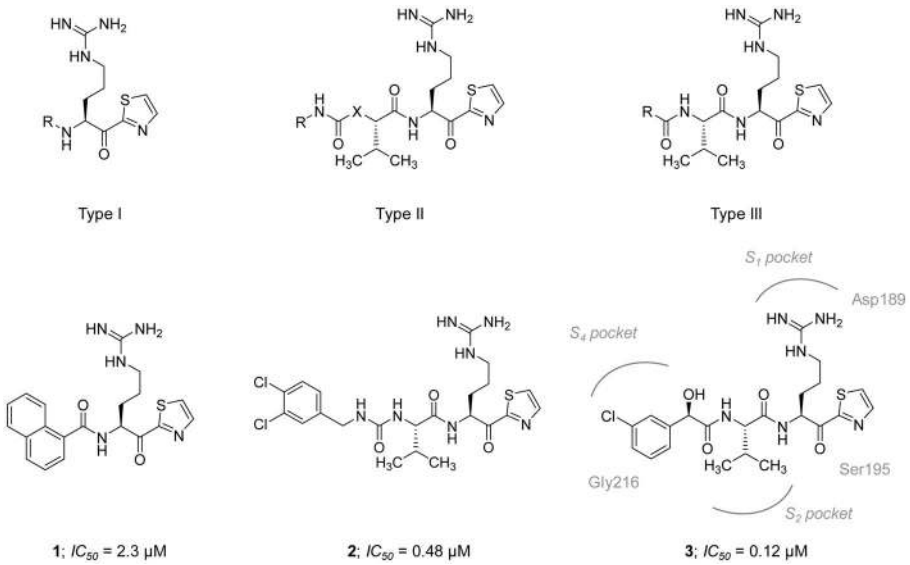

Figure 3. Chemical structures of the early α-ketothiazole guanidine-containing peptidomimetics that act as active site inhibitors of FXIa

Chemical structures of types I-III are provided along with representative inhibitors (**1–3**). The FXIa IC_{50} values are also provided in μM. Interactions between inhibitor **3** and residues in the active site of FXIa are also delineated (PDB ID: 2FDA).

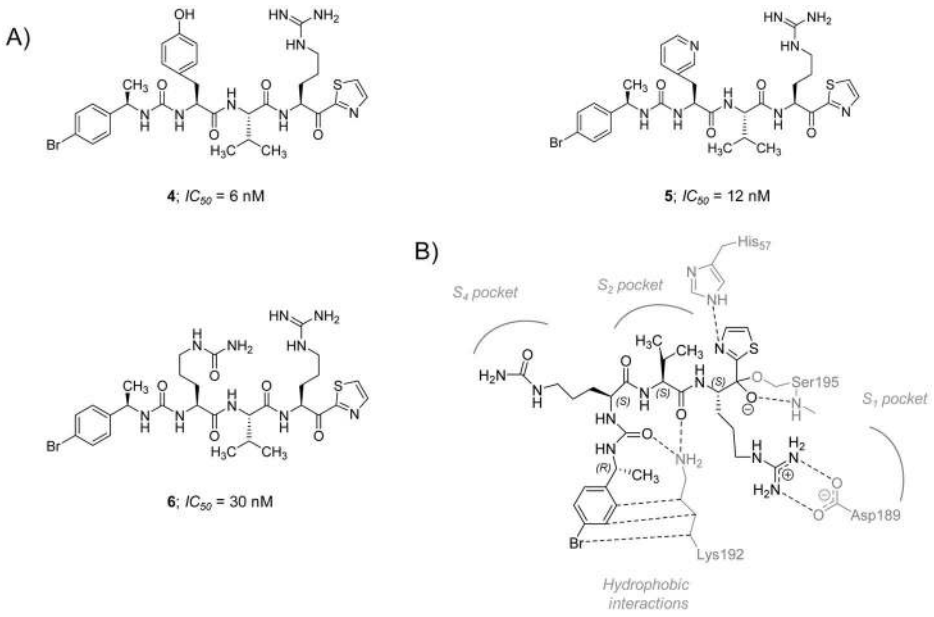

Figure 4. Chemical structures of the advanced α-ketothiazole guanidine-containing tetrapeptidomimetics that act as active site inhibitors of FXIa

A) Chemical structures of inhibitors **4–6** are provided along with their FXIa IC_{50} values in nM. B) Interactions between inhibitor **6** and residues in the active site of FXIa are also delineated (PDB ID: 1ZOM).

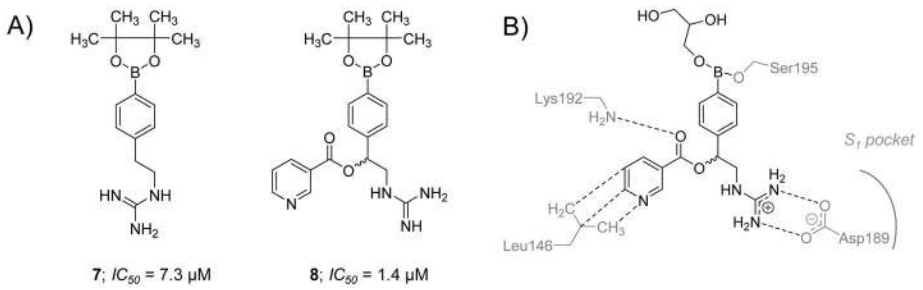

Figure 5. Chemical structures of aryl boronic acid derivatives that act as active site inhibitors of FXIa

A) Chemical structures of inhibitors **7** and **8** are provided along with their FXIa IC_{50} values in μM. B) Interactions between inhibitor **8** and residues in the active site of FXIa are also delineated (PDB ID: 1ZLR).

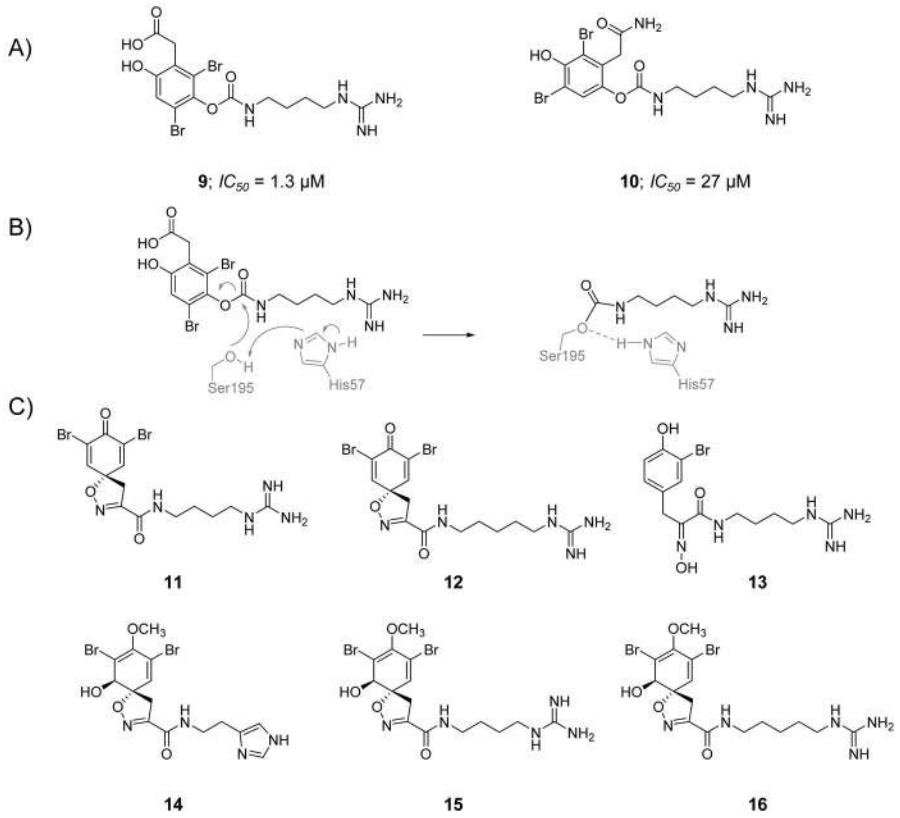

Figure 6. Chemical structures of clavatadines from marine sponge acting as active site inhibitors of FXIa

A) Chemical structures of clavatadine A, **9**, and B, **10**, are provided along with their FXIa IC_{50} values in μM. B) The carbamylation reaction between the carbamate group of clavatadine A and Ser195 of the catalytic triad of FXIa. C) Chemical structures for other clavatadines **11–16**.

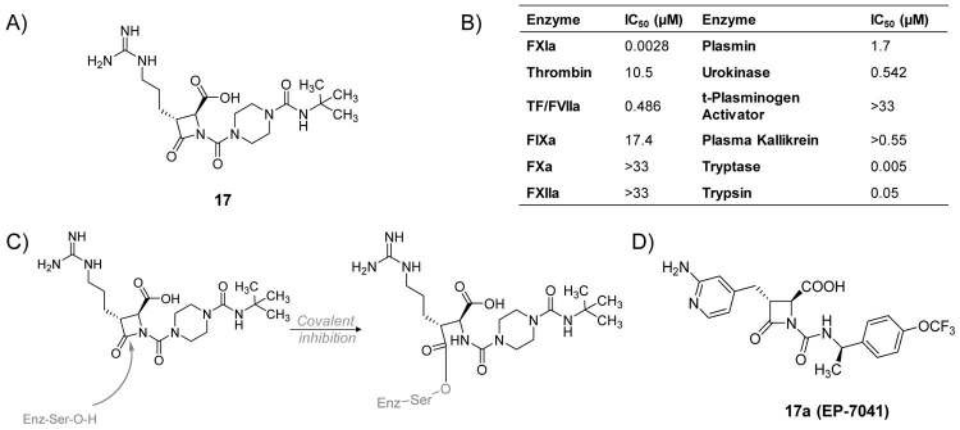

Enzyme	IC_{50} (μM)	Enzyme	IC_{50} (μM)
FXIa	0.0028	Plasmin	1.7
Thrombin	10.5	Urokinase	0.542
TF/FVIIa	0.486	t-Plasminogen Activator	>33
FIXa	17.4	Plasma Kallikrein	>0.55
FXa	>33	Tryptase	0.005
FXIIa	>33	Trypsin	0.05

Figure 7.

A) Chemical structure of β-lactam, active site inhibitor **17** of FXIa. B) The inhibition potencies (IC_{50} values in μM) of β-lactam **17** against a series of serine proteases. C) The acylation reaction between the β-lactam moiety of **17** and Ser195 residue of FXIa's active site. D) The chemical structure of inhibitor **17a** (Ep-7041) which just finished Phase I clinical trial.

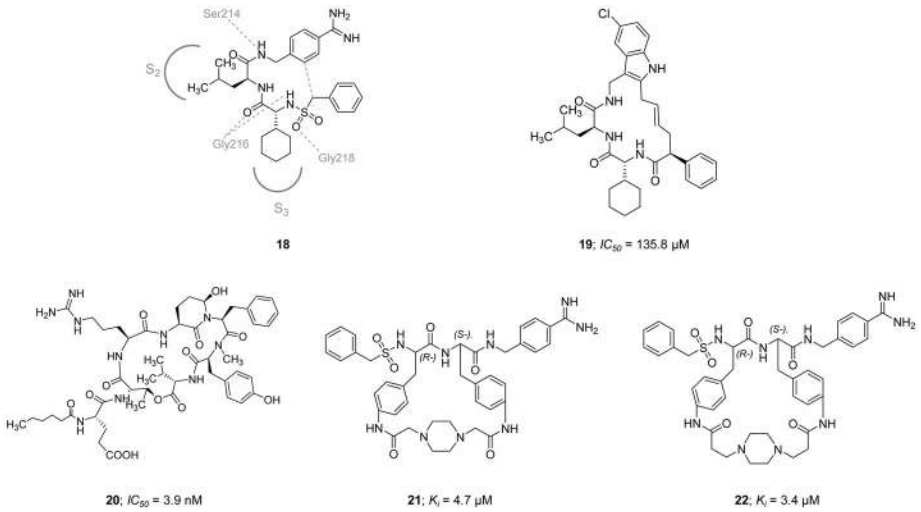

Figure 8.

Chemical structures of macrocyclic peptidomimetic, active site inhibitors **19**–**22** of FXIa along with their inhibitory parameters. Molecule **18** was exploited by Hanessian *et al.* to design the macrocyclic inhibitor **19**. For inhibitors 21 and 22, the stereochemistry is indicated by (L-) and (R-).

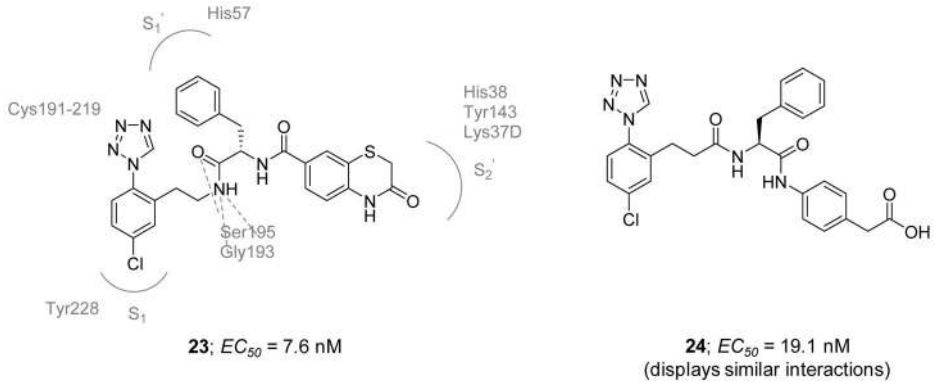

Figure 9.

Chemical structures of early 1-(4-chlorophenyl)-1H-tetrazole-based inhibitors **23** and **24** of FXIa which were exploited to obtain the first x-ray crystal structures of FXIa catalytic domain with nonbasic inhibitors (PDB IDs: 3SOS and 3SOR). Effective concentrations to inhibit FXIa are also provided in nM.

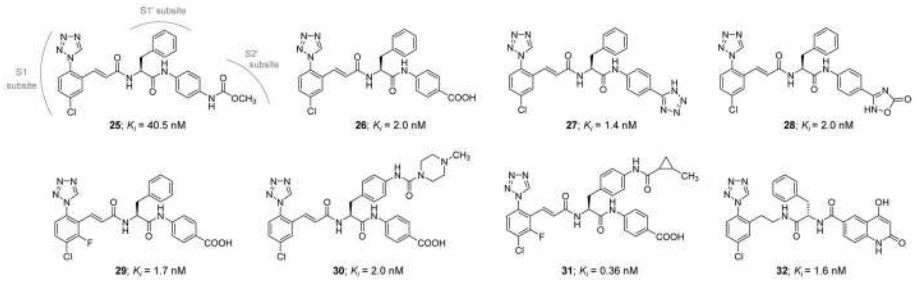

Figure 10.

Chemical structures of advanced 1-(4-chlorophenyl)-1H-tetrazole-based inhibitors **25–32**of FXIa. They are active site peptidomimetic inhibitors with K_i values in low nanomolar range. They follow the "P1-P1′-P2′" design concept.

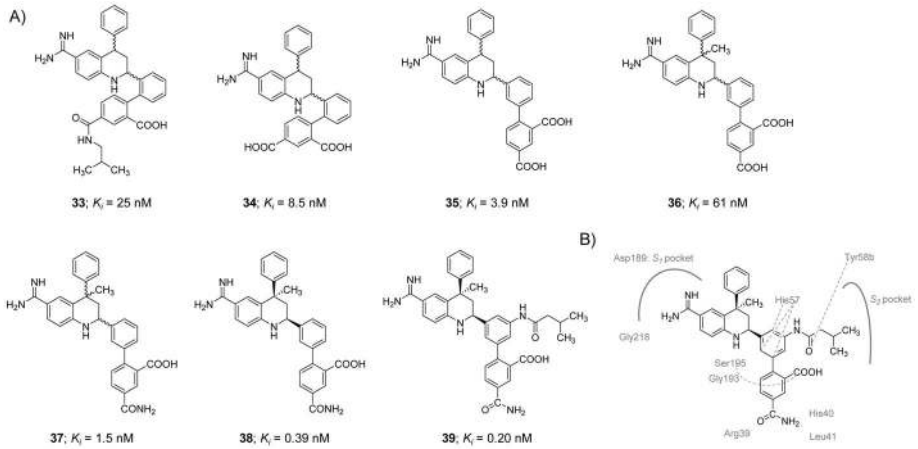

Figure 11.

A) Chemical structures of tetrahydroquinoline (THQ) derivatives **33–39** acting as active site, peptidomimetic inhibitors of FXIa. Inhibitors' *Ki* values are provided in nM. B) Interactions between inhibitor **39** and residues in the active site of FXIa are also delineated (PDB ID: 4NA7).

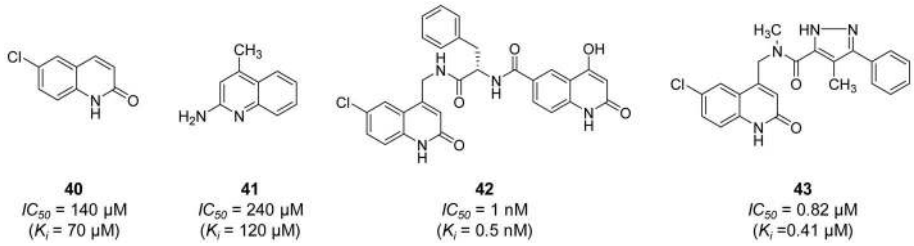

Figure 12.

Chemical structures of quinolin-2-one derivatives **40–43** acting as active site, peptide-mimetic inhibitors of FXIa. Inhibitiors' K_i and IC_{50} values are provided in nM and μM. Inhibitors were initially developed using fragment-based drug design concept.

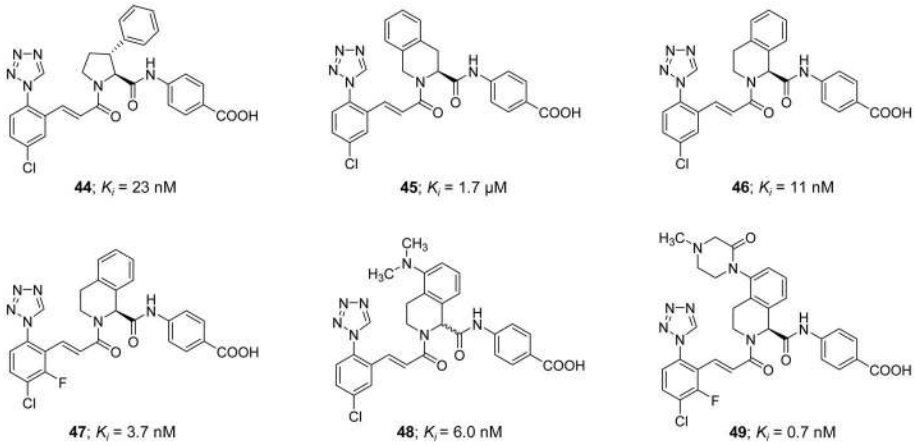

Figure 13.

Chemical structures of pyrrolidine **44** and tetrahydroisoquinoline (THIQ) derivatives **45–49** acting as active site, peptidomimetic inhibitors of FXIa. Inhibitors' *Ki* values are provided in nM (or μM).

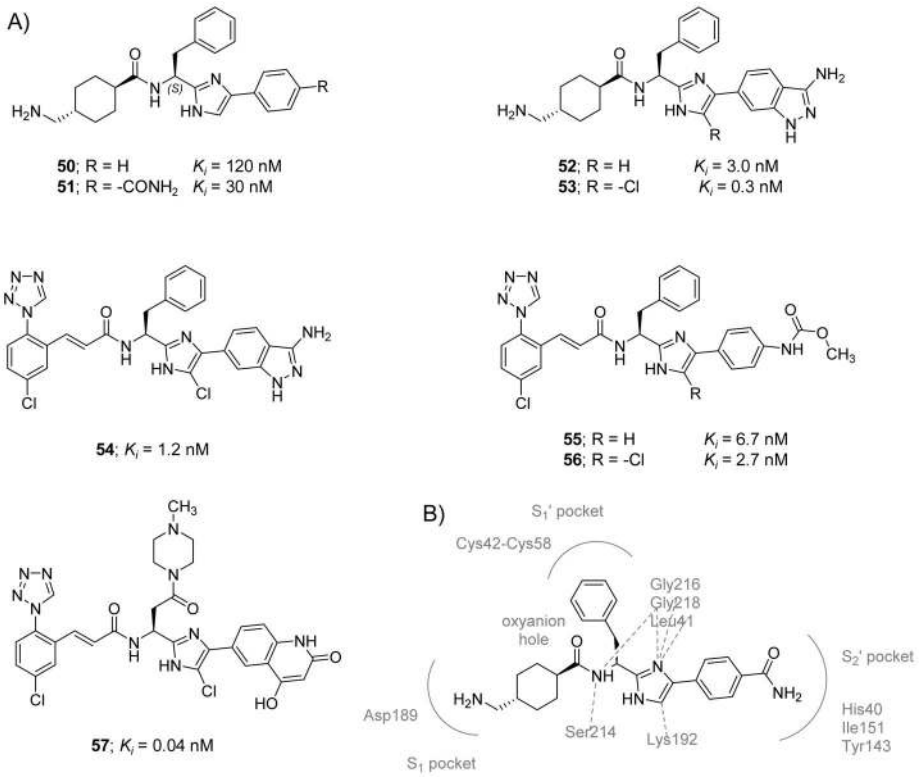

Figure 14. Chemical structures of imidazole-containing derivatives that act as active site tripeptidomimetic inhibitors of FXIa

A) Chemical structures of inhibitors **50–57** are provided along with their FXIa K_i values in nM. They follow the "P1-P1′-P2′" design concept. B) Interactions between inhibitor **51** and residues in the active site of FXIa are also delineated (PDB ID: 4TY6).

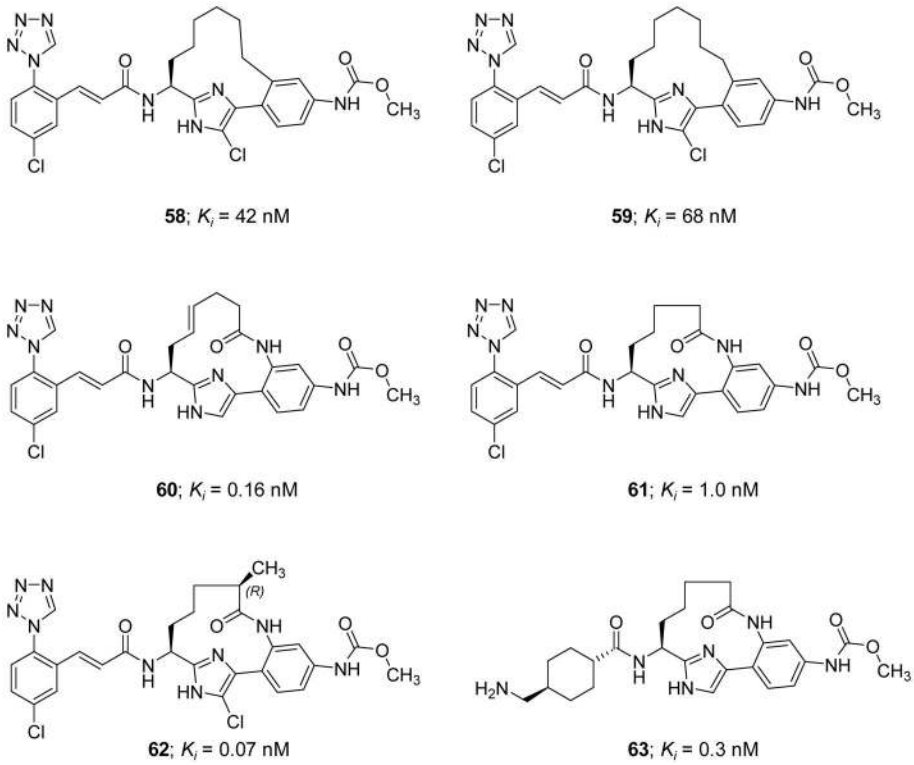

Figure 15.

Chemical structures of macrocyclic peptidomimetic **58–63** acting as active site inhibitors of FXIa. Inhibitors' K_i values are provided in nM. Corresponding acyclic inhibitors are imidazole-containing derivatives with P1 domain of 1-(4-chlorophenyl)-*1H*-tetrazole **58–61** or tranexamic acid **63**.

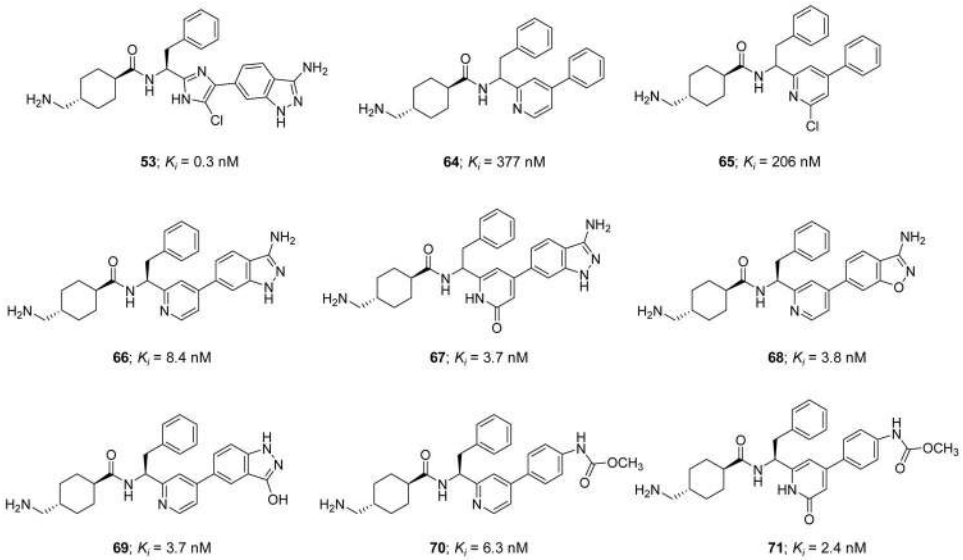

Figure 16.

Chemical structures of pyridine **64–66** and **68–70** and pyridinone **67** and **71**-containing derivatives which inhibit FXIa by binding to its active site. P1 domain is tranexamic acid. Inhibitors' K_i values are provided in nM.

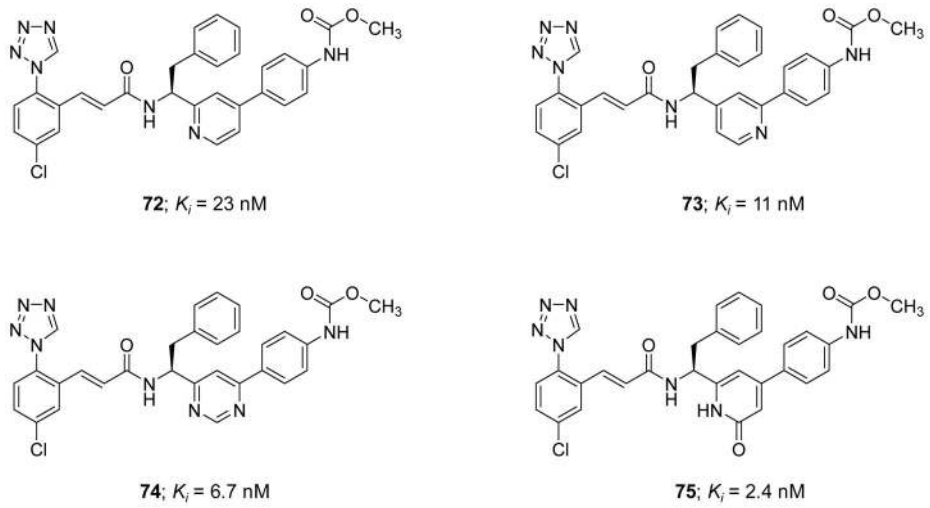

Figure 17.

Chemical structures of pyridine **72** and **73**, pyridinone **75**, and pyrimidine **74**-containing derivatives which inhibit FXIa by binding to its active site. P1 domain is 1-(4-chloro-phenyl)-*1H*-tetrazole. Inhibitors' K_i values are provided in nM.

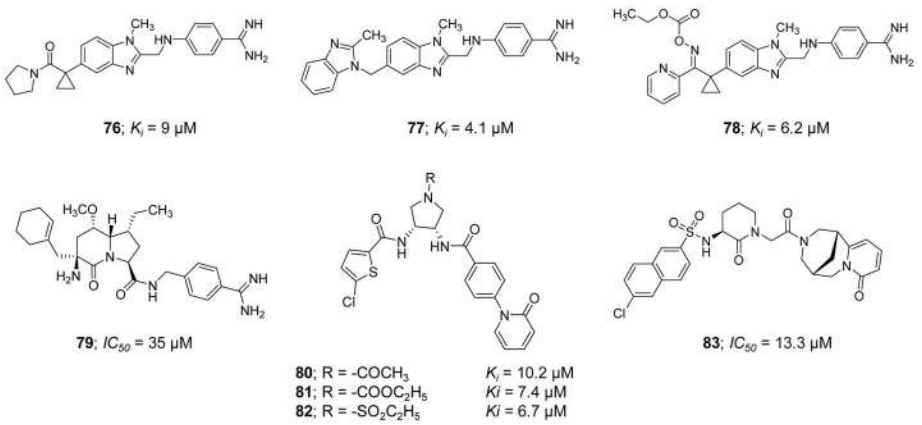

Figure 18.

Chemical structures of miscellaneous molecules that inhibit FXIa by binding to its active site. Chemical classes included are benzimidazole benzamidines **76–78**, indolizidinone **79**, cyclicdiamines **80–82**, and arylsulfonamidopiperidone **83**. These molecules mainly inhibit other serine proteases. Inhibitors' K_i values are provided in μM.

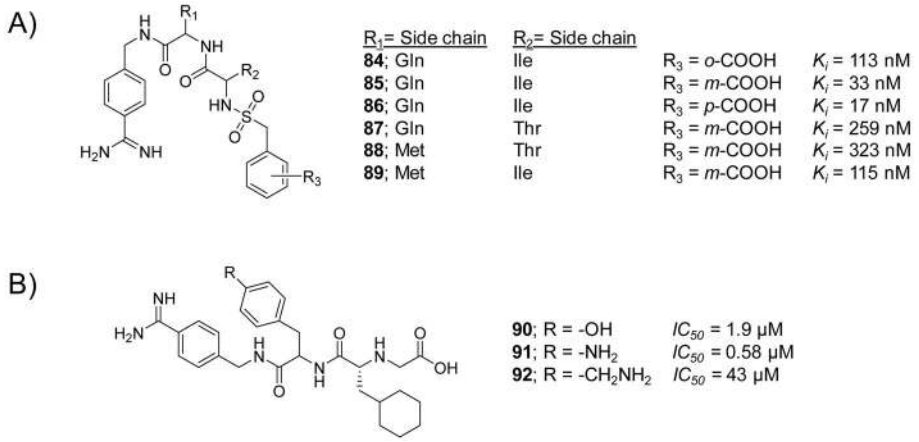

Figure 19.

Chemical structures of benzamidine-based inhibitors of FXIa **84–92**. A) Inhibitors **84–89** are also potent inhibitors of FVIIa. B) Inhibitors **90–92** are also potent inhibitors of APC. Provided are inhibitors' K_i and IC_{50} values in nM and μM.

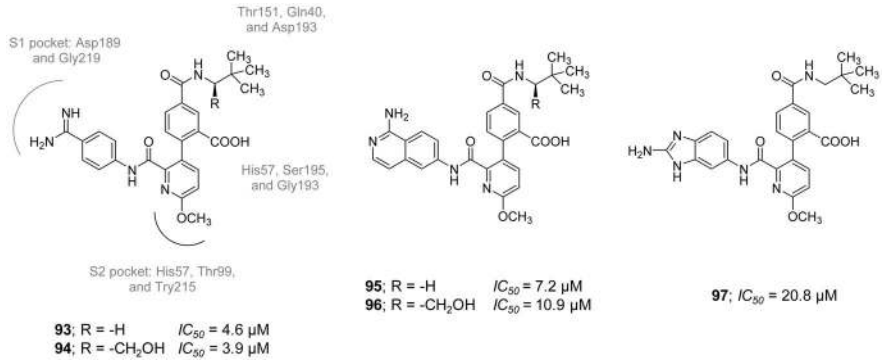

Figure 20.

Chemical structures of biaryl acid derivatives **93–97** which inhibit FXIa by binding to its active site. These molecules are more potent inhibitors of FVIIa. FXIa Ki values are provided in μM. Provided also are the interactions between inhibitors **93** and **94** and residues in the active site of FXIa.

A)

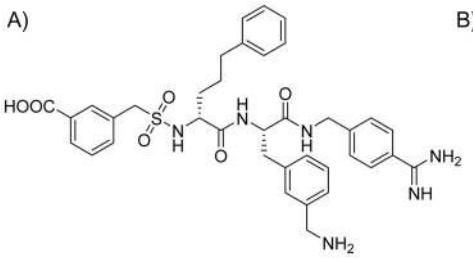

98; CU-2010
K_i = 18 nM

B)

Enzyme	CU-2010 K_i (nM)	CU-2020 (Pegylated CU-2010) K_i (nM)
FXIa	~26	~819
Plasma kallikrein	~0.04	~0.16
Plasmin	~2.2	~8.4
FXIIa	~4040	~892
FXa	~51	~81
Thrombin	~1423	~1553

Figure 21.

A) Chemical structure of CU-2010 **98** which inhibits FXIa with a K_i value of 18 nM. B) The inhibition profile of CU-2010 and its pegylated form against a series of related serine proteases. CU-2010 and CU-2020 were originally reported as antifibrinolytic agents.

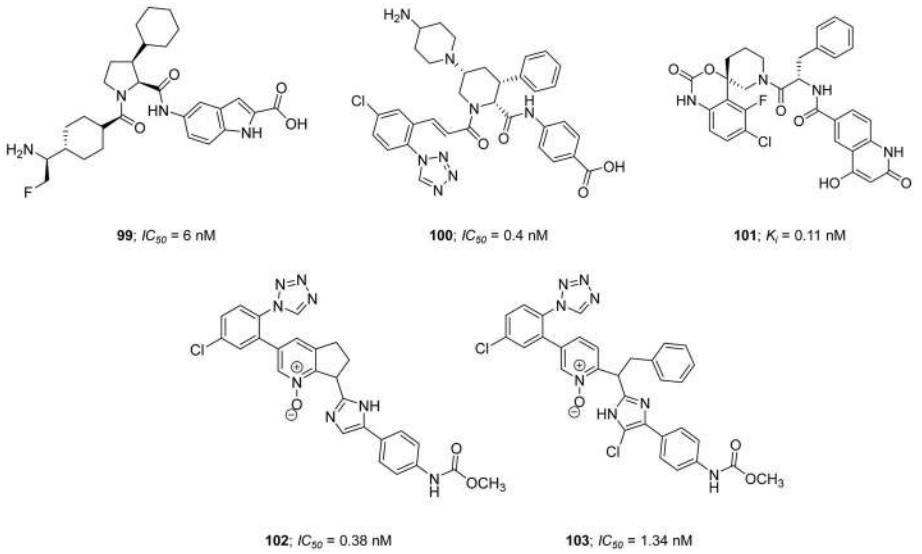

Figure 22.

Chemical structures of patented molecules **99–103** which demonstrated very potent inhibitory activity toward FXIa in the low nanomolar range. Chemical classes are pyrrolidine-2-carboxamide **99**, piperidine-2-carboxamide **100**, dihydrobenzoxazine **101**, cyclopentapyridine-*N*-oxide **102**, and pyridine-*N*-oxide **103**.

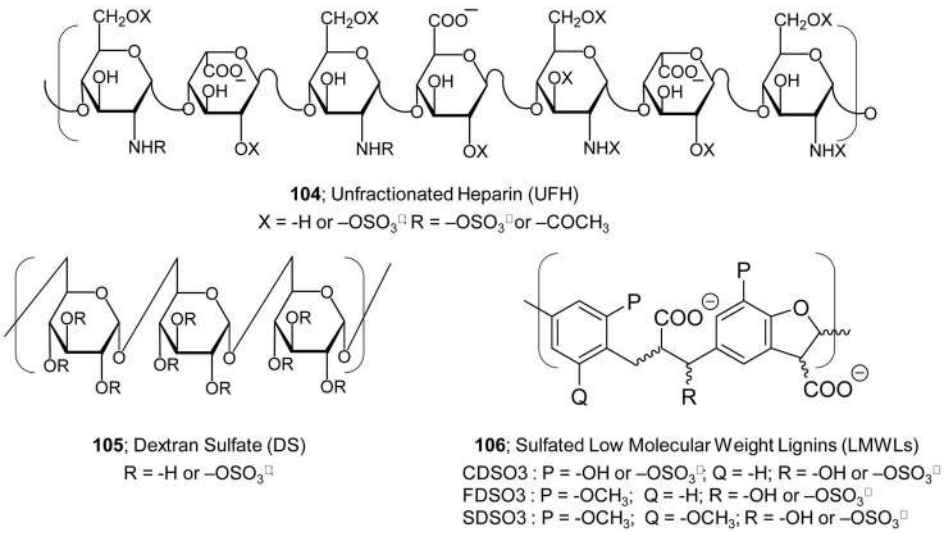

Figure 23.

Chemical structures of GAGs and their mimetics **104–106** as polymeric allosteric inhibitors of FXIa.

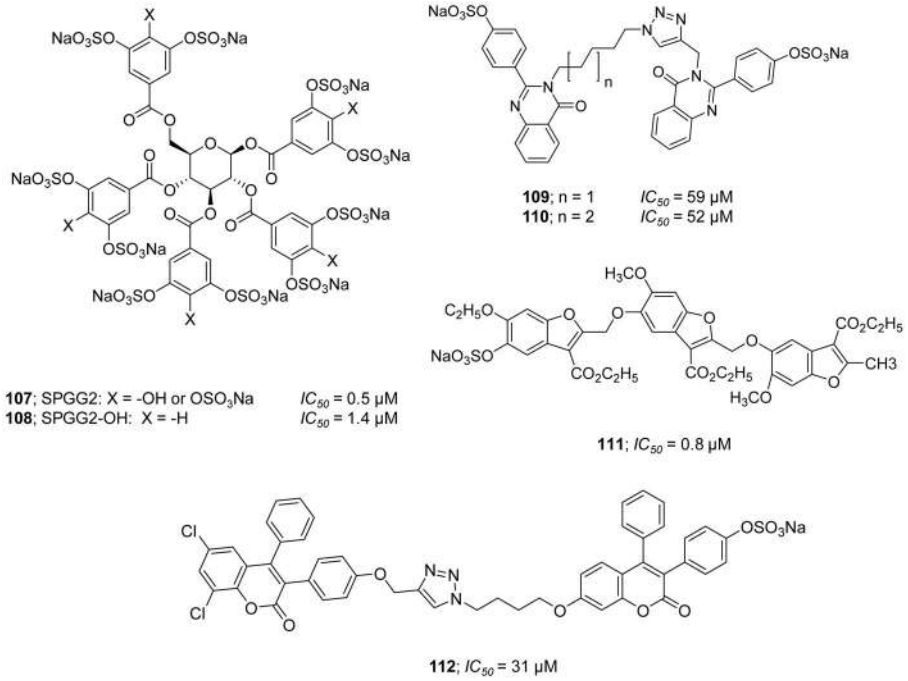

Figure 24.

Chemical structures of sulfated, nonsaccharide GAG mimetics **107–112** as small molecule, allosteric inhibitors of FXIa. They include decasulfated galloids **107** and **108**, disulfated quinazolinone dimers **109** and **110**, monsulfated benzofuran trimer **111**, and monosulfated coumarin dimer **112**. Inhibitors' IC_{50} values are also provided in μM.

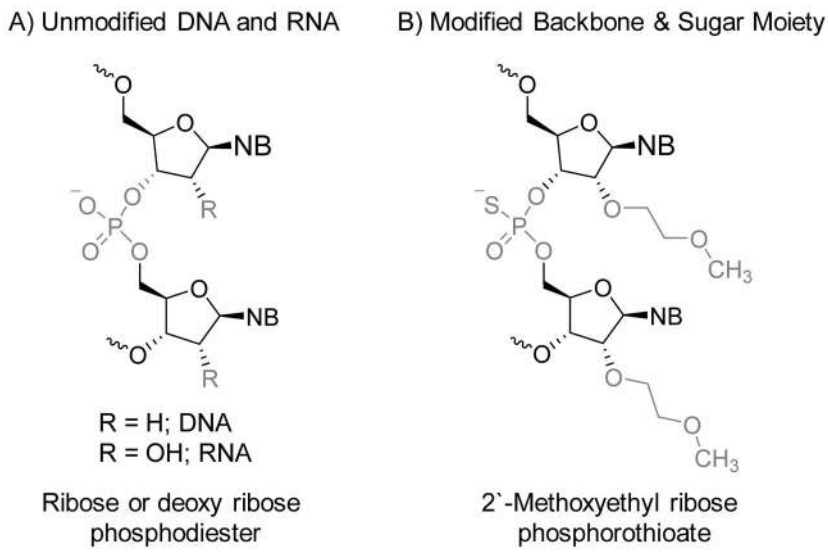

Figure 25.

Chemical structures of A) unmodified DNA or RNA sequence having ribose or deoxyribose sugar and phosphodiester linkage and B) modified oligonucleotide sequence used in the design of FXI ASO with 2′-methoxyethylribose sugar and phosphorothioate linkage. NB means nitrogenous base.

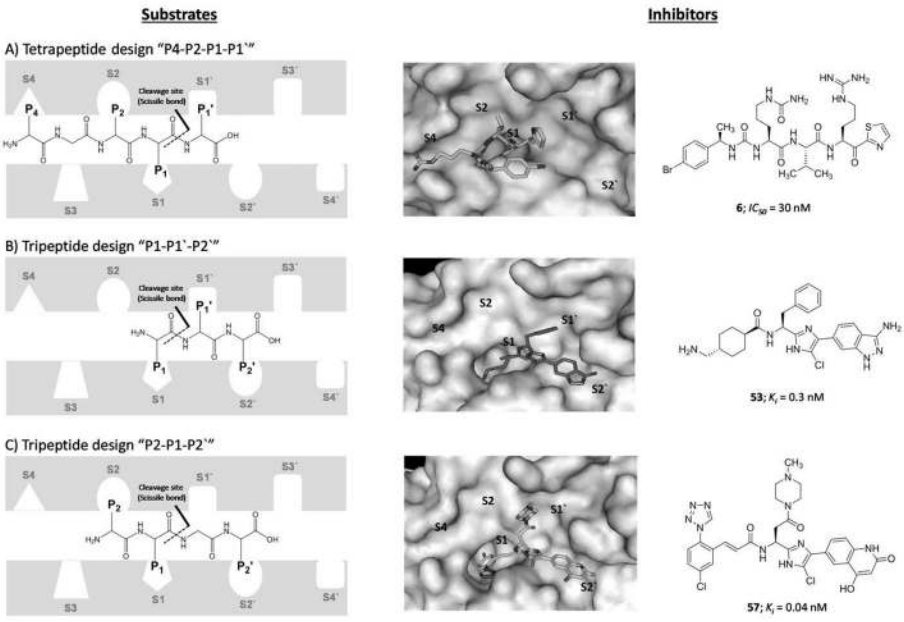

Figure 26.

The substrate-based concepts that were exploited to design active site peptidomimetic inhibitors of FXIa. A) Tetrapeptide design "P4-P2-P1-P1′" as with inhibitor **6** (K_i =30 nM; PDB ID: 1ZOM); B) Tripeptide design "P1-P1′-P2′" as with inhibitor **53** (K_i = 0.3 nM; PDB ID: 4TY7); and C) Tripeptide design "P2-P1-P2′" as with inhibitor **57** (K_i= 0.04 nM; PDB ID: 4Y8Z).